FIFTH EDITION

McKee's Pathology of the Skin

WITH CLINICAL CORRELATIONS

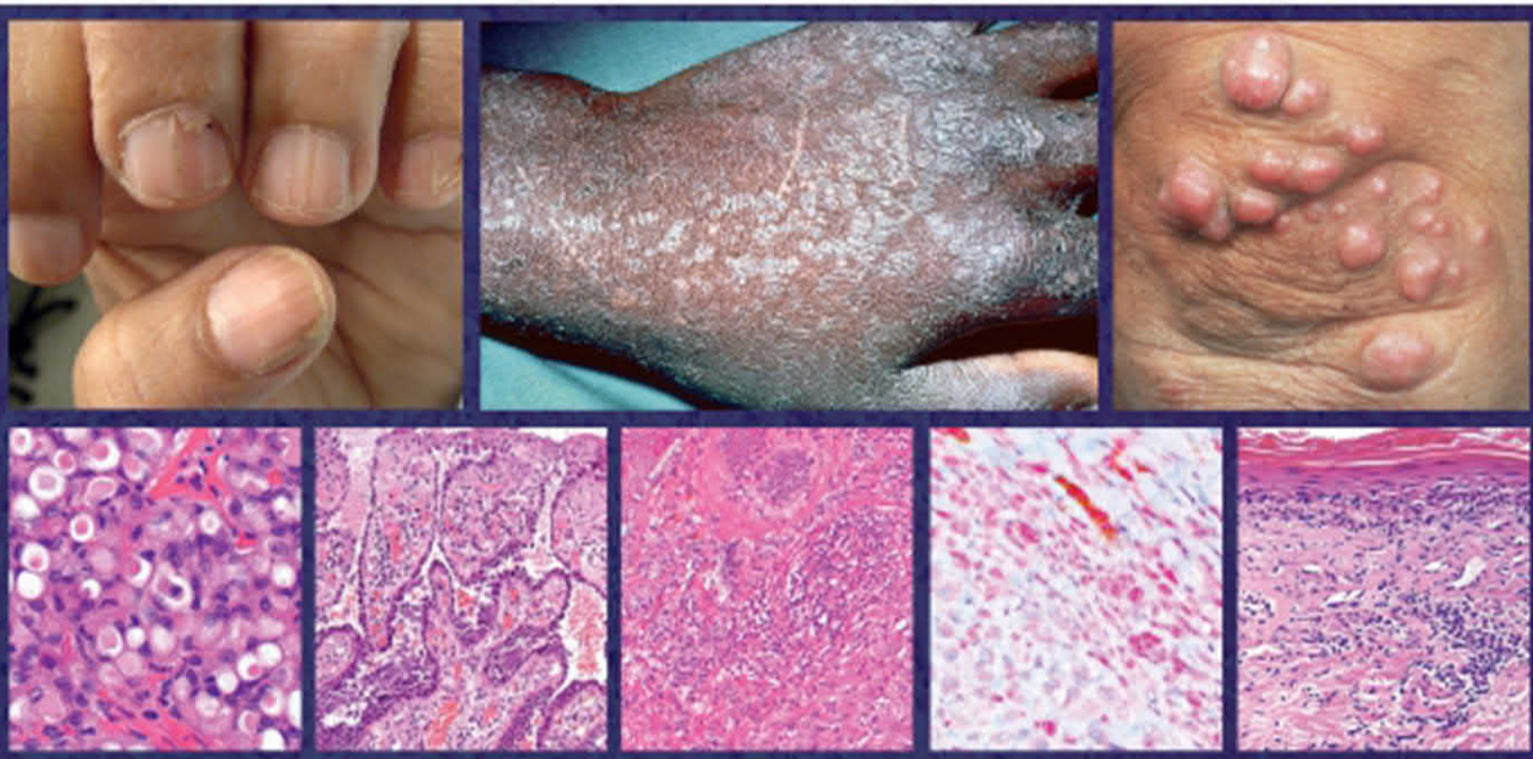

Eduardo Calonje
Thomas Brenn | Alexander J. Lazar | Steven D. Billings

ELSEVIER

McKee's

Pathology of the Skin

VOLUME ONE | FIFTH EDITION

McKee's

Pathology of the Skin

WITH CLINICAL CORRELATIONS

Eduardo Calonje MD, DipRCPath
Director of Dermatopathology
Department of Dermatopathology
St John's Institute of Dermatology
St Thomas' Hospital
London, UK

CO-EDITORS

Thomas Brenn MD, PhD, FRCPath
Professor
Department of Pathology & Laboratory Medicine, Section of Anatomic Pathology
Department of Medicine, Section of Dermatology
Cumming School of Medicine
University of Calgary
Calgary Laboratory Services and Alberta Health Services
Calgary, AB, Canada

Alexander J. Lazar MD, PhD
Professor
Departments of Pathology, Genomic Medicine and Dermatology
Sections of Dermatopathology, Soft Tissue & Bone Pathology, and Clinical Genomics
Faculty, Sarcoma Research Center and Graduate School of Biomedical Science
The University of Texas M.D. Anderson Cancer Center Houston, Texas, USA

Steven D. Billings MD
Professor
Co-Director Dermatopathology Section
Department of Anatomic Pathology
Cleveland Clinic
Cleveland, OH, USA

For additional online content visit **ExpertConsult.com**

ELSEVIER

ELSEVIER

First edition 1989
Second edition 1996
Third edition 2005
Fourth edition 2012
Fifth edition 2020

Notices

Practitioners and researchers must always rely on their own experience and knowledge in evaluating and using any information, methods, compounds or experiments described herein. Because of rapid advances in the medical sciences, in particular, independent verification of diagnoses and drug dosages should be made.

To the fullest extent of the law, no responsibility is assumed by Elsevier, authors, editors or contributors for any injury and/or damage to persons or property as a matter of products liability, negligence or otherwise, or from any use or operation of any methods, products, instructions, or ideas contained in the material herein.

ISBN: 978-0-7020-6983-3 (2 volume set)
eISBN: 978-0-7020-7552-0

Content Strategist: Michael J. Houston
Content Development Specialist: Louise Cook
Project Manager: Andrew Riley
Design: Renee Duenow
Illustration Manager: Nichole Beard
Marketing Manager: Melissa Fogarty

Printed in China
Last digit is the print number: 9 8 7 6 5 4 3 2 1

Contents

Preface to the fifth edition vii
List of contributors viii
Acknowledgments x
Dedication xi
Glossary of abbreviations xii

VOLUME ONE

1 The structure and function of skin 1
John A. McGrath

2 Specialized techniques in dermatopathology 35
Plamenka K. Randall, Boris C. Bastian, Jeffrey P. North, John Goldblum, John A. McGrath and Alexander J. Lazar

3 Disorders of keratinization 53
Dana Matoo and Vivianne Oji

4 Inherited and autoimmune subepidermal blistering diseases 118
Boštjan Luzar and John A. McGrath

5 Acantholytic disorders 171

6 Spongiotic, psoriasiform and pustular dermatoses 201

7 Lichenoid and interface dermatitis 241

8 Superficial and deep perivascular inflammatory dermatoses 283

9 Granulomatous, necrobiotic and perforating dermatoses 306

10 Inflammatory diseases of the subcutaneous fat 351
Boštjan Luzar and Eduardo Calonje

11 Diseases of the oral mucosa 389
Soek Bin Wan

12 Diseases of the anogenital skin 470
Eduardo Calonje, Flora Lewis, Chris Bunker, Diego Fernando Sánchez Martínez and Antonio L. Cubilla

13 Degenerative and metabolic diseases 559

14 Cutaneous adverse reactions to drugs 630

15 Neutrophilic and eosinophilic dermatoses 662

16 Vascular diseases 714

17 Idiopathic connective tissue disorders 771
Boštjan Luzar and Eduardo Calonje

18 Infectious diseases of the skin 826
Wayne Grayson and Eduardo Calonje

VOLUME TWO

19 Human immunodeficiency virus (HIV) and acquired immunodeficiency syndrome (AIDS)-associated cutaneous diseases 978
Stephen L. Walker and Wayne Grayson

20 Disorders of pigmentation 990

21 Diseases of collagen and elastic tissue 1015

22 Diseases of the hair 1051
Rodrigo Restrepo and Eduardo Calonje

23 Diseases of the nails 1129
Josette André, Ursula Baran and Anne Theunis

24 Tumors of the surface epithelium 1156

25 Melanocytic nevi 1234
Boštjan Luzar, Boris C. Bastian, Jeffrey P. North and Eduardo Calonje

26 Melanoma 1310
Jeffrey P. North, Boris C. Bastian and Alexander J. Lazar

27 Tumors of the conjunctiva 1383
Anne Y. Lin

28 Sentinel lymph node biopsies 1388
Alistair J. Cochran

29 Cutaneous lymphoproliferative diseases and related disorders 1403
John Goodlad and Eduardo Calonje

30 Cutaneous metastases and Paget disease of the skin 1520

31 Tumors of the hair follicle 1545

32 Tumors and related lesions of the sebaceous glands 1599

33 Tumors of the sweet glands 1611

34 Cutaneous cysts 1680

35 Connective tissue tumors 1698
Eduardo Calonje, Vasiliki Demetriou, Alexander J. Lazar

36 Animal models of skin disease 1895
John P. Sundberg, Lloyd E. King, Jr., Marcus Rosenberg, Qian Li, Joyce Little, Michael E. Wilke and C. Herbert Pratt

Index I-1

Preface to the fifth edition

It is unbelievable that it is more than 5 years since Phillip McKee announced that he was retiring and standing down as the editor of the textbook that he started as a solo author back in the early 1990s. This book, to which he devoted a large part of his life and career, became a household name many years ago and I am very lucky that he, with his boundless generosity, invited me to be part of it when the third edition was planned. Since then, "the book" has become an intrinsic part of my life and almost my whole existence since I became the main editor three years ago when Phillip retired. It is needless to say that Phillip is sorely missed not only as a teacher and friend, but also as somebody that for so many years devoted countless hours to something that can only be described as a labour of love. Thankfully we remain close friends and in communication. However, the void that he has left is difficult if not impossible to fill. I am eternally grateful to him for putting his trust in me and can only hope that I will not disappoint him.

Although for most of the 20th century, single author books were the norm and giants in the field of pathology and dermatology produced wonderful textbooks with little outside help, the amount of knowledge and information produced at an incredible rate in all fields make it impossible to perpetuate this trend and Phillip recognized this when the third edition was planned. Thomas Brenn and Alex Lazar continue to be associate editors of this textbook, as in the past, and their help has been as always invaluable, especially as the task is daunting when one has a full-time job to take care of. In this edition we have asked Steven Billings to join the team as a third co-editor and, although I never doubted the choice, he has surpassed expectations as somebody with incredible energy, knowledge and will to help in every possible way. Many of the previous contributors have been asked to contribute again and a few new ones have joined the effort with their knowledge and expertise. To all these contributors we are deeply indebted.

In the fourth edition we made the decision to provide the references online-only to allow us to expand the text and figures facilitating a more comprehensive textbook. Unfortunately, although following the same option this time, not much extra space is available and therefore the number of new images is limited. The editors, however, have been very generous in allowing extra text to keep up to date with new developments. They have also allowed us to include a new chapter entitled 'Animal Models of Skin Disease' by John P. Sundberg and colleagues which we believe is a valuable addition to the book.

A very esteemed and famous dermatopathologist has for many years started his lectures by predicting the demise of classical dermatopathology and its almost complete replacement by molecular techniques. In his view, it is a matter of a few years before this happens and light microscopy of sections stained with H&E will be a thing of the past or limited to places where newer techniques are not available. Although there is undoubtful truth in this, as clearly demonstrated in the fields of neoplasms and inherited diseases, it is also true that light microscopy remains the gold standard and that most of the diagnoses depend at least partially on the evaluation of sections stained in routine manner with the aid of special techniques. Our view is that all these techniques complement each other. Therefore, in the fifth edition we have tried to keep a balance between traditional diagnostic techniques and recent advances, particularly in the field of molecular diagnosis. It is difficult to keep up to date with the latest developments in the field as there has been an explosion of information as never before, particularly with regards to molecular mechanisms of disease. We have tried to reflect this in the book as accurate and as extensively as possible.

During the production of this book, I have been very lucky to work with two highly professional individuals that have gone out of their way to make my life easier. They are Louise Cook and Michael Houston. I had worked with both in the past and knew that every crisis no matter how big it seems, could be resolved with patience and resolution. For more than 2 years, I have had a weekly telephone conversation with Louise to sort out even the smallest problem. I will miss this. She has never let me down and I cannot thank her enough for her patience, her resilience and for just doing an amazing job.

This preface will not be complete if I did not acknowledge the person that has been unflinchingly there for me without asking for anything in return. My wife Claudia has given her love, her time, her patience and her understanding to help me complete this project. Having to share your marriage with a book is an unenviable task and she has done wonders.

EC
2018

List of contributors

The authors would like to acknowledge and offer grateful thanks for the input of all previous editions' contributors, without whom this new edition would not have been possible.

Josette André MD
Head of the Dermatology and Dermatopathology Department.
CHU Saint-Pierre - CHU Brugmann
Hôpital Universitaire des Enfants Reine Fabiola
Université Libre de Bruxelles
Brussels, Belgium

Boris C. Bastian MD, PhD
Professor of Dermatology and Pathology
University of California, San Francisco;
Gerson and Barbara Bass Baker Distinguished Professor in Cancer Research, UCSF
San Francisco, CA, USA

Marcus Bosenberg MD, PhD
Co-Leader of the Genomics, Genetics and Epigenetics Program
Yale Cancer Center;
Dermatopathologist, Departments of Dermatology and Pathology
Yale University School of Medicine
New Haven, CT, USA

Chris Bunker MA, MD, FRCP
Consultant Dermatologist
University College and Chelsea and Westminster Hospitals London;
Professor of Dermatology
University College London
London, UK

Alistair J. Cochran, MD
Distinguished Professor of Pathology and Laboratory Medicine and Surgery
Department of Pathology and Laboratory Medicine
David Geffen School of Medicine at UCLA
Los Angeles, CA, USA

Antonio L. Cubilla MD
Instituto de Patología e Investigación
Asuncion, Paraguay

Vasileia Damaskou MD
Consultant Histopathologist
2nd Department of Pathological Anatomy
National and Kapodistrian University of Athens
School of Medicine,
Attikon University Hospital,
Athens, Greece

John Goodlad MD, FRCPath
Consultant Haematopathologist and Honorary Senior Lecturer
Department of Pathology
Western General Hospital and University of Edinburgh, Edinburgh, UK

Wayne Grayson MBChB, PhD, FCPath(SA)
Consultant Anatomical Pathologist and Dermatopathologist
AMPATH National Laboratories;
Honorary Associate Professor
School of Pathology
University of the Witwatersrand, Johannesburg
Johannesburg, South Africa

Lloyd E. King Jr. MD, PhD
Professor of Medicine, Dermatology and Dermatopathology
Division of Dermatology, Department of Medicine
Vanderbilt University Medical Center
Nashville, TN, USA

Fiona Lewis MB ChB, MD, FRCP
Consultant Dermatologist
St John's Institute of Dermatology
Guy's and St Thomas' NHS Trust
London, UK

Qiaoli Li PhD
Department of Dermatology and Cutaneous Biology
Jefferson Institute of Molecular Medicine
Thomas Jefferson University
Philadelphia, PA, USA

Amy Y. Lin MD
Associate Professor of Pathology and Ophthalmology
University of Illinois College of Medicine
Chicago, IL, USA

Boštjan Luzar MD, PhD
Professor of Pathology
Consultant Pathologist
Institute of Pathology
Medical Faculty University of Ljubljana
Ljubljana, Slovenia

Diego Fernando Sánchez Martínez MD
Pathologist
Instituto de Patologia e Investigación
Asunción, Paraguay

John A. McGrath MD, FRCP, FMedSci
Mary Dunhill Chair in Cutaneous Medicine
St John's Institute of Dermatology
King's College London
Guy's Hospital
London, UK

Dieter Metze MD
Professor of Dermatology
Director, Dermatopathology Unit
Department of Dermatology
University Hospital Münster
Münster, Germany

Jeffrey P. North MD
Assistant Professor
Department of Dermatology
UCSF School of Medicine
San Francisco, CA, USA

Vinzenz Oji MD
Assistant Professor
Department of Dermatology
University Hospital Münster
Münster, Germany

C. Herbert Pratt PhD
Scientific Program Manager
Department of Research and Development
The Jackson Laboratory
Bar Harbor, ME, USA

Pratistadevi K. Ramdial MBChB, FCPath(SA)
Professor and Head
Department of Anatomical Pathology
Nelson R. Mandela School of Medicine
University of Kwazulu-Natal and the National Health Laboratory Service
Durban, South Africa

Rodrigo Restrepo MD
Director, Dermatopathology Fellowship Program
Universidad CES
Professor of Dermatopathology
Universidad Pontificia Bolivariana
Director, Laboratory of Pathology
Clinica Medellin
Medellin, Colombia

Ursula Sass MD
Assistant Professor
Dermatology and Dermatopathology Department
CHU Saint-Pierre
Université Libre de Bruxelles
Brussels, Belgium

John P. Sundberg DVM, PhD
Principal Investigator
Research and Development Department
The Jackson Laboratory
Bar Harbor, ME, USA

Anne Theunis MD
Assistant Professor
Dermatopathology and Pathology Department
CHU Saint-Pierre and Institut Bordet
Université Libre de Bruxelles
Brussels, Belgium

Jouni Uitto MD, PhD
Professor of Dermatology and Cutaneous Biology, and Biochemistry and Molecular Biology;
Chair, Department of Dermatology and Cutaneous Biology
Jefferson Institute of Molecular Medicine
Thomas Jefferson University
Philadelphia, PA, USA

Steve L. Walker PhD, MRCP (UK), DTM&H
Consultant Dermatologist and Associate Professor
Department of Clinical Research
London School of Hygiene and Tropical Medicine
London, UK

Michael V. Wiles PhD
Senior Director
Department of Technology Evaluation and Development
The Jackson Laboratory
Bar Harbor, ME, USA

Sook-Bin Woo DMD, MMSc
Associate Professor
Department of Oral Medicine, Infection and Immunity
Harvard School of Dental Medicine, Boston, MA, USA
Attending Dentist and Consultant Pathologist
Brigham and Women's Hospital
Boston, MA, USA
Co-Director
Center for Oral Pathology Strata Pathology Services Inc.,
Lexington, MA, USA

Acknowledgments

All the editorial team, including Louise Cook, Michael Houston, Thomas Brenn, Alex Lazar and Steven Billings have been invaluable in helping to carry this work to fruition and I am forever grateful for their efforts and hard work. My wife Claudia has never deserted me and has endured so much for the sake of my well-being that my admiration and love for her knows no boundaries. My children Matteo and Isabella have always supported me through thick and thin and I am indebted to them for this. Many people including colleagues and friends have made my life easier during these years and have helped in any way they can in order for me to complete this work. Many especially visiting fellows have had to endure lots and they have been always there for me not only with words of support but also with their help. I especially want to thank Drs Adriana Garcia Herrera, Eduardo Rozas, Fiona Lewis, Zlatko Marusic, Chao-Kai Hsu, Giri Raj, Tawatchai Suttikoon, László Fónyad, Erica Ahn, Agnes Pekar-Lukacs and Yi-Gou Feng. I am also forever grateful to my friends Celmira Manzano and Patricia Otero.

EC

The path of life is determined by the people we meet. There are many ways in which certain individuals touch our hearts, steer us in the right direction and help us achieve goals which would have been unattainable otherwise. Words aren't ever enough to really show one's true appreciation for the generosity, support and motivation received over the years.

My wonderful, loving parents, Sonja and Walter, have always been there for me and supported my every move. My professional life could have gone very wrong indeed had it not been for the kindness and gracious support from these truly unique mentors and teachers Uta Francke, Heinz Furthmayr, Ramzi Cotran and Christopher Fletcher. There is so much I owe to these two wonderful individuals who have become very close friends, Phillip McKee and Eduardo Calonje. Tinka, Yäelle and Pippa, thank you for all the color and joy you bring to my life and for keeping me humble and (relatively) sane.

TB

Our decidedly cynical postmodern outlook gives short shrift and virtually no quarter to being earnest and sincere in demeanor. Nonetheless, I find I that I am truly and greatly honored to have worked with my exceedingly talented three co-editors and the distinguished cast of chapter authors who stayed this long strange journey with us. Numerous gracious individuals have and continue to inspire and influence me and help me to find my way in life from mentors to colleagues and friends to fellows and students of various sorts and types. I am loath to attempt to name this entire cast of characters lest I neglect to list anyone in particular. Suffice it to say, you know who you are and my many glaring faults are indeed my own and exist despite what you have all tried so hard to do for me! To the many fellows and students who have endured learning with me over the years, please know that you definitely taught me at least as much if not more than I ever managed to impart to you. Your quite reasonable demands for clear, concise and reproducible diagnostic criteria and intellectual curiosity spur me to be my very best and have ignited a numerous studies and publications over the years. Truly, whatever success I have achieved is the product of intense exposure to the generosity of so many wonderfully talented and stimulating people.

AJL

I was surprised, humbled and deeply honored to be included as an editor on the book I use every day in practice. I am very grateful to Eduardo, Alex, and Thomas for including me and to Phillip McKee for his incredible contributions that are still present throughout this book. I would never have had this opportunity without the help and support of many people in my life. Notably, my parents for their support of my somewhat wandering path and my wife and daughter, Beth and Maeve, for their unending patience during the many hours spent on this book. I can never thank you enough. I am also deeply indebted to a number of mentors who have influenced me throughout my career, including Lawrence Roth, Thomas Ulbright, Thomas Davis, John Eble, Jenny Cotton, Sharon Weiss, and Andrew Folpe. I especially thank Antoinette Hood and the late William "Joe" Moores for teaching me dermatopathology. The influence of their wisdom is felt every day. Finally, I would like to thank my colleagues, residents and fellows who always teach me so much and inspire me.

SB

Dedication

To my wife Claudia, the light of my life and a person that I greatly admire in every respect.

To my children Matteo and Isabella.

EC

To Filippa.

TB

To my exceedingly patient and supportive family, Victoria, Elliott, Abigail and Sara.

AJL

To Beth, Maeve, Richard, Sally, Diane and Richard.

SB

Glossary of abbreviations

5-ARD	5-α-reductase
AA	alopecia areata
ACE	angiotensin converting enzyme [inhibitor]
AgNORs	argyrophilic nucleolar organizer regions
AHNMD	associated clonal hematological non-mast cell lineage disease
AIDS	acquired immunodeficiency syndrome
AILD	angioimmunoblastic lymphadenopathy with dysproteinaemia
ALA	aminolevulinic acid
ALK	anaplastic lymphoma kinase
ALK1	activin-like receptor kinase 1
ALM	acral lentiginous melanoma
AN	acanthosis nigricans
ANA	antinuclear antibodies
ANCA	neutrophil cytoplasmic antibodies
APO	apoptosis inhibitor 2
ARC	AIDS-related complex
ATF1	activating transcription factor 1
ATLL	adult T-cell leukemia/lymphoma
BANS	back, arm, neck and scalp [area]
BB	mid borderline leprosy
BCC	basal cell carcinoma
BCG	bacille Calmette–Guérin
b-FGF	basic fibroblast growth factor
BIDS	brittle sulfur-deficient hair, intellectual impairment, decreased fertility and short stature
BL	borderline lepromatous leprosy
BLAISE	Blaschko linear acquired inflammatory skin eruption
BMP	bone morphogenetic protein
BP	bullous pemphigoid
BPA	bullous pemphigoid antigen
BSAP	B-cell-specific activator protein
BSLE	bullous systemic lupus erythematosus
BT	borderline tuberculoid leprosy
CINeF	C1 inhibitor factor
CAD	chronic actinic dermatitis
cAMP	cyclic adenosine 3′-5′-monophosphate
c-ANCA	cytoplasmic antineutrophil cytoplasmic antibodies
CDC	Centers for Disease Control and Prevention
CEA	carcinoembryonic antigen
CGRP	calcitonin gene-related polypeptide
CHILD	congenital hemidysplasia with ichthyosiform nevus and limb defects [syndrome]
CK	cytokeratin
CLA	cutaneous lymphocyte antigen
CLL	chronic lymphocytic leukemia
CMG	capillary morphogenesis protein
CNS	central nervous system
CP	cicatricial pemphigoid (mucous membrane pemphigoid)
CRASP	complement regulator-acquiring surface protein
CREST	calcinosis, Raynaud's phenomenon, esophageal dysfunction, sclerodactyly, telangiectasia [syndrome]
CTCL	cutaneous T-cell lymphoma
dcSSc	diffuse cutaneous systemic sclerosis
DDEB	dominant dystrophic epidermolysis bullosa
DEB	dystrophic epidermolysis bullosa
DH	dermatitis herpetiformis
DIC	disseminated intravascular coagulation
DMF	direct immunofluorescence
DLE	discoid lupus erythematosus
DNCB	dinitrochlorobenzene
DSAP	disseminated superficial actinic porokeratosis
Dsc	desmocollin
dsDNA	double-stranded DNA
Dsg	desmoglein
DSP	disseminated superficial porokeratosis
EB	epidermolysis bullosa
EBA	epidermolysis bullosa acquisita
EBS	epidermolysis bullosa simplex
EBS-DM	epidermolysis bullosa simplex, Dowling–Meara
EBS-K	epidermolysis bullosa simplex, Koebner
EBS-MD	epidermolysis bullosa simplex with muscular dystrophy
EBS-WC	epidermolysis bullosa simplex, Weber–Cockayne
EBV	Epstein–Barr virus
ECE	endothelin-converting enzyme
ECM	extracellular membrane
EDS	Ehlers–Danlos syndrome
EGFR	endothelial growth factor receptor
ELAM	endothelial leukocyte adhesion molecule
ELISA	enzyme linked immunosorbent assay
EM	electron microscope
EMA	epithelial membrane antigen
ENA	extractable nuclear antigen
ENL	erythema nodosum leprosum
EPIDR	neutrophilic, polymorphic and pruritic eruptions associated with radiotherapy
EPPK	epidermolytic palmoplantar keratoderma
EPS	extracellular polysaccharide substance
ESR	erythrocyte sedimentation rate
ETA	exfoliative toxin A
ETB	exfoliative toxin B
Ev	epidermodysplasia verruciformis
EVER1	Ewing's sarcoma [protein receptor]
FACE	facial Afro-Caribbean childhood eruption
FADS	focal dermal hypoplasia deformation sequence
FAMMM	familial atypical multiple mole melanoma [syndrome]
FAP	familial adenomatous polyposis
FAPA	fever, aphthous stomatitis, pharyngitis, adenitis [syndrome]
FHT	fragile histidine triad
FIGURE	facial idiopathic granulomatous with regressive evolution
FISH	fluorescent in situ hybridization
GA	granuloma annulare
GABEB	generalized atrophic benign epidermolysis bullosa
GCDFP	gross cystic disease fluid protein
G-CSF	granulocyte colony stimulating factor
GFAP	glial fibrillary acidic protein
GM-CSF	granulocyte-macrophage colony stimulating factor
GSE	gluten sensitive enteropathy
GVHD	graft versus host disease
HA	hyperandrogenism
HAART	highly active antiretroviral therapy
HAIR-AN	hyperandrogenism–insulin resistance–acanthosis nigricans [syndrome]
HBV	hepatitis B virus
HDL	high density lipoprotein

HF	hemorrhagic fever
HG	herpes gestationis
HHV	human herpesvirus
HIT	heparin-induced thrombocytopenia [syndrome]
HIV	human immunodeficiency virus
HLA	human leukocyte antigen
HMFG	human milk fat globulin
HNPCC	hereditary non-polyposis colorectal carcinoma [syndrome]
HPF (hpf)	high power field
HPL	hyperlipoproteinemia
HPV	human papillomavirus
HRF	histamine releasing factor
HSP	heat shock protein
HSV	herpes simplex virus
HTLV	human T-cell lymphotropic virus
HTR	telomerase RNA
HUS	hemolytic uremic syndrome
IBD(D)	infections and IBDs (see IBDs above)
ICAM	intercellular adhesion molecule
ICH	endothelium cell histiocytosis
IDL	intermediate density lipoproteins
IEN	intraepidermal neutrophilic IgA dermatosis variant)
IFAP	ichthyosis follicularis–alopecia– photophobia [syndrome]
IFN	intermediate filament associated protein
Ig	interferon
IMF	immunoglobulin
INCEN	indirect immunofluorescence
IMF	inflammatory linear verrucous epidermal nevus
IP	immunofluorescence
IR	inducible protein (mononeopterin)
ISSVD	insulin resistance
JEB	International Society for the Study of Vulvovaginal Disease
JEB-H	junctional epidermolysis bullosa
JEB-nH	junctional epidermolysis bullosa, Herlitz
JEB-PA	junctional epidermolysis bullosa, non-Herlitz
KID	junctional epidermolysis bullosa with pyloric atresia
KOH	keratitis–ichthyosis–deafness [syndrome]
KPAF	potassium hydroxide
LB-N cells	keratinous pilaris atrophicans facei
LAD	lymphocyte and/or histiocytic Reed–Sternberg cell variants
LATS	linear IgA disease
LCA	long acting thyroid stimulator
LCH	leukocyte common antigen
LEBSL	Langerhans' cell histiocytosis
LDL	lateral cutaneous systemic sclerosis
LE	low density lipoprotein
LFA	lupus erythematosus
LH-RH	lymphocyte function-associated antigen
LL	luteinizing hormone-releasing hormone
LP	lamina lucida hyperplasia lymphoma
LPP	lichen planus
LPS	lichen planus pemphigoides
LS	lichen sclerosus
LYVE	lymphatic vessel endothelial [hyaluronan receptor]
MAC	membrane attack complex
MAI	M. avium intracellulare
MALT	mucosa-associated lymphoid tissue
MART-1	melanoma antigen recognized by T-cells 1
MBP	myelin basic protein
MC1R	melanocortin 1 receptor
MCGN	mesangiocapillary glomerulonephritis
MCP	molecule downregulation protein
M-CSF	macrophage colony stimulating factor
MCTD	mixed connective tissue disease
MDR	multidrug resistance gene
Mel-CAM	melanoma cell adhesion molecule
MEN	multiple endocrine neoplasia [syndrome]
MFH	malignant fibrous histiocytoma
MGS/GRO	melanoma growth stimulatory activity
MHC	major histocompatibility complex
mH	minor histocompatibility complex
MITF	microphthalmia transcription factor
MMP	matrix metalloproteinase
MMR	mismatch repair
MSA	muscle-specific actin
MSI	microsatellite instability
NADH	nicotinic adenine dinucleotide, reduced
nDNA	native [double-stranded] DNA
NEMO	nuclear factor (NF)-kappaB gene modulator
NF	neurofibromatosis
NF1	neurofibromatosis type I
NF2	neurofibromatosis type II
NFP	neurofilament protein
NIH	National Institutes of Health
NISH	non-isotopic in situ hybridization
NK	natural killer
NL	neutrophilic lipodystrophy
NRAMP1	natural resistance-associated macrophage protein 1
NSAIDs	non-steroidal anti-inflammatory drugs
NSE	neuron-specific enolase
OL EDA ID	osteopetrosis, lymphedema, anhidrotic ectodermal dysplasia, immunodeficiency [syndrome]
ORF	open reading frame
PAIN	periorbital intraepithelial neoplasia
p-ANCA	perinuclear cytoplasmic neutrophil antibodies
PAPA	pyogenic sterile arthritis, pyoderma gangrenosum and acne [syndrome]
PAS	periodic acid-Schiff
PBG	porphobilinogen
PCNA	proliferating cell nuclear antigen
PCR	polymerase chain reaction
PDGF(β)	platelet-derived growth factor β
PECAM	platelet endothelial cell adhesion molecule
PEGoma	pericardial epithelioid cell tumor
PGL	phenolic glycolipid
PGP	protein gene product
PGWG	poorly granulomatous
PI	protease inhibitor
PIBIDS	photosensitivity and IBIDS [see IBIDS above]
PILA	papillary intralymphatic angioendotheliomatosis
PLEVA	pityriasis lichenoides et varioliformis acuta
PNET	primitive neuroectodermal tumor
POEMS	polyneuropathy, organomegaly, endocrinopathy, M-protein and skin changes [syndrome]
PPD	purified protein derivative
PPDL	pure and primitive diffuse lymphoma
PPK	palmoplantar keratoderma
pRB	retinoblastoma protein
PSS	progressive systemic sclerosis
PTEN	phosphatase and tensin homolog
PUPPP	pruritic urticarial papules and plaques of pregnancy
PUVA	psoralen plus ultraviolet light of A [long wavelength
r-IL-2	recombinant interleukin 2
RBC	red blood cell
RDEB	recessive dystrophic epidermolysis bullosa
RDEB-HS	recessive dystrophic epidermolysis bullosa, Hallopeau–Siemens
RDEB-nHS	recessive dystrophic epidermolysis bullosa, non-Hallopeau–Siemens
RER	rough endoplasmic reticulum
RNP	ribonucleoprotein
RT-PCR	reverse transcriptase polymerase chain reaction

SA	syphilis, aleprosa
SAT	slowly adapting type I (mechanoreceptor)
SCLE	subacute cutaneous lupus erythematosus
scRNP	small cytoplasmic ribonucleic protein
SEA	staphylococcal enterotoxin A
SEB	staphylococcal enterotoxin B
Shh	Sonic Hedgehog
SIRDS	(sunscreens and IRDS (see IRDS above)
SIL	squamous intraepithelial lesion
SLE	systemic lupus erythematosus
SLL	small lymphocytic lymphoma
SMA	smooth muscle actin
snRNP	small nuclear ribonucleic protein
SPD	subcorneal pustular dermatosis
SPRRs	small proline rich proteins/cornifins
SPTL	subcutaneous panniculitis-like T-cell lymphoma
SRP	signal recognition particle
ssDNA	single stranded DNA
SSSS	staphylococcal scalded skin syndrome
STD	sexually transmitted disease
subcLD	subclavian dermis
TCR	T-cell receptor
TEN	toxic epidermal necrolysis
TFIIH	transcription/DNA repair factor IIH
TGF	transforming growth factor
thio-TEPA	triethylene thiophosphoramide
TIMP	tissue inhibitor of metalloproteinase
TNF	tumor necrosis factor
TORCH	toxoplasmosis, other infections, rubella, cytomegalovirus and herpes simplex [syndrome]
TRAPS	tumor necrosis factor receptor-associated periodic syndrome
TSST	toxic shock syndrome toxin
TT	tuberculoid leprosy
tTA	tetracycline transactivator [transcription factor]
TTF-1	thyroid transcription factor 1
tTG	tissue transglutaminase
TTP	thrombotic thrombocytopenic purpura
UPS	undifferentiated pleomorphic sarcoma
UPO	uroporphyrinogen
UPO-D	uroporphyrinogen decarboxylase
URR	upstream regulatory region
UV	ultraviolet
UVA	ultraviolet A
UVB	ultraviolet B
UVL	ultraviolet light
VCAM	vascular cell adhesion molecule
VEGF	vascular endothelial growth factor
VEGFR	vascular endothelial growth factor receptor
VIN	vulval intraepithelial neoplasia
VIP	vasoactive intestinal peptide
VLDL	very low density lipoprotein
VZV	varicella-zoster virus
wfh	wrinkle free [mouse model]
XP	xeroderma pigmentosum

See www.expertconsult.com for references and additional material

The structure and function of skin

John A. McGrath

CHAPTER 1

Introduction 1
Properties of skin 1
Normal epidermal histology 1
Regional variations in skin anatomy 2
Skin development 3
Keratinocyte biology 5
Epidermal stem cells 6
Skin barrier 8
Skin immunity 10
Melanocytes 11
Merkel cells 13
Intercellular junctions 15
Pilosebaceous units 16
Eccrine glands 18
Apocrine glands 21
Dermal–epidermal junction 22
Dermal collagen 26
Dermal elastic tissue 26
Ground substance 28
Fibroblast biology 29
Cutaneous blood vessels and lymphatics 29
Nervous system of the skin 32
Subcutaneous fat 33

Introduction

Skin is a double-layered membrane covering the exterior of the body and consists of a stratified cellular epidermis and an underlying dermis of connective tissue. In adults, the skin weighs over 5 kg and covers a surface area approaching 2 m^2. The epidermis is mainly composed of keratinocytes and is typically 0.05–0.1 mm in thickness. The dermis contains collagen, elastic tissue and ground substance and is of variable thickness, from 0.5 mm on the eyelid or scrotum to more than 5 mm on the back (*Fig. 1.1*).

The dermis is subdivided into a more superficial component (the papillary dermis) which is bounded inferiorly by the superficial vascular plexus and an underlying much thicker reticular dermis. Below the dermis is a layer of subcutaneous fat which is separated from the rest of the body by a vestigial layer of striated muscle.

Properties of skin

A key role of skin is to provide a mechanical barrier against the external environment. The cornified cell envelope and the stratum corneum restrict water loss from the skin while keratinocyte-derived endogenous antibiotics (defensins and cathelicidins) provide an innate immune defense against bacteria, viruses, and fungi. The epidermis also contains a network of about 2×10^9 Langerhans cells which serve as sentinel cells whose prime function is to survey the epidermal environment and to initiate immune responses against microbial threats. Melanin, which is mostly found in basal keratinocytes, provides some protection against DNA damage from ultraviolet radiation. An important function of skin is thermoregulation. Vasodilatation or vasoconstriction of the blood vessels in the deep or superficial plexuses helps regulate heat loss. Eccrine sweat glands are found at all skin sites and are present in densities of 100–600/cm^2; they play a role in heat control and aspects of metabolism. Secretions from apocrine sweat glands contribute to body odor. Skin lubrication and waterproofing is provided by sebum secreted from sebaceous glands. Subcutaneous fat has important roles in cushioning trauma as well as providing insulation and a calorie reserve. Fat also has an endocrine function and contributes to tissue remodeling and phagocytosis. Nails provide protection to the ends of the fingers and toes as well as being important in pinching and prising objects. Hair may have important social and psychological value. Skin also has a key function in synthesizing various metabolic products, such as vitamin D.

Normal epidermal histology

Although the basic structure is relatively constant at various skin sites, there are often clear differences which enable one to determine the site of origin. The epidermis consists of four clearly defined layers or strata:

- Basal cell layer (stratum basale)
- Prickle cell layer (stratum spinosum)
- Granular cell layer (stratum granulosum)
- Corneocyte layer (stratum corneum)

An eosinophilic acellular layer known as the stratum lucidum is sometimes seen in skin from the palms and soles (*Fig. 1.2*).

Basal cells are cuboidal or columnar with a large nucleus typically containing a conspicuous nucleolus. Small numbers of mitoses may be evident. Clear cells are also present in the basal layer of the epidermis; these represent melanocytes. Cells with clear cytoplasm seen in the stratum spinosum represent Langerhans cells. Very occasional Merkel cells may also be present but these are not easily identified in hematoxylin and eosin stained sections. Histologically, prickle cells are polygonal in outline, have abundant eosinophilic cytoplasm and oval vesicular nuclei, often with conspicuous nucleoli. Keratohyalin granules typify the granular cell layer (*Fig. 1.3*). The granular cells typically form three tightly packed layers, with individual cells adopting a tetrakaidecahedron shape. Skin integrity is maintained by a mobile layer of tight junctions that translocate from granular layer cell surface to base as individual keratinocytes transition to the uppermost granular cell layer. Thus the main impermeability plane in skin is between the first and second granular cell layers. Further maturation leads to loss of nuclei and flattening of the keratinocytes to form the plates of the corneocyte layer (stratum corneum). Adjacent cells are united at their free borders by intercellular bridges (prickles), which are most clearly identifiable in the prickle cell layer and in disease states of the skin where there is marked intercellular edema (spongiosis) (*Fig. 1.4*).

Toker cells represent an additional clear cell population, which may be found in nipple epidermis of both sexes in up to 10% of the population.[1] Toker cells are large, polygonal or oval and have abundant pale staining or clear cytoplasm with vesicular nuclei often containing prominent, albeit small, nucleoli. The cytoplasm is mucicarmine and Periodic acid-Schiff negative.[1] The cells may be distributed singly but more often they are found as small clusters, not uncommonly forming single layered ductules.[1] They are located along the basal layer of the epidermis or suprabasally and are also sometimes seen within the epithelium of the terminal lactiferous duct.

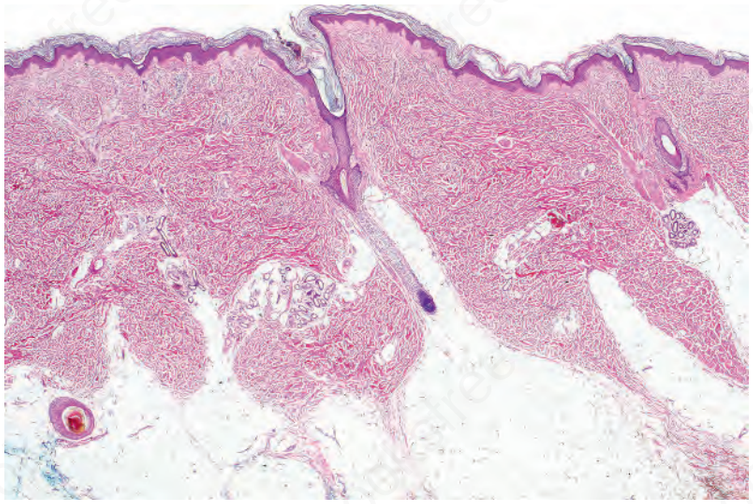

Fig. 1.1
Skin from forearm: there is a fairly thin epidermis. Compare the thickness of the dermis with that from the back (see *Fig. 1.5*).

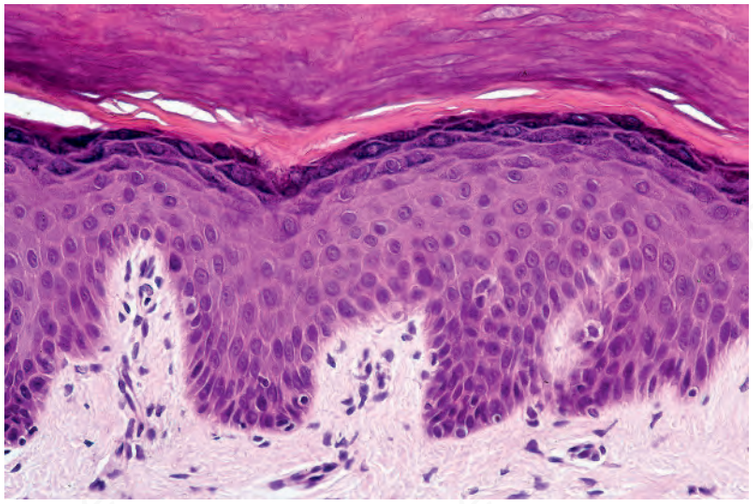

Fig. 1.2
Skin from palm: note the eosinophilic stratum lucidum clearly separating the granular cell layer from the overlying stratum corneum.

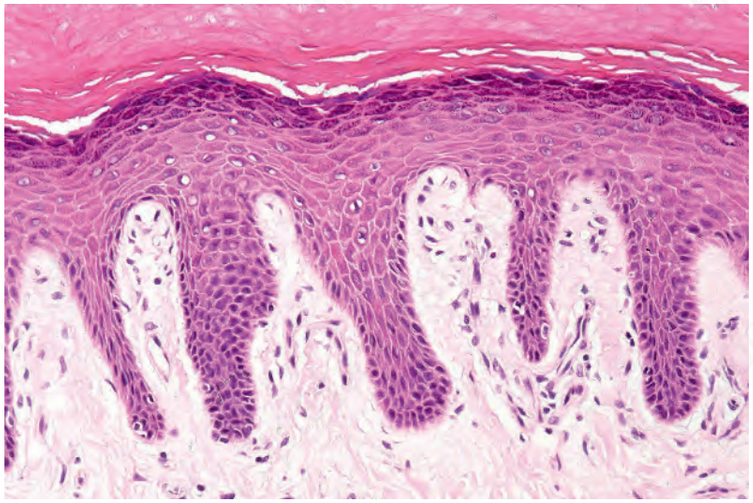

Fig. 1.3
Skin from palm: there is a conspicuous granular cell layer.

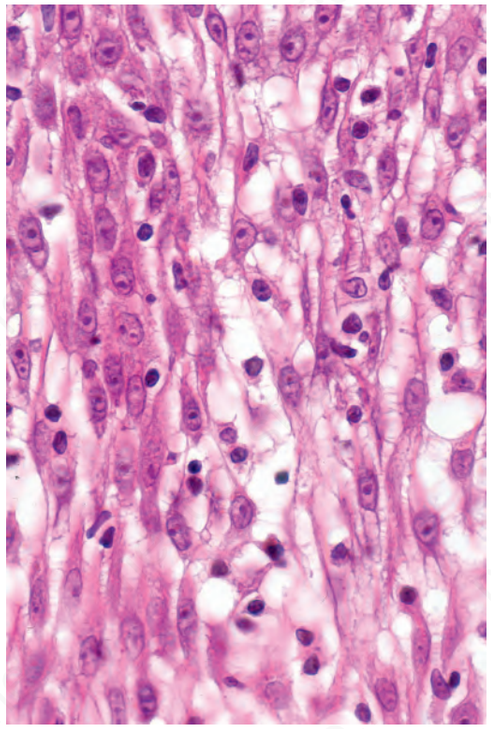

Fig. 1.4
Spongiosis: the intercellular bridges (prickles) are stretched and more visible in this biopsy from a patient with acute eczema.

Toker cells are of particular importance as they may be mistaken by the unwary as Paget cells. They are thought to be the source of mammary Paget disease in those exceptional cases where an underlying ductal carcinoma is absent.[2] Toker cells express CK7, AE1/AE3, CAM 5.2, epithelial membrane antigen (EMA), cerbB2, estrogen, and progesterone receptors.[3,4] They do not express p53 or CD138. Carcinoembryonic antigen (CEA) may also be present, albeit weakly.[4] Paget cells by way of contrast are often negative for estrogen and progesterone receptors and are p53 and CD138 positive.[4]

Regional variations in skin anatomy

There are two main kinds of human skin: glabrous skin (nonhairy skin) and hair-bearing skin. Glabrous skin is found on the palms and soles. It has a grooved surface with alternating ridges and sulci giving rise to the dermatoglyphics (fingerprints). Glabrous skin has a compact, thick stratum corneum, and contains encapsulated sense organs within the dermis but no hair follicles or sebaceous glands. In contrast, hair-bearing skin has both hair follicles and sebaceous glands but lacks encapsulated sense organs. Hair follicle size, structure and density can vary between different body sites. For example, the scalp has large hair follicles that extend into subcutaneous fat whereas the forehead has only small vellus hair-producing follicles although sebaceous glands are large. The number of hair follicles does not alter until middle life but there is a changing balance between vellus and terminal hairs throughout life. In hair-bearing sites, such as the axilla, there are apocrine glands in addition to the eccrine sweat glands. Sebaceous glands are active in the newborn, and from puberty onwards, and the relative activity modifies the composition of the skin surface lipids. The structure of the dermal–epidermal junction also shows regional variations in the number of hemidesmosomal-anchoring filament complexes (more in the leg than the arm). In the dermis, the arrangement and size of elastic fibers varies from very large fibers in perianal skin to almost no fibers in the scrotum. Marked variation in the cutaneous blood supply is found between areas of distensible skin such as the eyelid and more rigid areas such as the fingertips.

Regional variation in skin structure is illustrated in *Figs 1.5–1.20*.

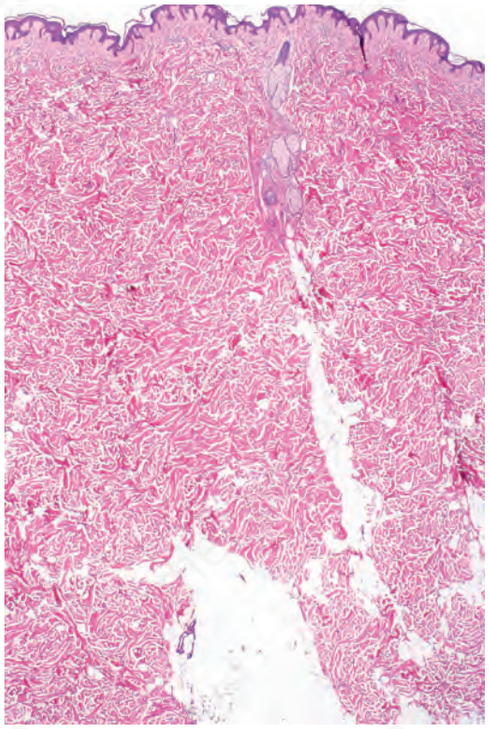

Fig. 1.5
Skin from the lower back: at this site the dermis is very thick and is characterized by broad parallel fascicles of collagen.

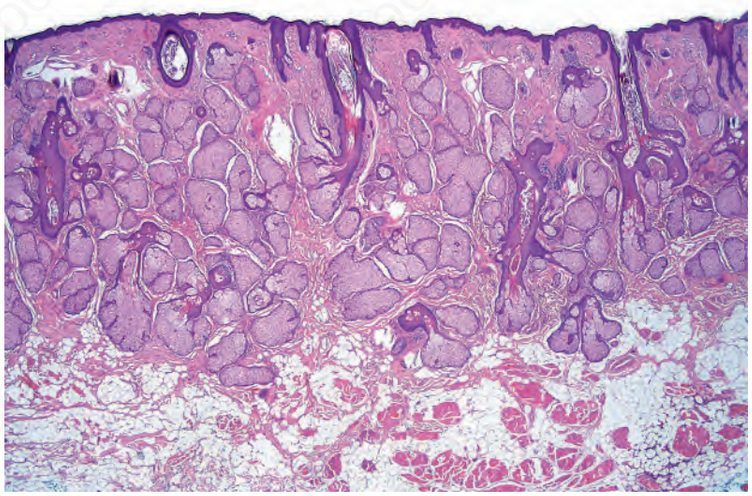

Fig. 1.6
Skin of the nose: there are conspicuous sebaceous glands: at this site, they often drain directly onto the skin surface. These appearances should not be confused with that of sebaceous hyperplasia.

Skin development

Two major embryological elements juxtapose to form skin. These comprise the prospective epidermis that originates from a surface area of the early gastrula, and the prospective mesoderm that comes into contact with the inner surface of the epidermis during gastrulation. The mesoderm generates the dermis and is involved in the differentiation of epidermal structures such as hair follicles.[1] Melanocytes are derived from the neural crest. After gastrulation, there is a single layer of neuroectoderm on the embryo surface: this layer will go on to form the nervous system or the skin epithelium, depending on the molecular signals (e.g., fibroblast growth factors or bone morphogenic proteins) it receives.[2] The embryonic epidermis consists of a

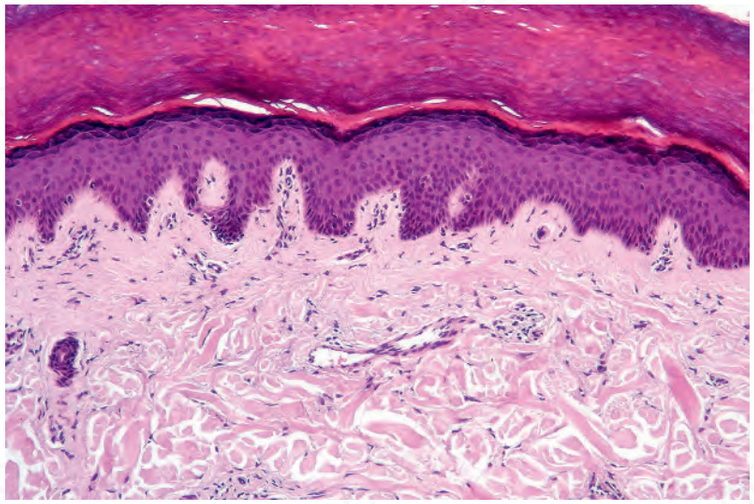

Fig. 1.7
Skin from the sole of the foot: this is typified by a thickened stratum corneum and prominent epidermal ridge pattern. The dermis is relatively dense at this site. Similar features are seen on the palms and ventral aspects of the fingers and toes.

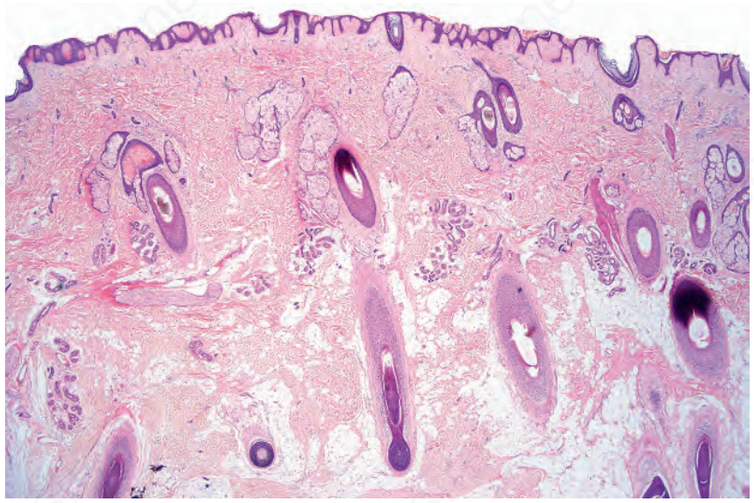

Fig. 1.8
Skin from the scalp: there are numerous terminal hair follicles with many of the bulbs in the subcutaneous fat.

single layer of multipotent epithelial cells which is covered by a special layer known as periderm that is unique to mammals. Periderm provides some protection to the newly forming skin as well as exchange of material with the amniotic fluid. During pregnancy, periderm is present until 24 weeks' gestation whereupon it is shed into the amniotic fluid. One key transcription factor in generating both an embryonic epidermal monolayer as well as a differentiated epidermis is p63.[3] Developmental signals induced by p63 occur before any keratin is generated. The embryonic dermis is at first very cellular and at 6–14 weeks three types of cell are present: stellate cells, phagocytic macrophages and granule-secretory cells, either melanoblasts or mast cells (*Fig. 1.21*). From weeks 14 to 21, fibroblasts are numerous and active, and perineural cells, pericytes, melanoblasts, Merkel cells and mast cells can be individually identified. Hair follicles and nails are evident at 9 weeks. Sweat glands are also noted at 9 weeks on the palms and the soles.[4] Sweat glands at other sites and sebaceous glands appear at 15 weeks. Touch pads become recognizable on the fingers and toes by the sixth week and development is maximal by the 15th week. The earliest development of hair occurs at about 9 weeks in the regions of the eyebrow, upper lip and chin. Sebaceous glands first appear as hemispherical protuberances on the posterior surfaces

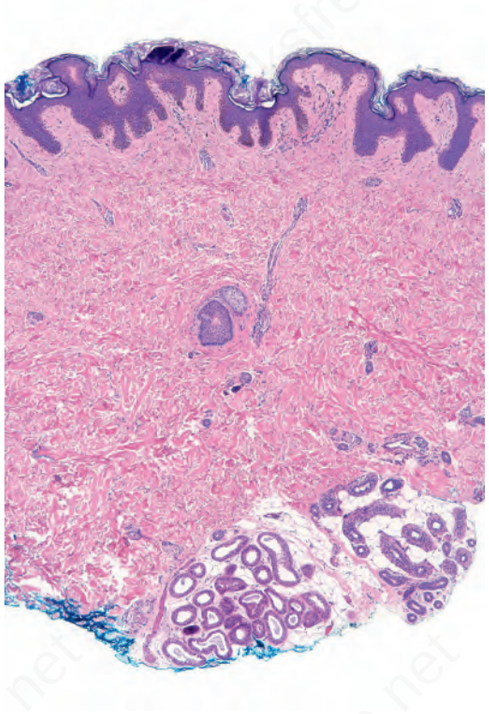

Fig. 1.9
Skin from axilla: apocrine glands as seen at the bottom of the field are typical for this site.

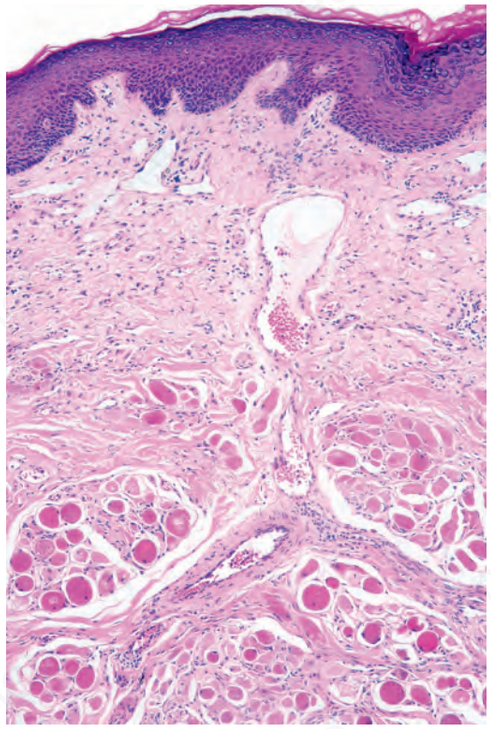

Fig. 1.11
Skin from the outer aspect of the lip: note the keratinizing stratified squamous epithelium and skeletal muscle fibers.

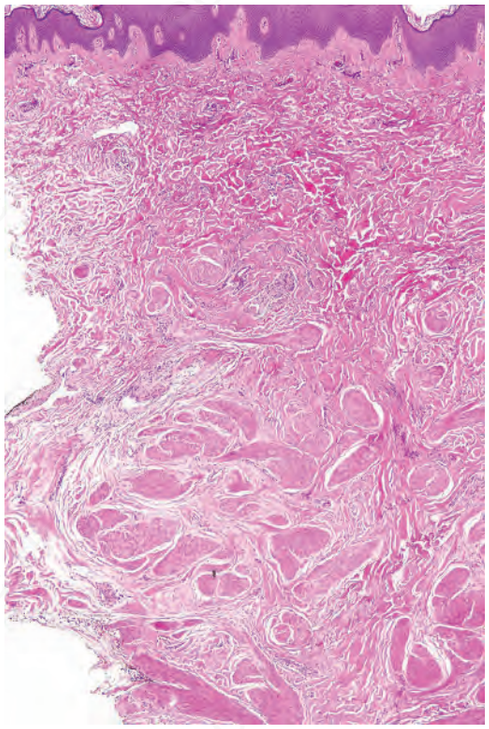

Fig. 1.10
Skin of areola: there are abundant smooth muscle fibers: lactiferous ducts may also sometimes be present (not shown).

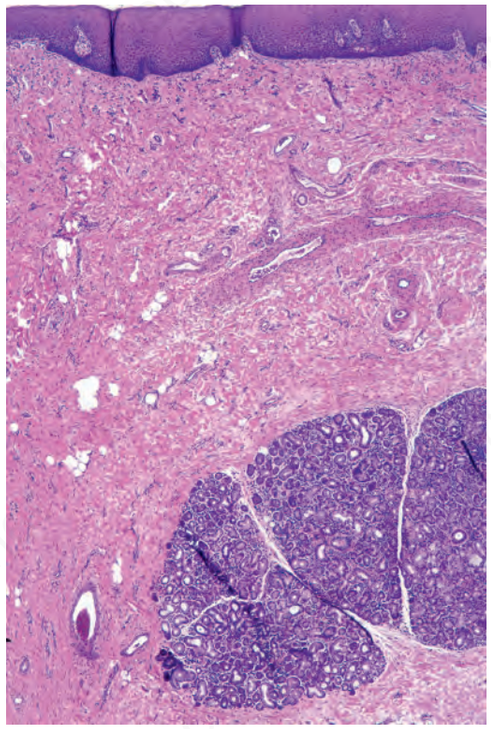

Fig. 1.12
Mucosal aspect of lip: at this site the squamous epithelium does not normally keratinize. Minor salivary glands as shown in this field are not uncommonly present.

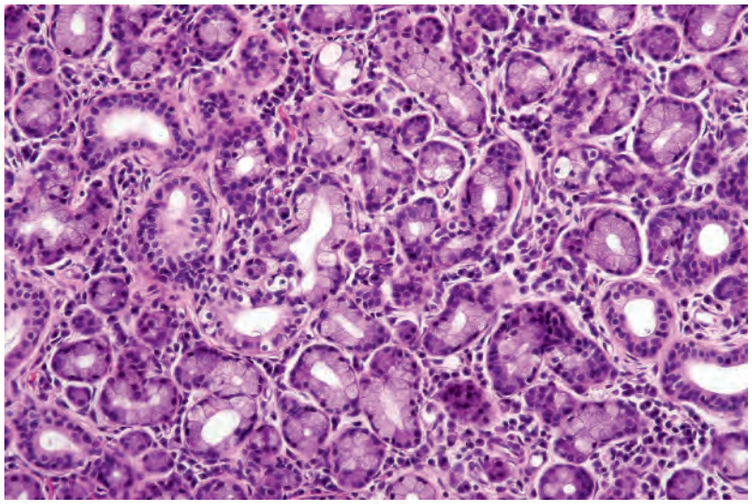

Fig. 1.13
Mucosal aspect of lip: close-up view of the salivary gland shown in *Fig. 1.12*.

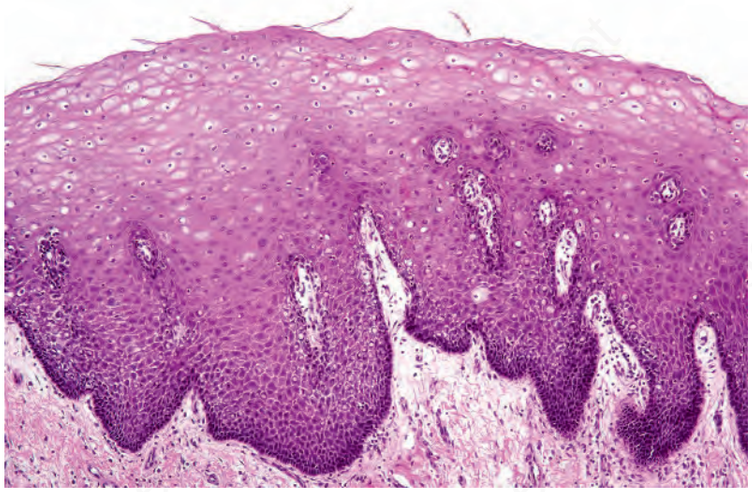

Fig. 1.14
Mucosal aspect of lip: the cytoplasm of the keratinocytes is often rich in glycogen.

of the hair pegs and become differentiated at 13–15 weeks. Langerhans cells are derived from the monocyte–macrophage–histiocyte lineage and enter the epidermis at about 12 weeks. Merkel cells appear in the glabrous skin of the fingertips, lip, gingiva and nail bed, and in several other regions, around 16 weeks. Although some cells of the dermis may migrate from the dermatome (venterolateral part of the somite) and take part in the formation of the skin, most of the dermis is formed by mesenchymal cells that migrate from other mesodermal areas.[5] These mesenchymal cells give rise to the whole range of blood and connective tissue cells, including the fibroblasts and mast cells of the dermis and the fat cells of the subcutis. In the second month, the dermis and subcutis are not discernible as distinct skin layers but collagen fibers are evident in the dermis by the end of the third month. Later, the papillary and reticular layers become established and, at the fifth month, the connective tissue sheaths are formed around the hair follicles. Elastic fibers are first detectable at 22 weeks.

Keratinocyte biology

The cytoskeleton of all mammalian cells, including epidermal keratinocytes, comprises actin containing microfilaments ≈7 nm in diameter, tubulin containing microtubules 20–25 nm in diameter, and filaments of intermediate

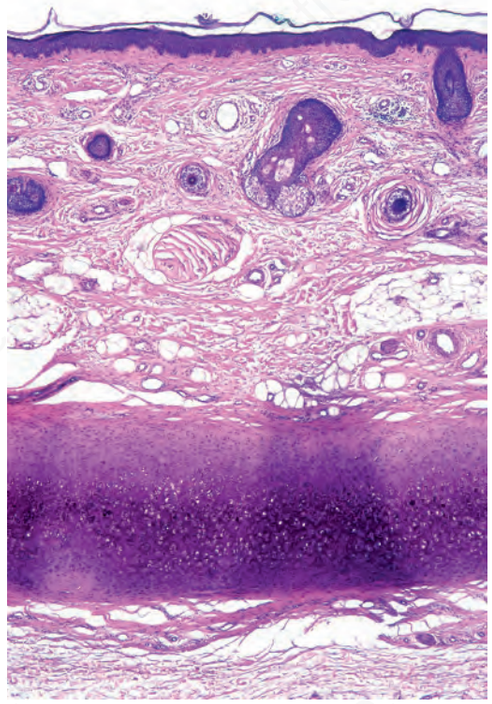

Fig. 1.15
Skin from the ear: note the vellus hairs, and a fairly thin dermis overlying the auricular cartilage.

size, 7–10 nm in diameter, known as intermediate filaments. There are six types of intermediate filaments of which keratins are the filaments in keratinocytes (*Figs 1.22*, *1.23*). The human genome possesses 54 functional keratin genes located in two compact gene clusters, as well as many nonfunctional pseudogenes, scattered across the genome.[1] Keratin genes are very specific in their expression patterns. Each one of the many highly specialized epithelial tissues has its own profile of keratins. Hair and nails express modified keratins containing large amounts of cysteine which forms numerous chemical cross-links to further strengthen the cytoskeleton. The genes encoding the keratins fall into two gene families: type I (basic) and type II (acidic) and there is coexpression of particular acidic–basic pairs in a cell- and tissue-specific manner. Keratin heterodimers are assembled into protofibrils and protofilaments by an antiparallel stagger of some complexity. Simple epithelia are characterized by the keratin pair K8/K18, and the stratified squamous epithelia by K5/K14. Suprabasally, keratins K1/K10 are characteristic of epidermal differentiation (*Fig. 1.24*). K15 is expressed in some interfollicular basal keratinocytes as well as keratinocytes within the hair-follicle bulge region at the site of a population of multipotent stem cells. K9 and K2 expression is site restricted in skin: K9 to palmoplantar epidermis and K2 to superficial interfollicular epidermis.

Apart from their structural properties, keratins may also have direct roles in cell signaling, stress responses and apoptosis.[2] In epidermal hyperproliferation, as in wound healing and psoriasis, expression of suprabasal keratins K6/K16/K17 is rapidly induced.

Currently, 21 of the 54 known keratin genes have been linked to monogenic genetic disorders, and some have been implicated in more complex traits, such as idiopathic liver disease or inflammatory bowel disease.[3,4] The intermediate filament database has now recorded over 40 diseases and more than 400 mutations involving keratins (www.interfil.org). The first genetic disorder of keratin to be described was epidermolysis bullosa simplex, which involves mutations in the genes encoding K5 or K14 (*Fig. 1.25*). About half of the keratin genes are expressed in the hair follicle, and mutations in these genes may underlie cases of monilethrix as well as hair and nail ectodermal dysplasias.[5]

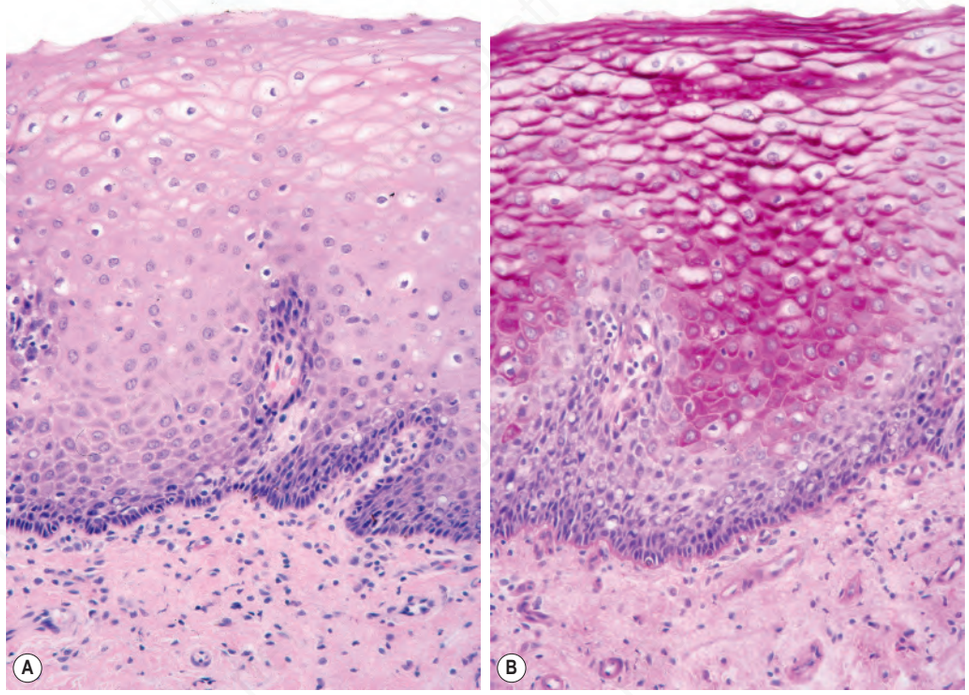

Fig. 1.16
(**A**, **B**) Vulval vestibule: at this site the stratum corneum is absent and there is no granular cell layer. The suprabasal keratinocytes have clear cytoplasm due to abundant glycogen and revealed by the periodic acid-Schiff reaction.

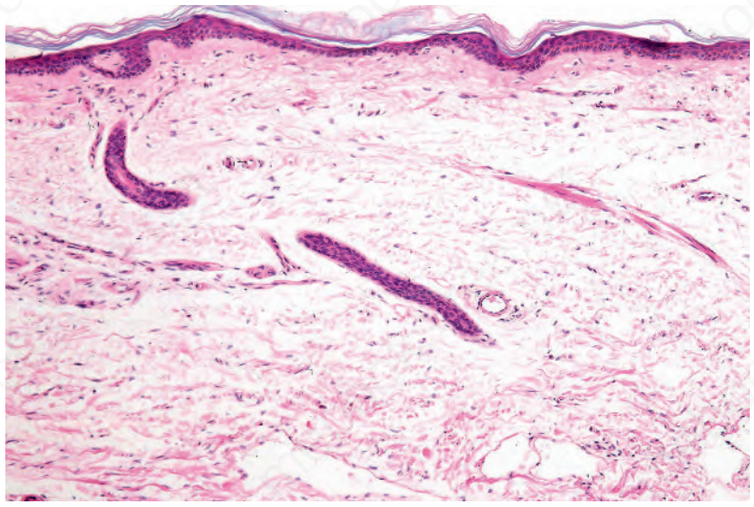

Fig. 1.17
Variation of skin: sample of skin from the forearm of a 92-year-old female. Note the epidermal thinning and dermal atrophy.

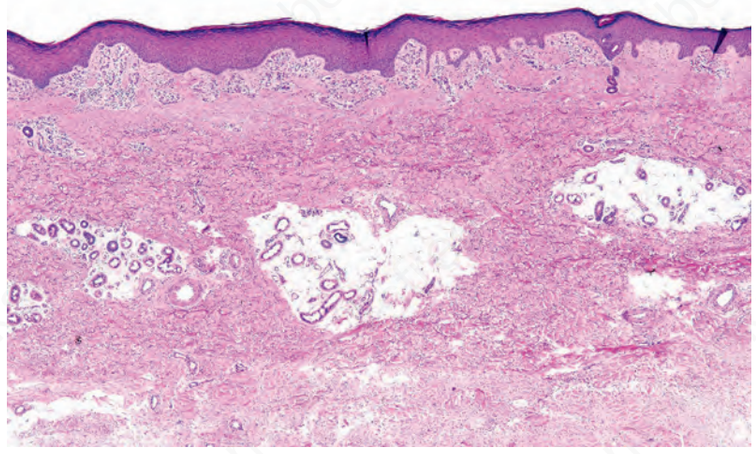

Fig. 1.18
Stasis change: skin from the lower leg. Although abnormal, the presence of stasis change characterized in this example by papillary dermal lobular capillary proliferation is a very common feature at this site.

Epidermal stem cells

To maintain, repair and regenerate itself, the skin contains stem cells which reside in the bulge area of hair follicles, the basal layer of interfollicular epidermis and the base of sebaceous glands (*Fig. 1.26*).[1] Stem cells are able to self-renew as well as give rise to differentiating cells.[2] It is not clear, however, whether every basal keratinocyte or only a proportion of cells is a stem cell.[3] Two possible hypotheses have emerged. One theory divides basal keratinocytes into epidermal proliferation units, which comprise one self-renewing stem cell and about 10 tightly packed transient amplifying cells, each of which is capable of dividing several times and then exiting the basal layer to undergo terminal differentiation.[4] This unit gives rise to a column of larger and flatter cells that culminates in a single hexagonal surface. The process of division of basal cells in this model is viewed as a symmetric process in which equal daughter cells are generated with the basal cells progressively reducing their adhesiveness to the underlying epidermal basement membrane, delaminating and committing to terminal differentiation. The alternative theory is that some basal cells (perhaps up to 70% of cells in murine studies) can undergo asymmetric cell division, shifting their spindle orientation from lateral to perpendicular.[5] Asymmetric cell divisions provide a means of maintaining one proliferative daughter while the other daughter cell is committed to terminal differentiation. Asymmetric cell divisions, therefore, can bypass the need for transient amplifying cells.

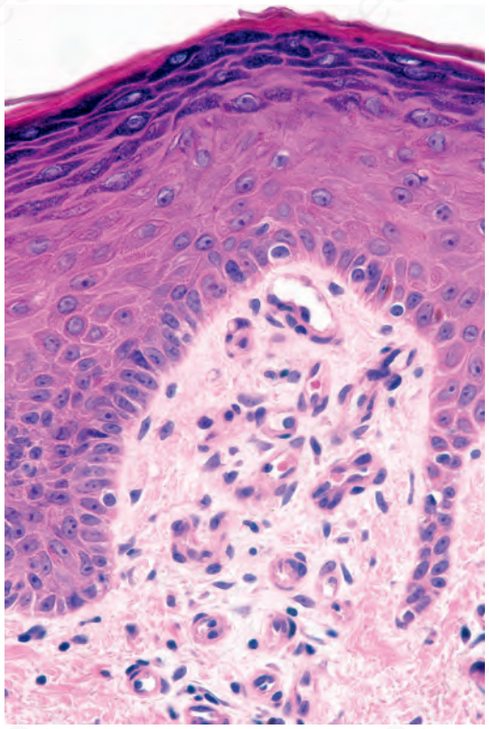

Fig. 1.19
Stasis change: high-power view.

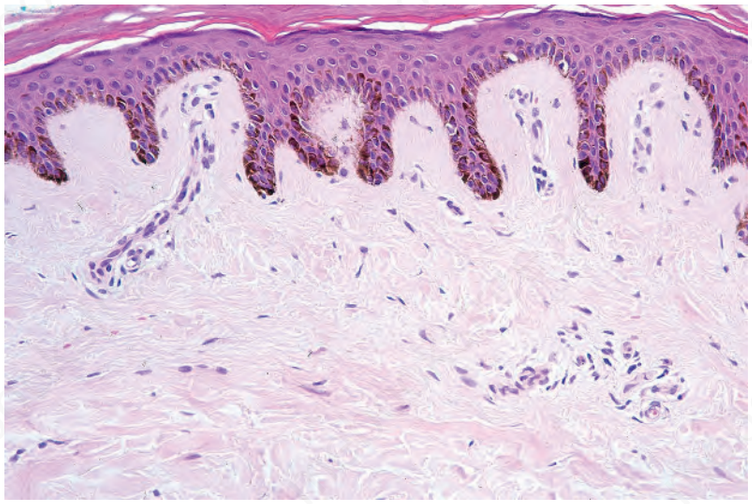

Fig. 1.20
Variation of normal skin: in dark-skinned races, the presence of intense basal cell melanin pigmentation is a normal histologic finding.

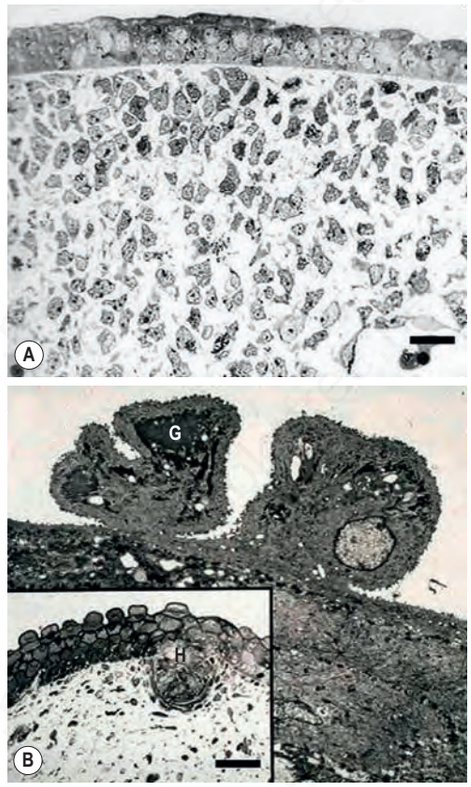

Fig. 1.21
(**A**, **B**) Development of normal human fetal skin: (**A**) at 7 weeks' gestation, the epidermis is only two cell layers thick but the dermis appears very cellular; (**B**) at 19 weeks' gestation the skin has an outer layer specific to mammals known as periderm. This contains surface blebs which are full of glycogen (*G*). Also present is a hair peg (*H*). This downgrowth of the epidermis is the first histologic step in generating a hair follicle. Bar = 25 μm.

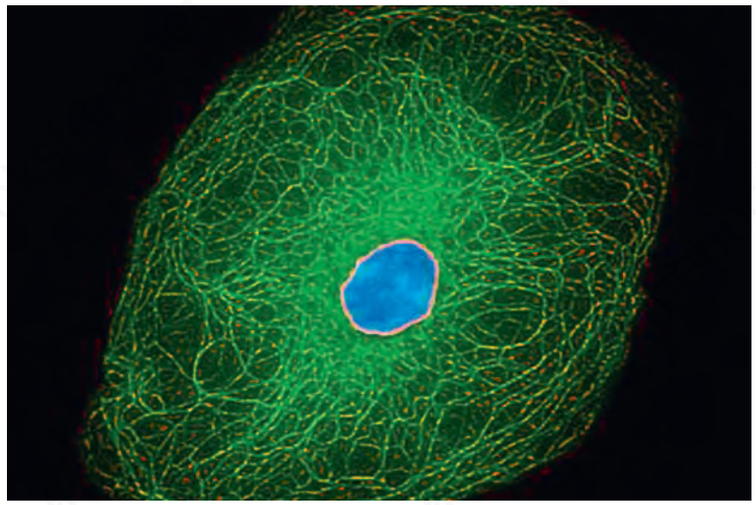

Fig. 1.22
Cytoskeleton of a keratinocyte: the major intermediate filament of a keratinocyte is keratin, highlighted in green.

Hair follicle stem cells are found in the bulge regions below the sebaceous glands (*Fig. 1.27*). The bulge area stem cells generate cells of the outer root sheath (ORS), which drive the highly proliferative matrix cells next to the mesenchymal papillae. After proliferating, matrix cells differentiate to form the hair channel, the inner root sheath (IRS) and the hair shaft. Hair follicle stem cells can also differentiate into sebocytes and interfollicular epidermis. Despite this multipotency, however, the follicle stem cells only function in pilosebaceous unit homeostasis and do not contribute to interfollicular epidermis unless the skin is wounded.[6]

Apart from stem cells in the hair follicles, sebaceous glands and interfollicular epidermis, other cells in the dermis and subcutis may have stem cells properties. These include cells that have been termed skin-derived precursors (SKPs), which can differentiate into both neural and mesodermal progeny.[7] In addition, a subset of dermal fibroblasts can have adipogenic, osteogenic, chondrogenic, neurogenic and hepatogenic differentiation potential.[8] Skin wounding can also induce mobilization and recruitment of inflammatory and noninflammatory cells (including epithelial progenitors) from bone marrow.[9]

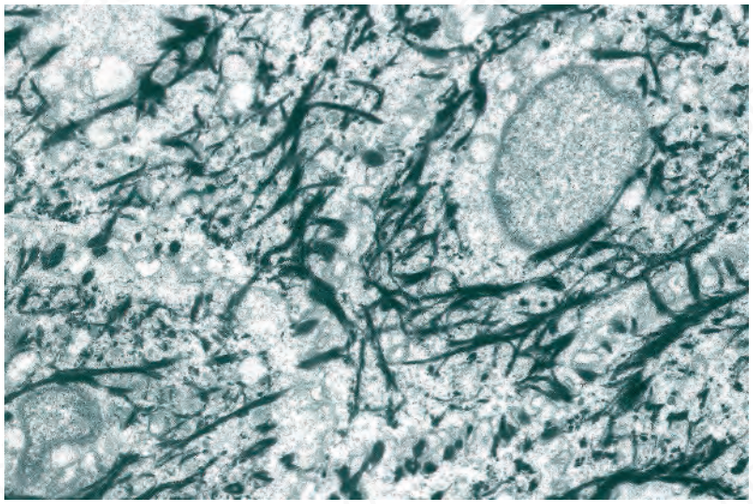

Fig. 1.23
Mid-prickle cell layer of normal epidermis: the abundant keratin filaments (tonofibrils) form a distinct interlacing lattice within the cytoplasm of keratinocytes.

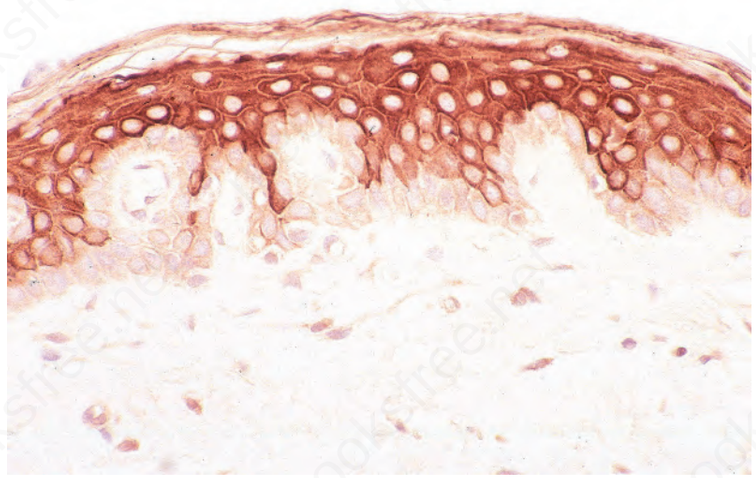

Fig. 1.24
Normal skin: suprabasal keratinocytes preferentially express keratins 1 and 10 as shown in this picture. Anti-Keratin1 antibody courtesy of I.M. Leigh, MD, Royal London Hospital Trust, London, UK.

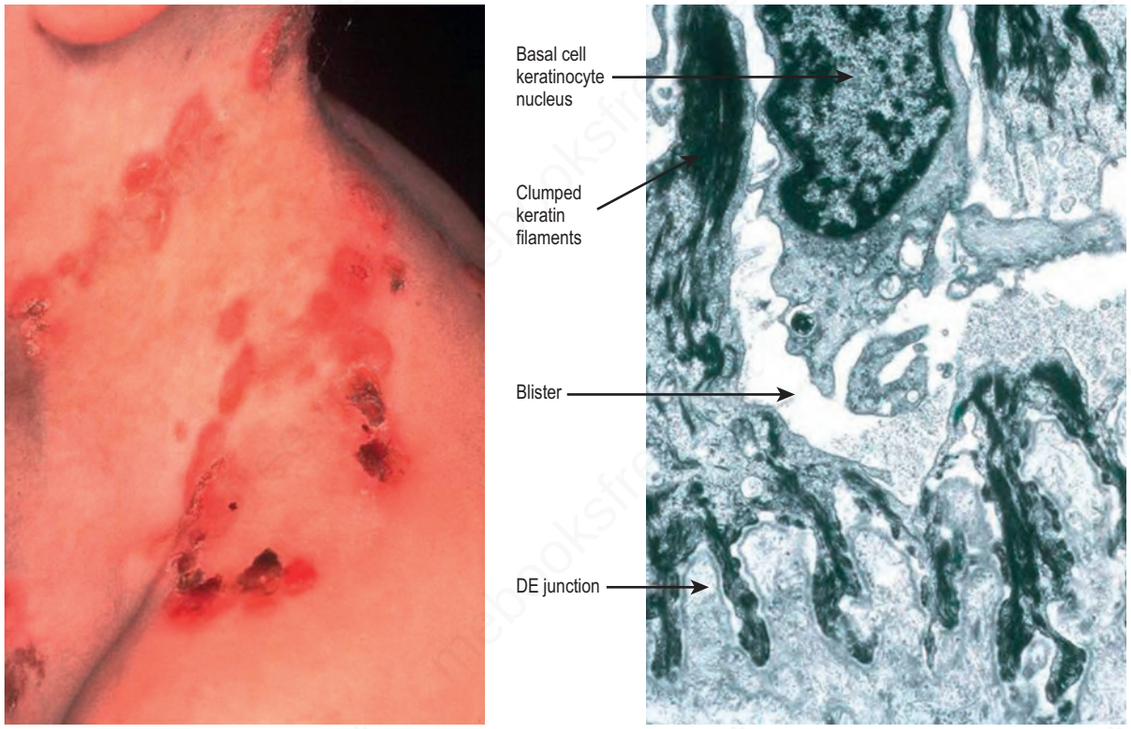

Fig. 1.25
Clinicopathologic consequences of mutations in the keratin 14 gene: (*left*) typical appearances of generalized severe epidermolysis bullosa simplex which usually results from heterozygous missense mutations in *KRT14* or *KRT5*; (*right*) ultrastructurally, there is keratin filament disruption and clumping as well as a plane of blistering just above the dermal–epidermal (DE) junction.

Skin barrier

A major function of the epidermis is to form a barrier against the external environment. To achieve this, terminal differentiation of keratinocytes results in formation of the cornified cell envelope. This physical barrier is rendered highly insoluble by the formation of glutamyl-lysyl isodipeptide bonds between envelope proteins, catalyzed by transglutaminases.[1] Several different proteins contribute to construction of the cornified cell envelope, including involucrin, and the family of small proline-rich proteins (SPR1), including cornifin or SPR1 and pancornulins. Other envelope proteins include skin-derived anti-leucoproteases (SKALP)/elafin and keratolinin/cystatin. Some precursors of the cornified envelope are delivered by granules: small, smooth, sulfur-rich L granules contain the cysteine-rich protein loricrin, and accumulate in the stratum granulosum.[2] Loricrin is the major component of the cornified envelope. Profilaggrin in F granules may make a minor contribution to the envelope. Membrane-associated proteins that contribute to the cornified envelope include the plakin family members, periplakin, envoplakin, epiplakin, desmoplakin as well as plectin. Formation of the cornified cell envelope is triggered by a rise in intracellular calcium levels.[3] This leads to cross-link formation between plakins and involucrin catalyzed by

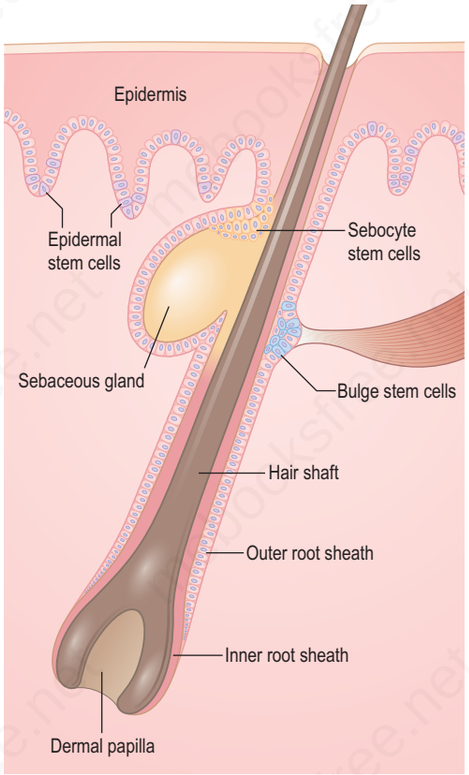

Fig. 1.26
Diagrammatic representation of the location of stem cells in human skin: stem cells are located within the bulge area of hair follicles (where the arrector pili muscle attaches) as well as in the basal keratinocyte layer in the interfollicular epidermis and at the base of sebaceous glands. Stem cells from the bulge area are capable of regenerating all parts of the pilosebaceous unit and interfollicular skin.

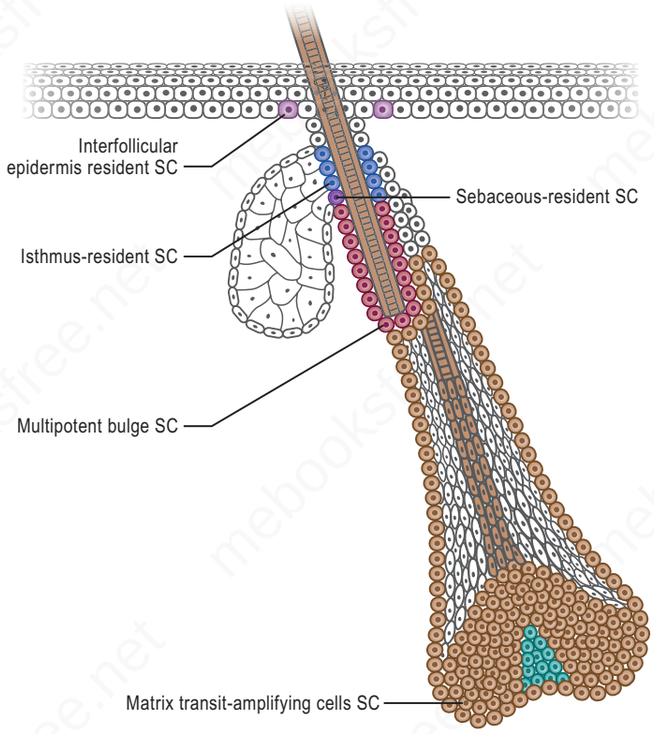

Fig. 1.27
Epidermis contains multiple resident stem cell (SC) compartments and transit-amplifying progeny. Within the bulge area of hair follicles, stem cells are multipotent, residing in the permanent portion of the hair follicle. Interfollicular stem cells reside in the basal layer of the epidermis. Resident progenitors of the hair follicle isthmus and sebaceous gland are located within the hair ORS that is above the bulge and below the sebaceous gland.

transglutaminases. Other desmosomal proteins are then also cross-linked, forming a scaffold along the entire inner surface of the plasma membrane. Ceramides from the secreted contents of lamellar bodies are then esterified onto glutamine residues of the scaffold proteins. The cornified cell envelope is reinforced by the addition of a variable amount of SPRs, repetin, trichohyalin, cystostatin α, elafin and LEP/XP-5 (skin-specific protein). Although most desmosomal components are degraded, keratin intermediate filaments (mostly K1, K10 and K2) may be cross-linked to desmoplakin and envoplakin remnants.

In the upper stratum spinosum and stratum granulosum lipid is synthesized and packaged into lamellated membrane-bound organelles known as membrane-coating granules, lamellar granules or Odland bodies (*Fig. 1.28*).[4] They are found adjacent to the cell membrane with alternating thick and thin dense lines separated by lighter lamellae of equal width, consistent with packing of flattened discs within a membrane boundary. These granules contain phospholipids, glycolipids and free sterols and move towards the plasma membrane as the cells move through the granular layer where they cluster at the cell membrane. They fuse with the plasma membrane, dispersing their contents into the intercellular space. Polar lipids from the lamellar granules are remodeled into neutral lipids in the intercellular space between corneocytes, thereby contributing to the barrier.

Within the granular layer of the epidermis, the main keratinocyte proteins are keratin and filaggrin, which together contribute approximately 80–90% of the mass of the epidermis and are ultrastructurally represented by the keratohyalin granules (*Fig. 1.29*). Filaggrin is initially synthesized as profilaggrin, a ≈500-kDa highly phosphorylated, histidine-rich polypeptide. During the post-translational processing of profilaggrin, the individual filaggrin polypeptides, each ≈35 kD, are proteolytically released. These are then dephosphorylated, a process that assists keratin filament aggregation and explains the origin of the name 'filaggrin' (filament aggregating protein) (*Fig. 1.30*). Typically, there are 10 highly homologous filaggrin units, although the number of filaggrin repeat units is variable and genetically determined, with duplications of filaggrin repeat units 8 and/or 10 in some individuals. Fewer filaggrin repeats leads to dryer skin. Loss-of-function mutations in filaggrin are very common, occurring in up to 10% of the European population. These mutations lead to reduced or absent keratohyalin granules, and are the cause of ichthyosis vulgaris as well as constituting a major risk factor for atopic dermatitis (*Fig. 1.31*).[5]

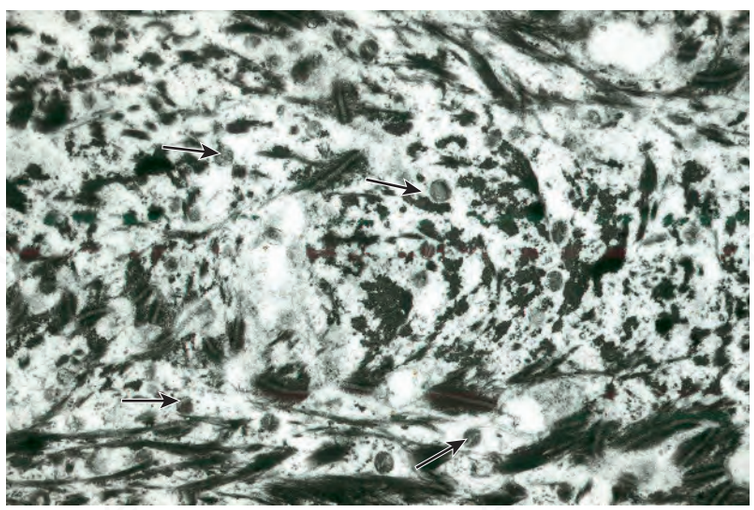

Fig. 1.28
Granular cell layer: note the keratohyalin and membrane coating granules (*arrowed*).

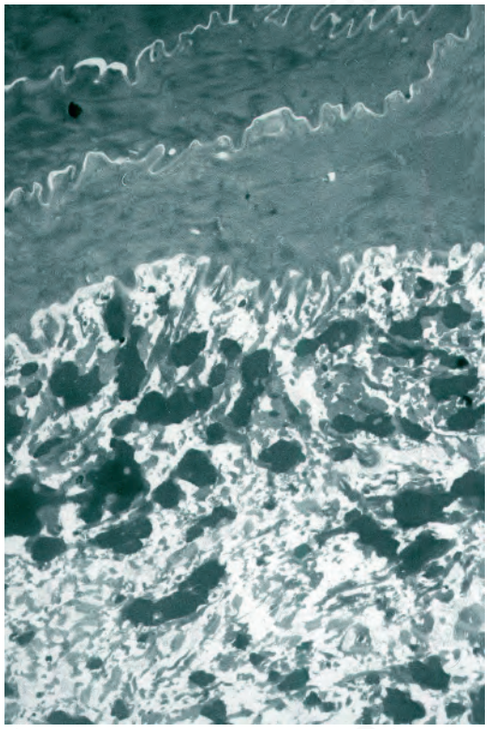

Fig. 1.29
Stratum corneum: keratohyalin granules are present just beneath the keratin lamellae.

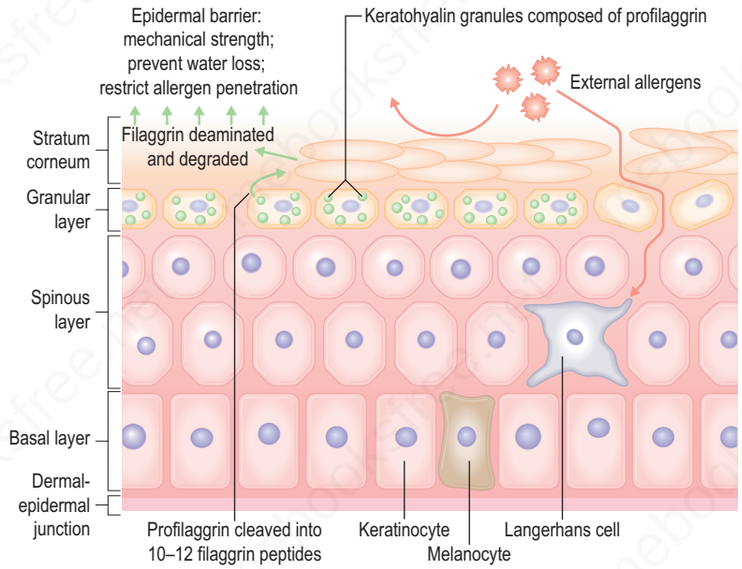

Fig. 1.30
Function of filaggrin in human skin: this is the major component of keratohyalin granules. In the granular layer profilaggrin is cleaved into filaggrin peptides subsequent deamination and degradation provides the skin with mechanical strength and restricts transepidermal water loss. Filaggrin also prevents allergen penetration. In the absence of filaggrin, for example caused by common mutations in the filaggrin gene, external allergens may penetrate the epidermis and encounter Langerhans cells. This may lead to the development of atopic dermatitis as well as other atopic manifestations and systemic allergies.

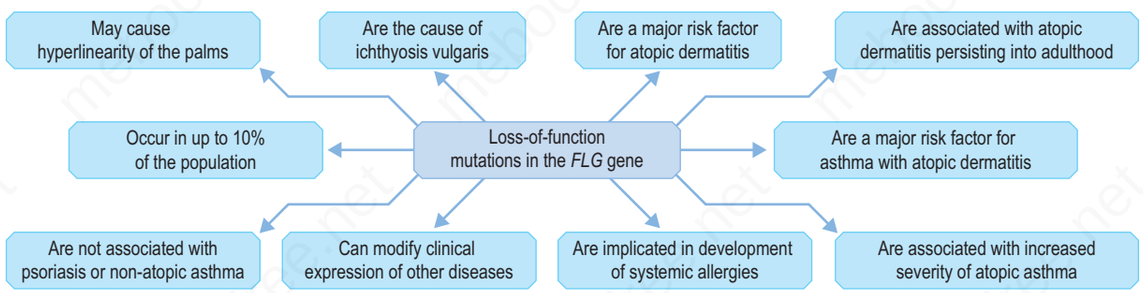

Fig. 1.31
Functional consequences of loss-of-function mutations in the filaggrin gene, which can affect up to 10% of the people in some populations.

Within the stratum corneum, the main intercellular adhesive structures are the corneodesmosomes. These complexes become modified from desmosomes at the most superficial layer of the stratum granulosum, the main difference being the presence of corneodesmosin in the extracellular portion. Corneodesmosomes are structurally different from desmosomes in that they are homogeneously electron-dense and their attachment plaques are integrated into the cornified cell envelopes. When the extracellular regions of corneodesmosomes are fully degraded, desquamation occurs. The degradation process of corneodesmosomes is carefully controlled by a number of proteases and their inhibitors. The most important proteases are the kallikrein-related peptidases, which are physiologically regulated by the lympho-epithelial Kazal-type related inhibitor. Other proteolytic regulators include matriptase, meprin and mesotrypsin. Mutations in some of these proteases or their inhibitors underlie different forms of ichthyosis, often with skin barrier impairment as well as hypotrichosis.[6]

Skin immunity

Skin possesses both innate and adaptive immune responses to defend against microbial pathogens and thereby prevent infection. Nevertheless, skin also encourages colonization by certain microorganisms to promote a cutaneous ecosystem known as the microbiome. This skin microbial community, which varies considerably with body region, interacts with host immunity to create homeostasis, with dysbiosis contributing to the pathogenesis of some skin diseases, including atopic dermatitis and rosacea.[1] One of the primary immune responses of skin is the synthesis, expression and release of antimicrobial peptides (*Fig. 1.32*).[2] There are dozens, possibly hundreds, of antimicrobial peptides in the skin, including cathelicidins, β-defensins, substance P, regulated on activation, normal T cell expressed and secreted (RANTES), Ribonuclease (RNase) 2, 3, and 7, and S100 calcium-binding protein A7 (S100A7). Many of these peptides have antimicrobial action against bacteria, viruses, and fungi. In the stratum corneum there is an effective chemical barrier maintained by the expression of S100A7 (psoriasin).[3] This antimicrobial substance is very effective at killing *Escherichia coli*. Subjacent to this in the skin there is another class of antimicrobial peptides, such as RNASE7, which is effective against a broad spectrum of microorganisms, especially enterococci.[4] Below this in the living layers of the skin are other antimicrobial peptides including the β-defensins.[5] The antimicrobial activity of most peptides occurs as a result of unique structural characteristics that enable them to disrupt the microbial cell membrane while leaving human cell membranes intact. The antimicrobial peptides can have immunostimulatory and immunomodulatory capacities as well as being chemotactic for

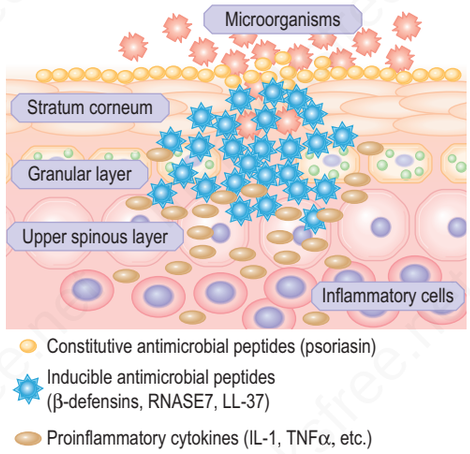

Fig. 1.32
Innate immunity in the skin: the physical barrier is complemented by an innate immune response that targets bacteria, viruses and fungi and prevents them from invading the skin. These peptides include constitutive and inducible substances against a broad range of organisms.

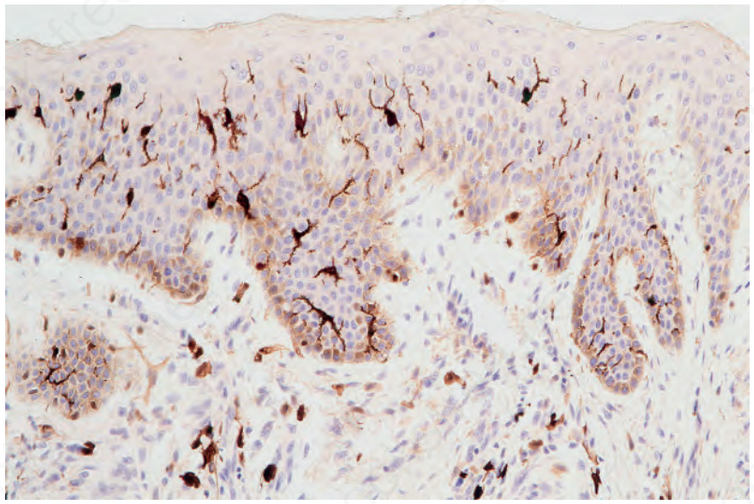

Fig. 1.33
Langerhans cells express S100 protein: note the conspicuous dendritic processes.

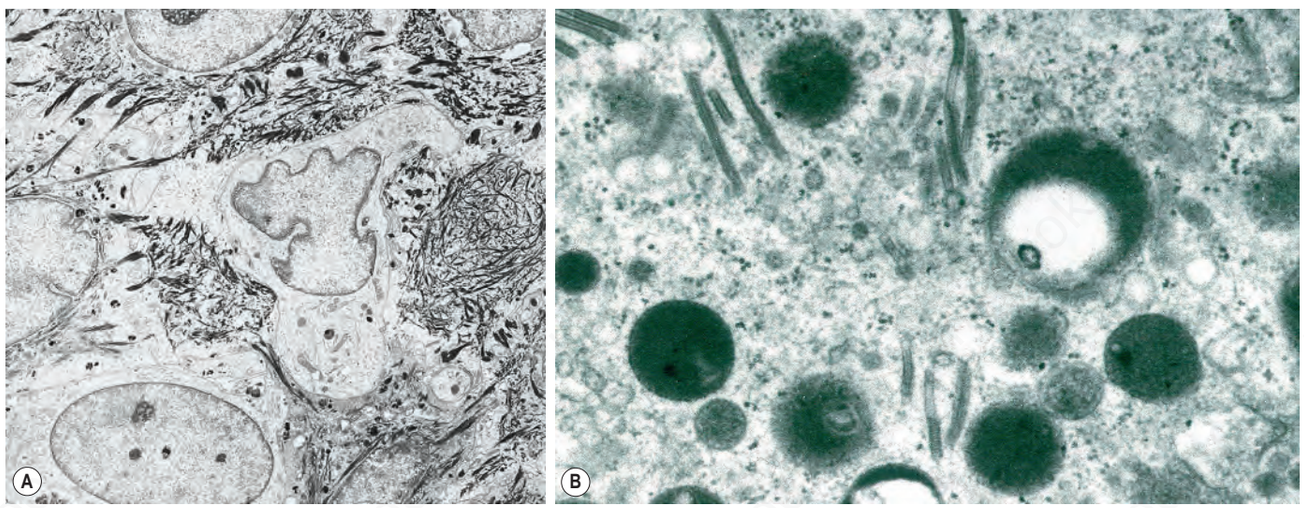

Fig. 1.34
(**A**, **B**) Langerhans cell: (**A**) note the characteristic lobulated nucleus. Dendritic processes are evident, (**B**) typical rod forms with the characteristic trilaminar structure.

distinct subpopulations of leukocytes and other inflammatory cells.[6] Some peptides have additional roles in signaling host responses through chemotactic, angiogenic, growth factor and immunosuppressive activity. These peptides are known as alarmins.[7] Alarmins may also stimulate parts of the host defense system, such as barrier repair and recruitment of inflammatory cells.

Skin immunity is also provided by a distinct population of antigen presenting cells in the epidermis known as Langerhans cells (*Fig. 1.33*). These are dendritic cells that were first described by Langerhans, who demonstrated their existence in human epidermis by staining with gold chloride. Without stimulation, Langerhans cells exhibit a unique motion termed 'Dendrite Surveillance Extension And Retraction Cycling Habitude (dSEARCH)'.[8] This is characterized by rhythmic extension and retraction of dendritic processes between intercellular spaces. When exposed to antigen, there is greater dSEARCH motion and also direct cell-to-cell contact between adjacent Langerhans cells which function as intraepidermal macrophages, phagocytosing antigens among keratinocytes. Langerhans cells can be found throughout the epidermis, extending superficially to within the granular cell layer. Stimulated Langerhans cells then leave the epidermis and migrate via lymphatics to regional lymph nodes. In the paracortical region of lymph nodes the Langerhans cell expresses protein on its surface to present to a T lymphocyte that can then undergo clonal proliferation. Langerhans cells, in combination with macrophages and dermal dendrocytes, represent the skin's mononuclear phagocyte system.[9] By electron microscopy, Langerhans cells have a lobulated nucleus, a relatively clear cytoplasm and well-developed endoplasmic reticulum, Golgi complex and lysosomes. They also possess characteristic granules which are rod or racquet-shaped (*Fig. 1.34*). These 'Birbeck' granules represent subdomains of the endosomal recycling compartment and form at sites where the protein Langerin accumulates.

Besides antigen detection and the processing role by epidermal Langerhans cells, cutaneous immune surveillance is also carried out in the dermis by an array of macrophages, T cells and dendritic cells. These immune sentinel and effector cells can provide rapid and efficient immunologic back-up to restore tissue homeostasis if the epidermis is breached. The dermis contains a very large number of resident T cells. Indeed, there are approximately 2×10^{10} resident T cells, which is twice the number of T cells in the circulating blood. Dermal dendritic cells may also have potent antigen-presenting capacities or the potential to develop into CD1a-positive and Langerin-positive cells. Dermal immune sentinels are capable of acquiring an antigen-presenting mode, a migratory mode or a tissue resident phagocytic mode.[10]

Melanocytes

Melanocytes are pigment-producing cells and are found in the skin, inner ear, choroid and iris of the eye. In skin, melanocytes are located in the

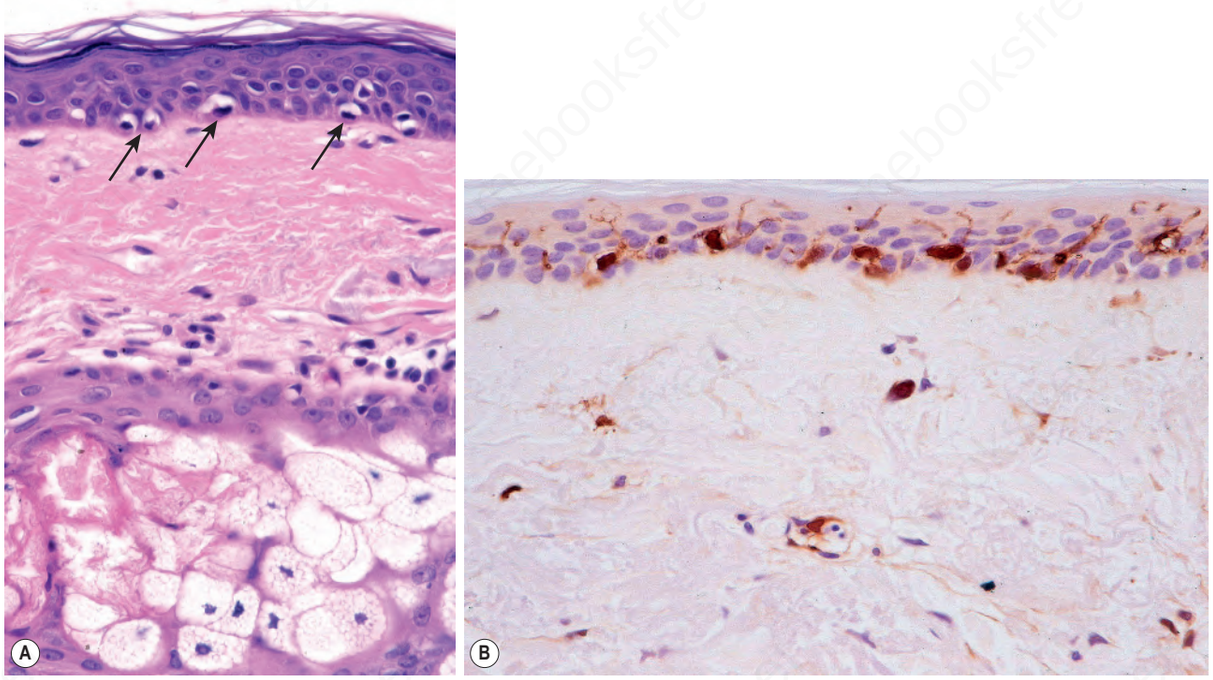

Fig. 1.35
(**A**, **B**) Normal epidermis: melanocytes are seen along the basal layer of the epidermis. The cytoplasmic vacuolation is a fixation artifact; (**B**) melanocytes can be highlighted with S100-protein immunohistochemistry. Note the dendritic processes.

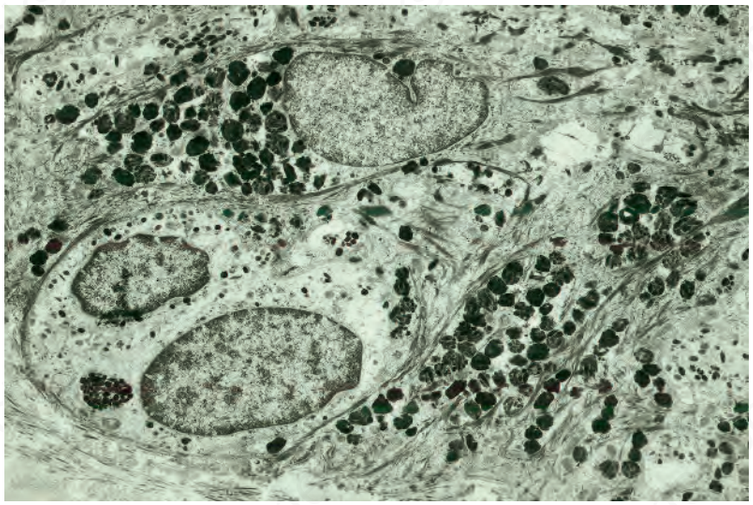

Fig. 1.36
Normal melanocyte: it has abundant pale cytoplasm and scattered solitary melanosomes. Note the absence of tonofibrils and desmosomes.

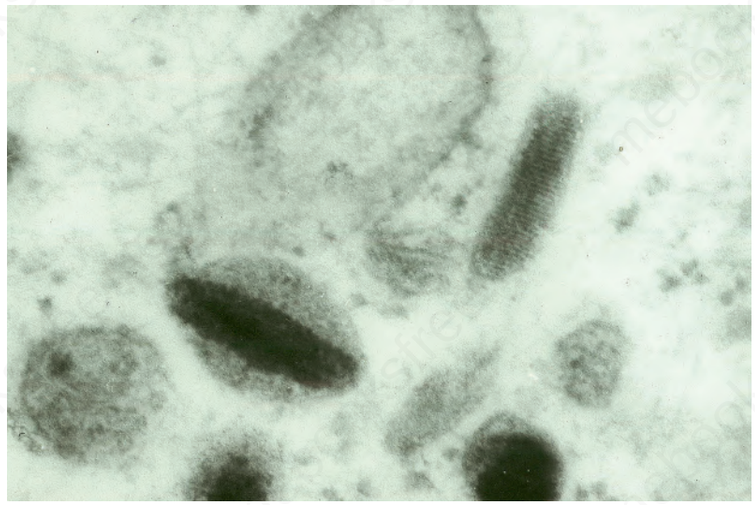

Fig. 1.37
Melanosome: note the typical striated internal structure.

basal keratinocyte layer. The ratio of melanocytes to basal cells ranges from approximately 1:4 on the cheek to 1:10 on the limbs. They appear as vacuolated cells in hematoxylin and eosin stained sections (*Fig. 1.35*). Ultrastructurally, melanocytes have pale cytoplasm and are devoid of tonofilaments, hemidesmosomes, and desmosomes (*Fig. 1.36*). They are easily recognized by their specific cytoplasmic organelles (melanosomes) which are derived from the smooth endoplasmic reticulum. Melanosomes are believed to represent a specialized variant of lysosome (*Fig. 1.37*). The function of melanocytes is the production of melanin, a complex of pigmented proteins that vary in color from yellow to red to brown or black and accounts for the various skin colors within and among races. Melanin protects the mitotically active basal epidermal cells from the injurious effects of ultraviolet light, which accounts for individuals with less pigmentation (fair-haired and light-skinned) having a much greater risk of sunburn and developing cutaneous malignancies (squamous cell and basal cell carcinomas, and melanoma). The mechanism involves absorbing or scattering ultraviolet radiation and/or its photoproducts. Other functions of melanin include control of vitamin D_3 synthesis and local thermoregulation.

In skin and hair, two forms of melanin pigment are produced; eumelanin and pheomelanin. Eumelanin is a brown or black pigment and is synthesized from tyrosine; it is particularly found in dark-colored races, whereas, pheomelanin has a yellow-red color and is synthesized from tyrosine and cysteine; it predominates in Caucasian skin.

Melanocytes also possess melanocyte-specific receptors including melanocortin-1 (MC1R) and melatonin receptors.[1] The activation or the inhibition of melanocyte-specific receptors can augment normal melanocyte function, skin color, and photoprotection. Moreover, receptor polymorphisms are known to underlie red hair phenotypes, as well as skin pallor

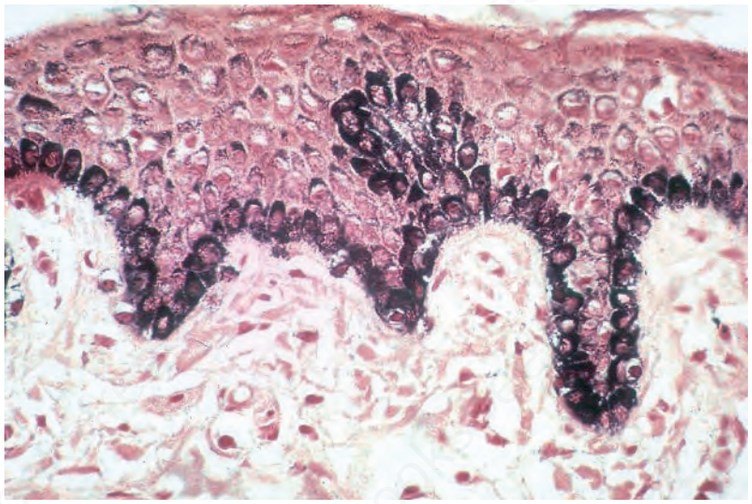

Fig. 1.38
Normal epidermis: this section of black skin has been stained by the Masson–Fontana reaction for melanin. Note the heavy pigmentation, which is present in both melanocytes and keratinocytes.

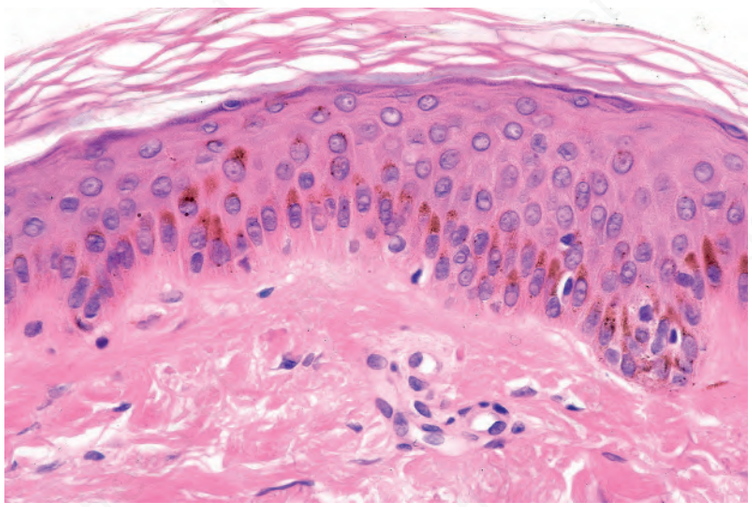

Fig. 1.39
Melanin pigment: actinically damaged skin. Note that the melanin pigment is located in a 'cap' overlying the keratinocyte nuclei.

or freckles (ephelides).[2] Hair graying reflects abnormalities in melanocyte signaling. Notably, Notch transcription factor signaling in melanocytes is essential for the maintenance of proper hair pigmentation, including regeneration of the melanocyte population during hair follicle cycling.[3]

Melanin is transferred from melanocytes in melanosomes to neighboring keratinocytes in the epidermis and into the growing shaft in hair follicles and can be identified by silver techniques such as the Masson-Fontana reaction (*Fig. 1.38*). Transport occurs along the dendritic processes of the melanocytes and the melanosomes are engulfed as membrane-bound (lysosomal) single or compound melanosomes by a group of adjacent largely basally located keratinocytes (epidermal melanin unit) where they are typically seen in an umbrella-like distribution over the outer aspect of the nucleus (*Fig. 1.39*). A compound melanosome typically contains from three to six single melanosomes. In heavily pigmented skin and dark hair, melanosomes remain solitary and are longer than those seen in melanogenesis in paler races. Other cells that may contain compound melanosomes include macrophages (melanophages), melanoma cells and, occasionally, Langerhans cells, the other type of epidermal dendritic cell. Macromelanosomes (giant melanosomes) measure several microns in diameter and therefore are readily visible in hematoxylin and eosin stained sections (*Fig. 1.40*).

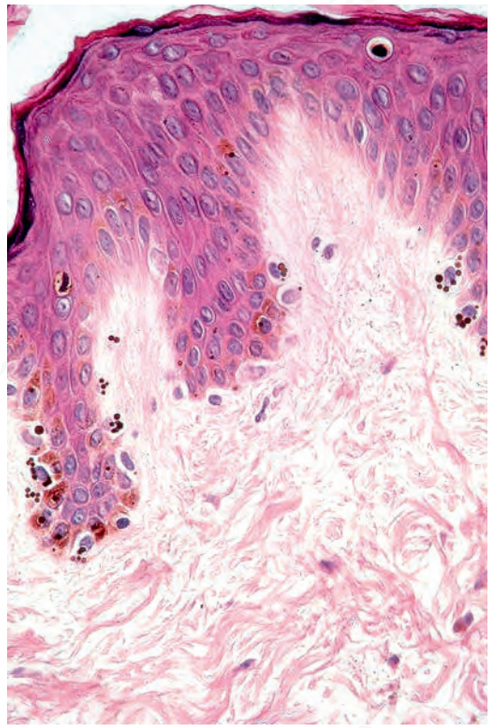

Fig. 1.40
Macromelanosomes: note the large spherical melanosomes in the cytoplasm of the melanocytes.

They may be encountered in normal skin, in lentigines, dysplastic nevi, Spitz nevi, in the café-au-lait macules of neurofibromatosis and in albinism. A key protein involved in melanosome assembly is NCKX5, encoded by the gene *SLC24A5*.[4] Loss of expression of this gene in mice results in marked changes in skin color with loss of pigment. Mature melanosomes of eumelanin are ellipsoidal in shape, while pheomelanin-producing melanosomes are spherical.

Merkel cells

Merkel cells are postmitotic cells scattered throughout the epidermis of vertebrates and constitute 0.2–0.5% of epidermal cells.[1] Merkel cells represent part of the affector limb in cutaneous slowly adapting type-1 (SA1) mechanoreceptors and are therefore particularly concerned with touch sensation. They are located amongst basal keratinocytes and are mainly found in hairy skin, tactile areas of glabrous skin, taste buds, the anal canal, labial epithelium and eccrine sweat glands. In glabrous skin, the density of Merkel cells is ≈50 per mm^2. Sun-exposed skin may contain twice as many Merkel cells as non-sun-exposed skin.[2] Numerous Merkel cells can be found in actinic keratoses.[3] Merkel cells cannot be recognized in conventional hematoxylin and eosin stained sections. Rather, immunohistochemistry, particularly using antikeratin antibodies (e.g., to keratin 20), or electron microscopy, is necessary for their identification (*Figs 1.41 and 1.42*).

Ultrastructurally, Merkel cells appear oval with a long axis of ≈15 µm orientated parallel to the basement membrane (*Fig. 1.43*). They also have a large bilobed nucleus and clear cytoplasm which reflects a relative scarcity of intracellular organelles. Merkel cells contain numerous neurosecretory granules, each 50 nm to 160 nm across; these are found opposing the junctions with the sensory nerve ending (*Fig. 1.44*). Merkel cells contain keratin filaments, particularly keratin filament types 8, 18, 19, and 20, which are characteristic of simple epithelium and fetal epidermis. Immunocytochemically, Merkel cells also express neuropeptides including synaptophysin, vasoactive intestinal peptide (VIP) and calcitonin gene-related polypeptide (CGRP).[4,5] They contain neuron-specific proteins including neuron-specific enolase (NSE) and protein gene product (PGP) 9.5.[6] In addition, Merkel cells express desmosomal proteins, membranous neural cell adhesion molecule and nerve

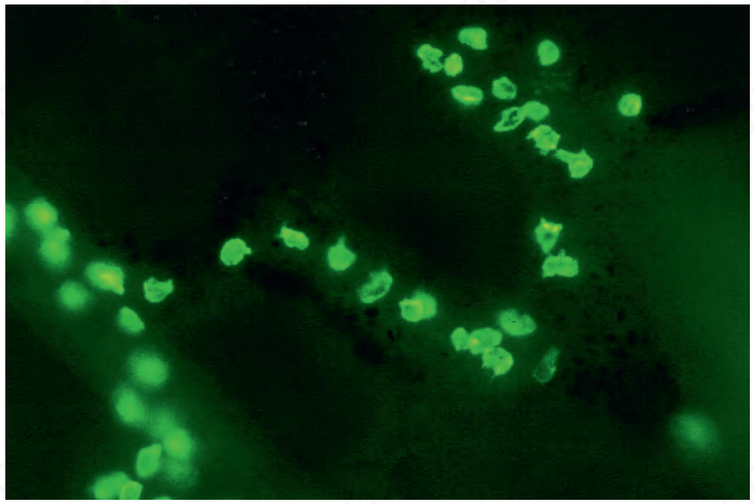

Fig. 1.41
Merkel cells: separated human epidermis showing a striking linear arrangement (troma-1 antibody). By courtesy of J.P. Lacour, MD, and J.P. Ortonne, MD, University of Nice, France.

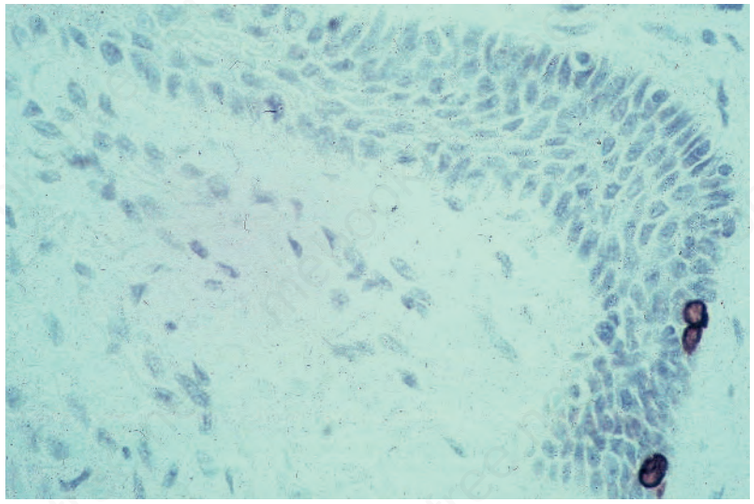

Fig. 1.42
Merkel cell: positive labeling for CAM 5.2 identifies Merkel cells in this obliquely sectioned epidermal ridge.

growth factor receptor.[7–9] Merkel cells show a positive uranaffin reaction.[10] Merkel cells form close connections with sensory nerve endings and secrete or express a number of these peptides.[11] The close contact between Merkel cells and nerve fibers represents a Merkel cell–neurite complex, but there is no clear evidence of synaptic transmission, although numerous vesicles can be identified in neurons apposed to Merkel cells.[12]

Human skin contains an extensive neural network that contains cholinergic and adrenergic nerves and myelinated and unmyelinated sensory fibers. Moreover, the skin also contains several transducers involved in the perception of touch, pressure, and vibration, including Ruffini organs surrounding hair follicles, Meissner corpuscles, Vater–Pacini corpuscles located in the deep layer of the dermis, and nerve endings which pass through the epidermal basement membrane. Some of these contain Merkel cells which form the Merkel cell–neurite complex, while others are free nerve endings. The cell bodies for all these neurons reside in the dorsal root ganglion. The Merkel cell–neurite complexes are thought to serve as mechanoreceptors and to be responsible for the sensation of touch via Piezo2-dependent transmission channels.[13] They are clustered near unmyelinated sensory nerve endings, where they group and form 'touch spots' at the bottom of rete ridges. These complexes are also known as hair discs, touch domes, touch

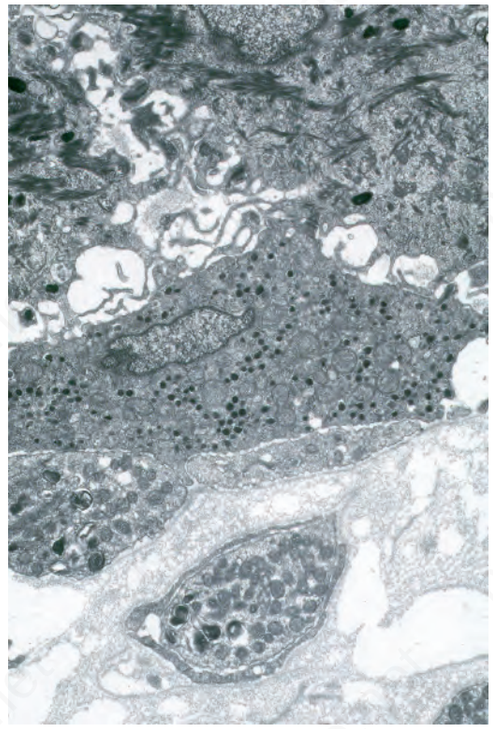

Fig. 1.43
Merkel cell: a heavily granulated Merkel cell is present in the midfield. This is located immediately adjacent to a small nerve fiber.

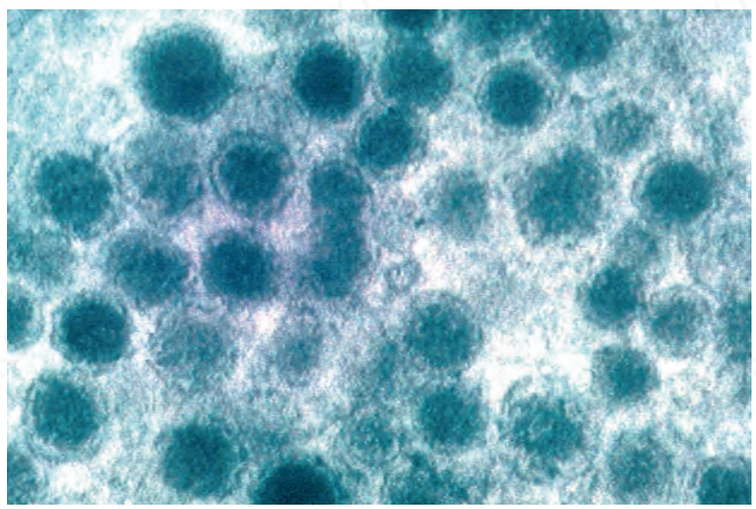

Fig. 1.44
Merkel cell granules: they are membrane bound and measure approximately 150 nm in diameter. By courtesy of A.S. Breathnach, MD (1977) Electron microscopy of cutaneous nerves and receptors. Journal of Investigative Dermatology 69, 8–26. Blackwell Publishing Inc., USA.

corpuscles, or Iggo discs. The complex is innervated by a single, slowly adapting type 1 nerve fiber. In hairy skin, Merkel cells also cluster in the rete ridges and in the ORS of the hair follicle where the arrector pili muscles attach. The function of Merkel cells in hair follicles is unclear, although they may be involved in the induction of new anagen cycles.

There are two hypotheses for the origin of Merkel cells: one possibility is that they differentiate from epidermal keratinocyte-like cells and the other is that they arise from stem cells of neural crest origin that migrated during embryogenesis, in similar fashion to melanocytes.[14] Merkel cell hyperplasia is a common histologic finding and may accompany keratinocyte hyperproliferation as well as being frequently seen in adnexal tumors such as

nevus sebaceus, trichoblastomas, trichoepitheliomas, and nodular hidradenomas.[15] Merkel cell hyperplasia is associated with hyperplasia of nerve endings that occurs in neurofibromas, neurilemomas, nodular prurigo, or neurodermatitis.

Intercellular junctions

Desmosomes are the major intercellular adhesion complexes in the epidermis. They anchor keratin intermediate filaments to the cell membrane and link adjacent keratinocytes (*Fig. 1.45*). Desmosomes are found in the epidermis, myocardium, meninges and cortex of lymph nodes. Ultrastructurally, desmosomes contain plaques of electron-dense material running along the cytoplasm parallel to the junctional region, in which three bands can be distinguished: an electron-dense band next to the plasma membrane, a less dense band, and then a fibrillar area (*Fig. 1.46*).[1] Identical components are present on opposing cells which are separated by an intercellular space of 30 nm within which there is an electron-dense midline. There are three main protein components of desmosomes in the epidermis: the desmosomal cadherins, the armadillo family of nuclear and junctional proteins, and the plakins (*Fig. 1.47*).[2] The transmembranous cadherins comprise mostly heterophilic associations of desmogleins and desmocollins. There are four main epidermis-specific desmogleins (Dsg1–4) and three desmocollins (Dsc1–3). These show differentiation-specific expression. For example, Dsg1 and Dsc1 are found predominantly in the superficial layers of the epidermis whereas Dsg3 and Dsc3 show greater expression in basal keratinocytes. The intracellular parts of the cadherins interact with the keratin filament network via the desmosomal plaque proteins, mainly desmoplakin, plakoglobin and plakophilin.[1]

Clues to the biologic function of these desmosomal components have arisen from various inherited and acquired human diseases.[3,4] Naturally occurring human mutations have been reported in ten different desmosome genes with variable skin, hair and heart abnormalities and several desmosomal proteins serve as autoantigens in immunobullous blistering skin diseases such as pemphigus (*Figs 1.48 and 1.49*).[5] Antibodies to multiple desmosomal proteins may develop in diseases such as paraneoplastic pemphigus through the phenomenon of epitope spreading.[6] Cleavage of the extracellular domain of Dsg1 has also been demonstrated as the basis of staphylococcal scalded skin syndrome and bullous impetigo.[7]

Adherens junctions are recognized ultrastructurally as electron-dense transmembrane structures, with two opposing membranes separated by approximately 20 nm, that form links with the actin skeleton.[8] They are 0.2–0.5 μm in diameter and can be found as isolated cell junctions or in association with tight junctions and desmosomes. Adherens junctions are expressed early in skin development and contribute to epithelial assembly, adhesion, barrier formation, cell motility and changes in cell shape. They may also spatially coordinate signaling molecules and polarity cues as well as serving as docking sites for vesicle release. Adherens junctions contain two basic adhesive units: the nectin-afadin complex and the classical cadherin complex.[9,10] The nectins form a structural link to the actin cytoskeleton via afadin (also known as AF-6) and may be important in the initial formation of adherens junctions. The cadherins form a complex with the catenins (α-, β-, and p120 catenin) and help mediate adhesion and signaling. Cell signaling via β-catenin can activate several pathways linked to morphogenesis and cell fate determination.

Inherited gene mutations of the adherens junction proteins plakoglobin and P-cadherin have been reported. Plakoglobin mutations result in Naxos disease (woolly hair, keratoderma, cardiomyopathy).[3] P-cadherin mutations underlie autosomal recessive hypotrichosis with juvenile macular dystrophy as well as ectodermal dysplasia-ectrodactyly-macular dystrophy (EEM) syndrome, in which there is hypotrichosis, macular degeneration, hypodontia and limb defects, including ectrodactyly, syndactyly and camptodactyly.[11,12]

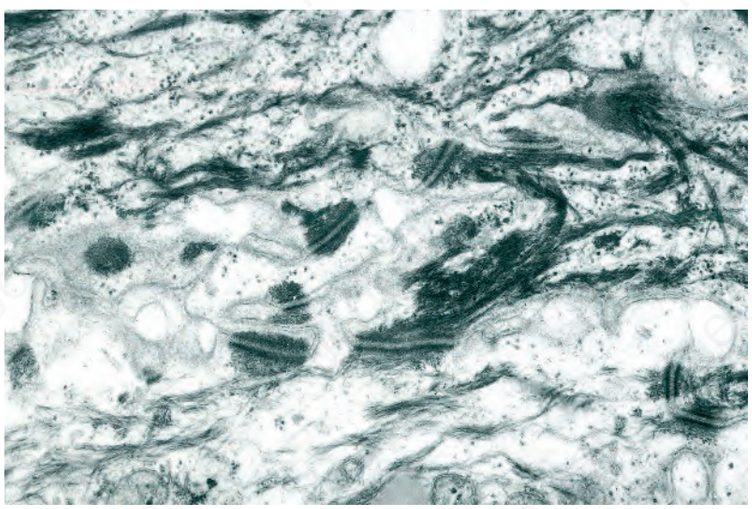

Fig. 1.45
Mid-prickle cell layer of normal epidermis: there are complex interdigitations between adjacent cell membranes with numerous desmosomal junctions.

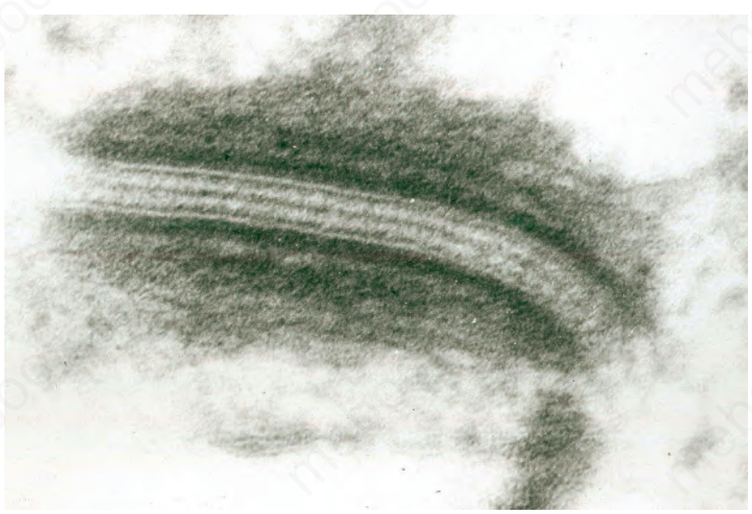

Fig. 1.46
Mid-prickle cell layer of normal epidermis showing the stratified nature of the desmosome.

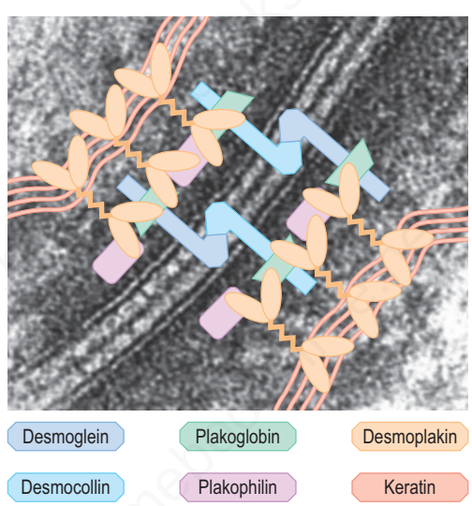

Fig. 1.47
Protein composition of a desmosome junction between adjacent keratinocytes. The keratin filament network of two keratinocytes is linked by a series of desmosomal plaque proteins and transmembranous molecules to create a structural and signaling bridge between the cells.

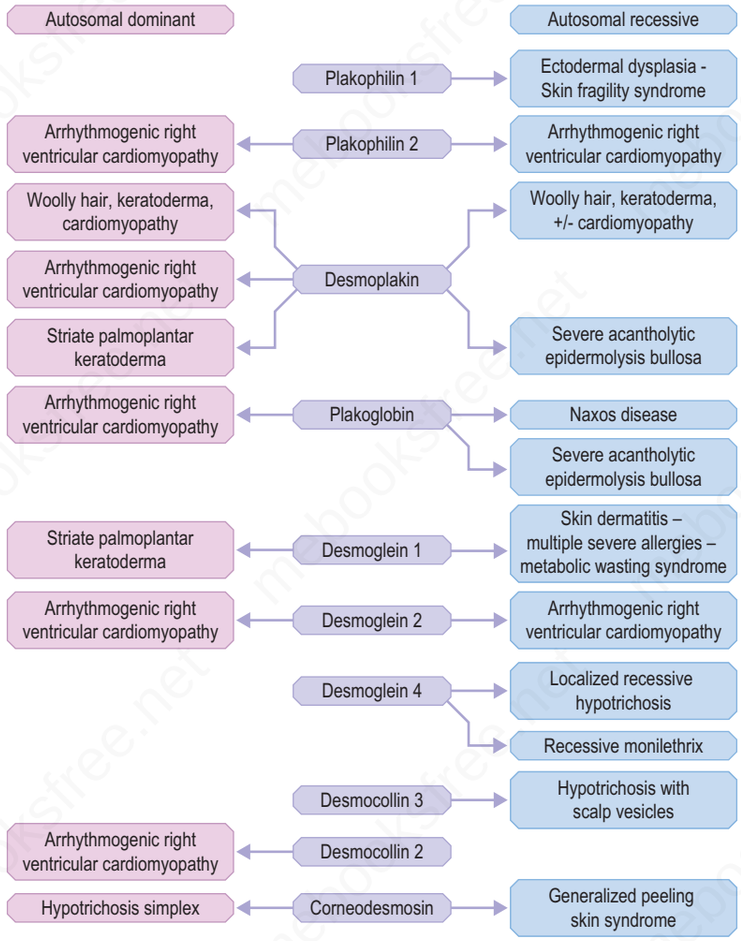

Fig. 1.48
Genetic disorders of desmosomes: autosomal dominant or autosomal recessive mutations in ten different structural components of desmosomes may give rise to specific diseases that can affect skin, hair or heart or combinations thereof.

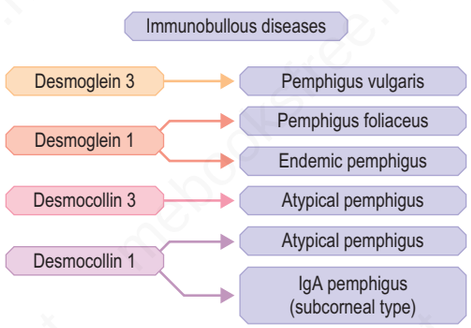

Fig. 1.49
Immunobullous diseases of desmosomes: intraepidermal blistering can arise through autoantibody disruption of four separate desmosomal proteins which leads to different clinical variants of pemphigus.

Gap junctions represent clusters of intercellular channels, known as connexons, which form connections between the cytoplasm of adjacent keratinocytes (and other cells).[13] Formation of a connexon involves assembly of six connexin subunits within the Golgi network. This complex is then transported to the plasma membrane where connexons associate with other connexons (homotypic or heterotypic) to form a gap junction. To date, 13 different human connexins have been described. The formation and stability of gap junctions can be regulated by protein kinase C, Src kinase, calcium concentration, calmodulin, adenosine 3′,5′-cyclic monophosphate (cAMP) and local pH.[14] The connexins are classified into three groups (α, β and γ) according to their gene structure, overall gene homology and specific sequence motifs.[15] Apart from the connexins, vertebrates also contain another class of gap junction proteins, the pannexins, which are related to the innexins found in nonchordate animals. The function of gap junctions is to allow sharing of low molecular mass metabolites (< 1000 Da) and exchange of ions between neighboring cells. Gap junction communication is essential for cell synchronization, differentiation, cell growth and metabolic coordination of avascular organs, including epidermis.[14]

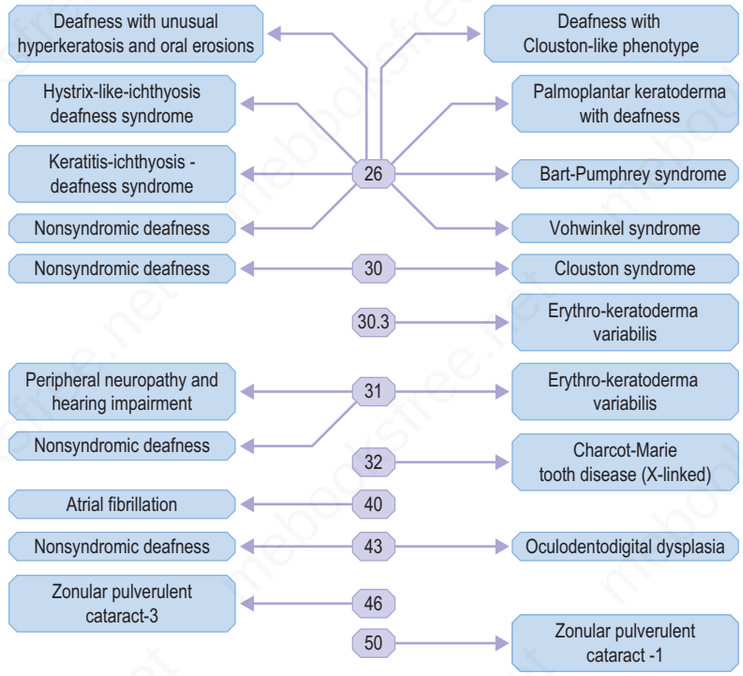

Fig. 1.50
Genetic disorders of connexins: nine different human connexin molecules are associated with different inherited diseases. Mutations in the four low molecular weight connexins shown at the top of the diagram are associated with a spectrum of skin pathology, as highlighted.

Inherited abnormalities in genes encoding four different connexins (Cx26, 30, 30.3 and 31) have been detected in several forms of keratoderma and/or hearing loss (*Fig. 1.50*). Nondermatologic disorders can also arise from mutations in some higher molecular weight connexins (Cx32, 40, 43, 46 and 50).

Tight junctions contribute to skin barrier integrity and maintaining cell polarity, although in simple epithelia they are major regulators of permeability.[8] An important function is to regulate the paracellular flux of water-soluble molecules between adjacent cells.[16] The main structural proteins of tight junctions are the claudins, of which there are approximately 24 subtypes, as well as the IgG-like family of junctional adhesion molecules (JAMs) and the occludin group of proteins. The principal claudins in the epidermis are claudin 1 and 4. These transmembranous proteins can bind to the intracellular zonula occudens proteins ZO-1, ZO-2, ZO-3 which interact with the actin cytoskeleton.[8,17]

Clinically, abnormalities in tight junction proteins can result in skin, kidney, ear and liver disease. Inherited gene mutations in claudin 1 have been reported in a few pedigrees with diffuse ichthyosis, hypotrichosis, scarring alopecia and sclerosing cholangitis.[18,19]

Pilosebaceous units

There are four classes of pilosebaceous unit: terminal on the scalp and beard; apopilosebaceous in axilla and groin; vellus on the majority of skin; and sebaceous on the chest, back and face. The dermal papilla is located at the base of the hair follicle and is associated with a rich extracellular matrix. Around the papilla are germinative (matrix) cells that have a very high rate of division, and give rise to spindle-shaped central cortex cells of

the hair fiber, and the single outer layer of flattened overlapping cuticle cells. A central medulla is seen in some hairs, with regularly stacked condensed cells interspersed with air spaces or low-density cores. The cortical cells are filled with keratin intermediate filaments orientated along the long axis of the cell, interspersed with a dense interfilamentous protein matrix. The cuticular cells are morphologically distinct, with flattened outward-facing cells, with three layers inside the cuticle of condensed, flattened protein granules: endocuticle, exocuticle and 'a' layer.[1] Around the cuticle is the IRS, which is composed of three distinct layers of cells that undergo keratinization: the IRS cuticle, the Huxley layer and the outermost Henle layer.[2] Differentiation in the IRS involves the development of trichohyalin granules, with 8–10 nm filaments orientated in the direction of hair growth. The IRS moves up the follicle, forming a support for the hair fiber, and degenerates above the sebaceous gland. The outermost layer is the ORS, which is continuous with the epidermis and expresses epithelial keratins, K5/K14, K1/K10 and K6/K16 in the upper ORS and K5/K14/K17 in the deeper ORS.

Normal growth of the hair fiber is 300–400 μm/day. Hair growth is generated by the high rate of proliferation of progenitor cells in the follicle bulb. There are three phases of cyclical hair growth: anagen, when growth occurs; catagen, a regressing phase; and telogen, a resting phase. The follicle re-enters anagen, and the old hair is replaced by a new one.

Immediately above the basal layer in the hair bulb, cells undergo a secondary pathway of 'trichocyte' or hair differentiation, and express a further complex group of keratins, the hard keratins.[2] Two families of hair keratins, types I and II, are present in mammals, which have distinctive amino- and carboxy-terminals with high levels of cysteine residues but lack the extended glycine residues of epidermal keratins. The proteins differ from epithelial keratins in position on two-dimensional gels but form acidic and basic groups. The nomenclature for human keratins and keratin-associated proteins was updated in 2006 and 2012, respectively.[3,4]

Mutations in hair keratin genes have been found to cause autosomal dominant forms of the human disease monilethrix. More common hair variants, such as curly hair, may be explained by dynamic changes during hair growth.[5] Curvature of curly hair is programmed from the very basal area of the follicle and the bending process is linked to a lack of axial symmetry in the lower part of the bulb, affecting the connective tissue sheath, ORS, IRS and the hair shaft cuticle.

Sebaceous glands usually develop as lateral protrusions from the ORS of hair follicles, but at certain sites, such as the eyelids, lips, areolae, nipples and labia minora, they appear to arise independently and drain directly onto the skin's surface (*Figs 1.51 and 1.52*). They are widespread in distribution, being found everywhere on the body except on the palms and soles. They are particularly abundant on the face and scalp, in the midline of the back and about the perineum, and are concentrated around the orifices of the body (*Fig. 1.53*). Those of the eyelid are known as the glands of Zeis and the meibomian glands. Sebaceous glands within the areolae are known as Montgomery tubercles. The largest sebaceous glands are associated with small vellus hairs in specialized pilosebaceous units known as sebaceous follicles (facial pores).

Sebaceous glands consist of several lipid-containing lobules, usually connected to a hair follicle (*Fig. 1.54*). Each lobule is composed of an outer layer of small cuboidal or flattened basophilic germinative cells, from which arises the inner zone of lipid-laden vacuolated cells with characteristic crenated nuclei (*Fig. 1.55*). The secretions drain into the sebaceous duct, which joins the hair follicle at the level of the infundibulum (*Fig. 1.56*). The duct is lined by keratinizing stratified squamous epithelium and is continuous with the external root sheath. The glands are holocrine because their secretions depend on complete degeneration of the acini, with release of all the cells' lipid contents to become sebum.

Immunohistochemically, the sebaceous cells label strongly for EMA but they do not express CEA or low molecular weight keratin (CAM 5.2) or S100 protein (*Fig. 1.57*). Ultrastructurally, the mature sebaceous gland shows gradual accumulation of variably sized, nonmembrane-bound, lipid inclusions in differentiating cells. Numerous mitochondria, ribosomes and

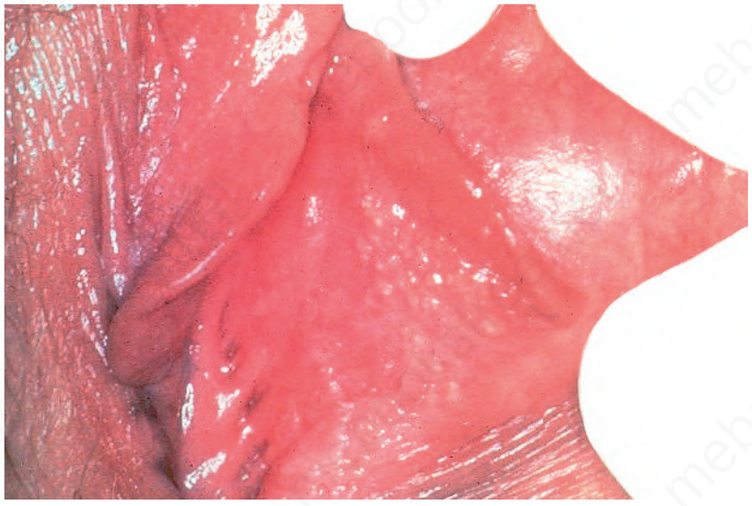

Fig. 1.51
Sebaceous glands: on the inner aspect of the labia these appear as tiny yellow papules (Fordyce spots). By courtesy of S.M. Neill, MD, Institute of Dermatology, London, UK.

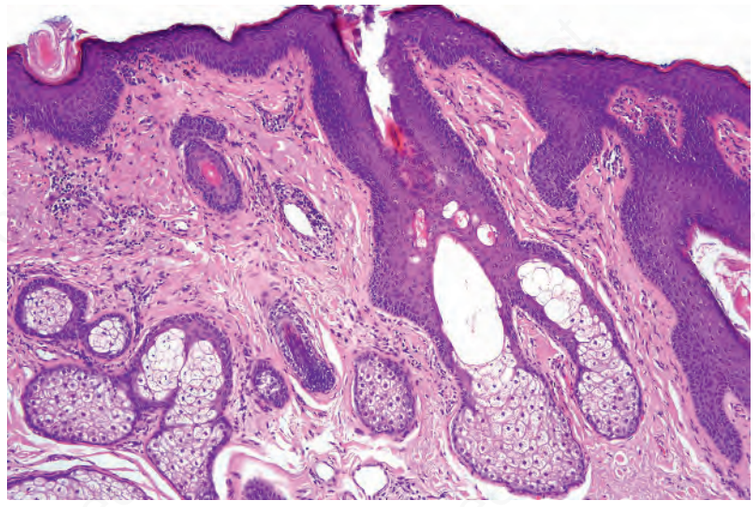

Fig. 1.52
Normal vulva: sebaceous glands are conspicuous, but arise independently of a hair follicle and open directly onto the surface epithelium.

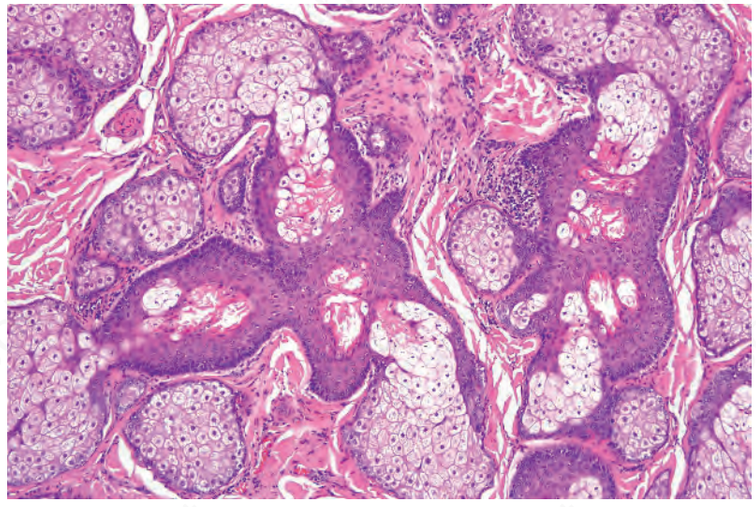

Fig. 1.53
Nose: sebaceous glands are particularly numerous at this site.

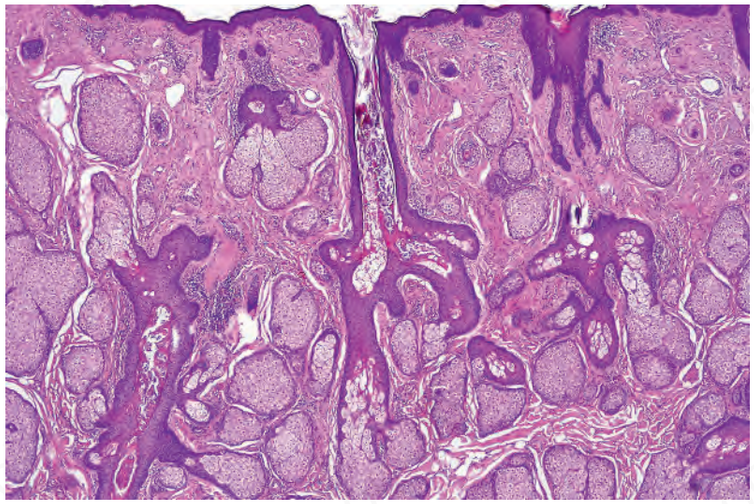

Fig. 1.54
Nose: multiple sebaceous glands are evident.

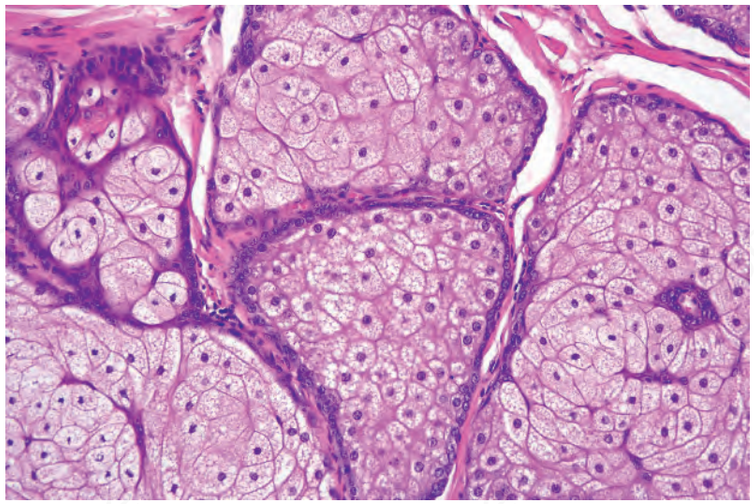

Fig. 1.55
Sebaceous lobule: germinative cells are basophilic and flattened. With maturation the cells acquire their characteristic 'bubbly' cytoplasm.

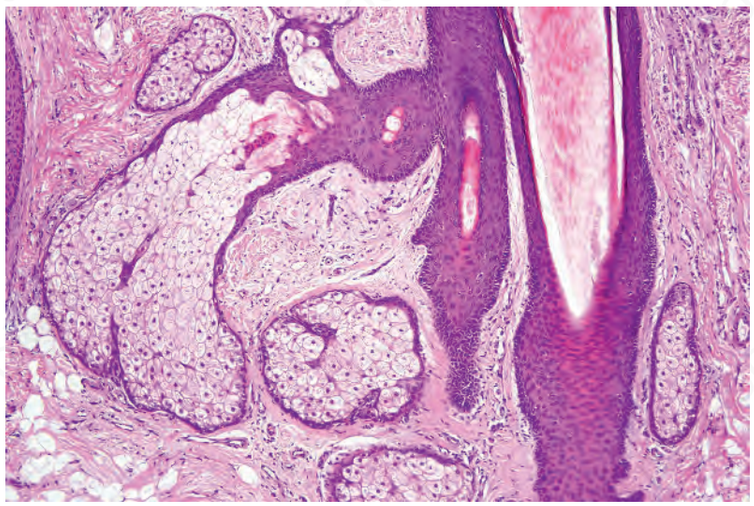

Fig. 1.56
Sebaceous duct: this is lined by keratinizing stratified squamous epithelium; it is continuous with the external root sheath.

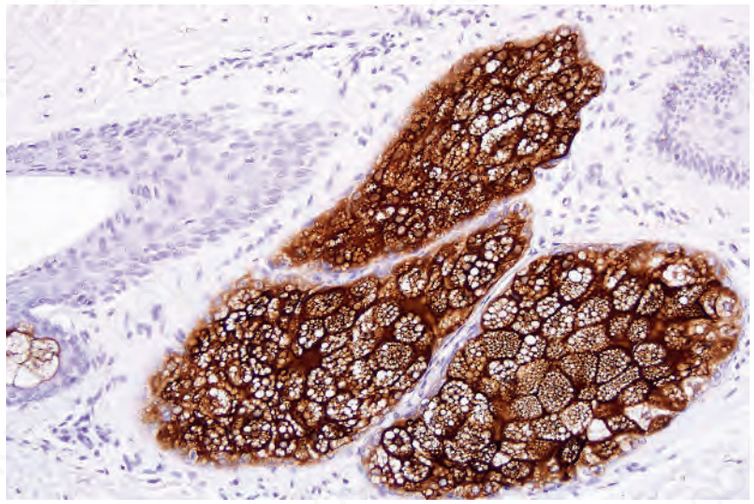

Fig. 1.57
Sebaceous gland: the epithelial cells normally strongly express EMA.

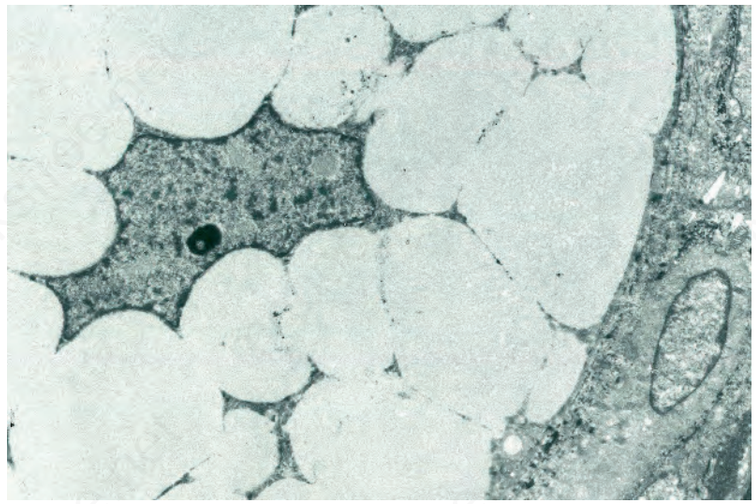

Fig. 1.58
Sebaceous gland: in this field from the center of a sebaceous lobule, the cytoplasm is completely distended with lipid droplets. Germinative cells are evident in the right-lower quadrant.

membrane-bound vesicles may also be evident. As the cells mature before their disintegration, the lipid droplets completely fill the cytoplasm and compress the centrally located nucleus (*Fig. 1.58*).

The secretion of sebaceous glands is sebum, an exceedingly complicated lipid mixture that includes triglycerides (57%), wax esters (26%) and squalene (12%). Its function includes waterproofing, control of epidermal water loss, and a protective function, inhibiting the growth of fungi and bacteria. Secreted sebum undergoes significant changes due to the presence of *Propionibacterium acnes* (triglyceride hydrolysis) within the pilosebaceous canal and *Staphylococcus epidermidis* (cholesterol ester formation) on the perifollicular skin. Skin surface lipid is composed of a mixture of sebum and epidermal lipids.

Eccrine glands

Human sweat glands are generally divided into two types: eccrine and apocrine.[1] The eccrine gland is the primary gland responsible for thermoregulatory sweating in humans.[2] Eccrine sweat glands are distributed over nearly the entire body surface. The number of sweat glands in humans varies greatly, ranging from 1.6 to 4.0 million.

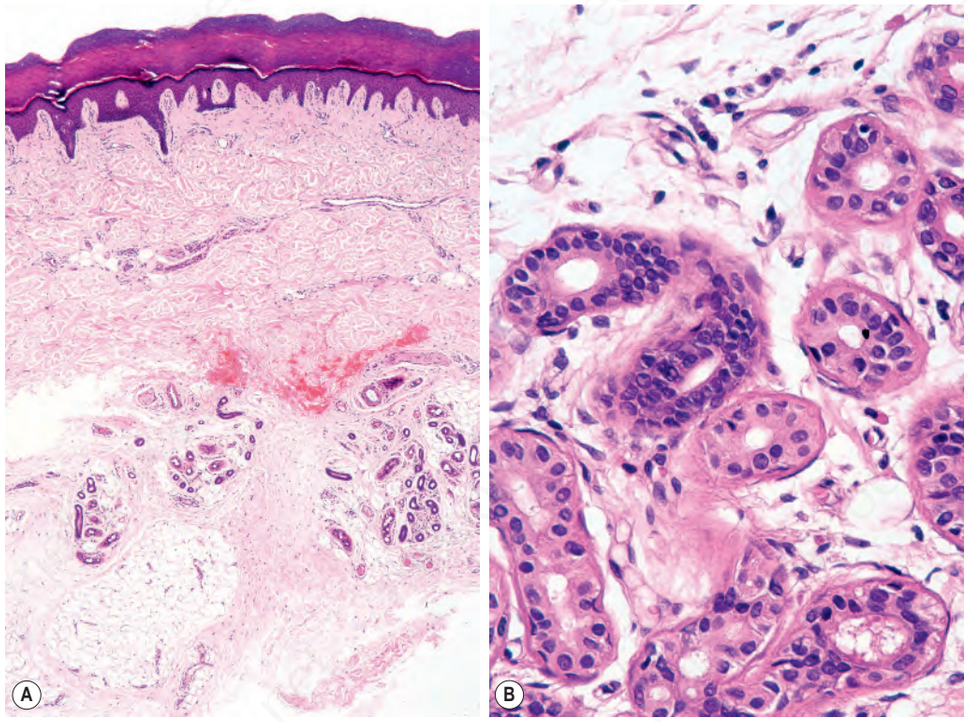

Fig. 1.59
Eccrine gland: (**A**) palmar skin showing numerous eccrine glands located in the deep reticular dermis and subcutaneous fat, (**B**) the secretory unit is in the lower field. Sections through the coiled duct are evident in the upper field. The epithelium of the duct is more darkly stained than that of the glandular component.

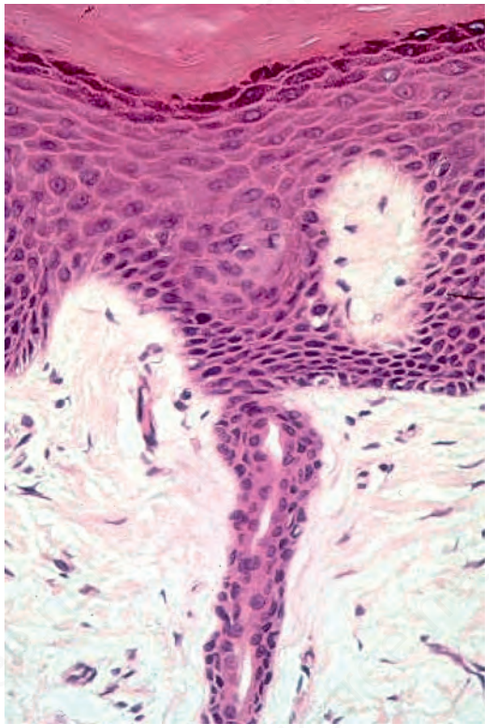

Fig. 1.60
Eccrine gland: high-power view of eccrine straight duct.

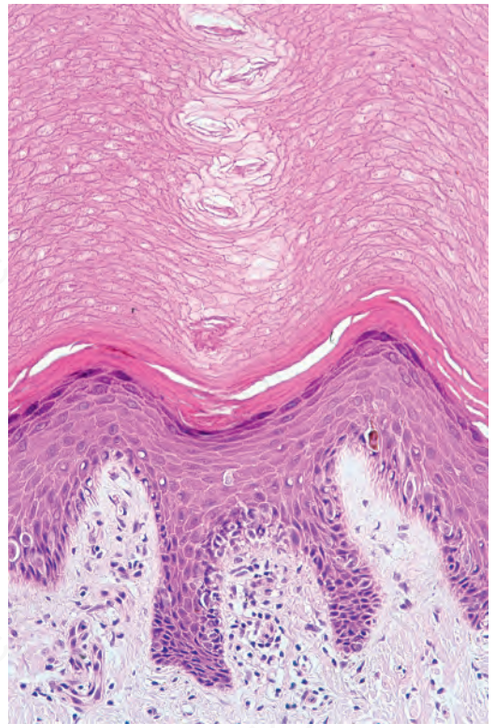

Fig. 1.61
Eccrine gland: most superficially, the duct coils through the stratum corneum.

Histologically, eccrine sweat glands are divided into four subunits: a highly vascularized coiled secretory gland, a coiled dermal duct, a straight dermal duct, and a coiled intraepidermal duct (the acrosyringium) (*Fig. 1.59*). The secretory coil is located in the lower dermis, and the duct extends through the dermis and opens directly onto the skin surface (*Figs 1.60*, *1.61*). The active sweat glands are present most densely on the sole, forehead and palm, somewhat less on the back of the hand, still less on the lumbar region, and the lateral and extensor surfaces of the extremities, and least on the trunk and the flexor and medial surfaces of the extremities. The uncoiled dimension of the secretory portion of the gland is approximately 30–50 μm in diameter and 2–5 mm in length. The size of the adult secretory coil ranges 1–8 × 10^{-3} mm^3. The secretory component lies in the

lower reaches of the reticular dermis or around the interface between the dermis and subcutaneous fat and is surrounded by a thick basement membrane and loose connective tissue often rich in mucin. It embodies an outer discontinuous layer of contractile myoepithelial cells and an inner layer of secretory cells comprising two cell types: large clear pyramidal cells, which appear to be responsible for water secretion, and smaller, darkly staining mucopolysaccharide-containing cells (probably secreting a glycoprotein), which are much less commonly seen. Between adjacent cells are canaliculi, which open into the lumen of the tubule (see below). Sometimes the secretory lobules show striking clear cell change due to glycogen accumulation (*Fig. 1.62*). The myoepithelial cells contract in response to cholinergic stimuli. They have spindled cell morphology and are distributed in a spiral, parallel array along the long axis of the secretory tubule. On the basis of their expression of keratin filaments, they appear to be of ectodermal rather than mesenchymal derivation. They do not label for vimentin. Myoepithelial cells therefore develop from the epithelial cells of the tip of the secretory coil and not, as might be expected, from adjacent mesenchymal cells. The dermal duct components consist of a double layer of cuboidal basophilic cells. The duct is not merely a conduit, but has a biologically active function, modifying the composition of eccrine secretion and, particularly, the reabsorption of water. The intraepidermal portion of the sweat duct opens directly onto the surface of the skin. A myoepithelial layer is absent.

The secretory unit is strongly labeled by CAM 5.2 (both cytoplasmic and membranous) and Ber-EP4 and there is luminal accentuation (*Fig. 1.63*). The ductal component is completely negative. EMA can be detected along the luminal aspect of the secretory unit and outlining the intercellular canaliculi. It is also present around the luminal border of the duct, and is often present in large quantities within the lumen. CEA is present in a similar distribution to EMA although secretory labeling tends to be rather focal and somewhat weaker while the ductal lumen is more strongly outlined. The myoepithelial cells can be identified by antibodies to S100 protein, desmin and smooth

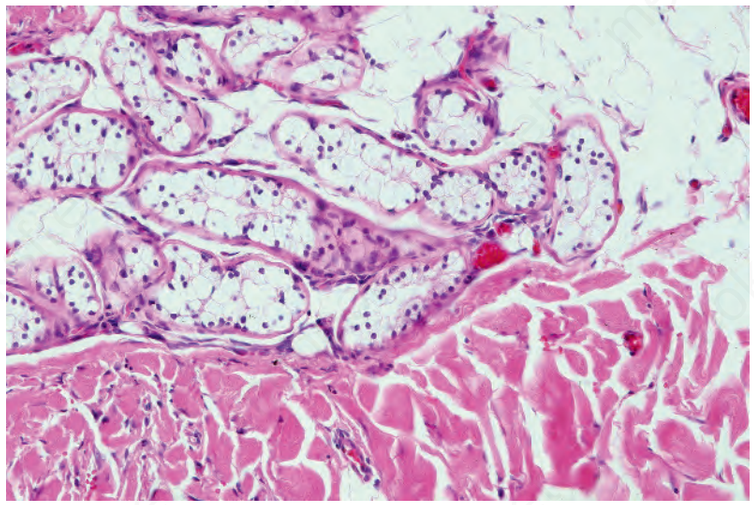

Fig. 1.62
Eccrine gland: excessive glycogen has resulted in vacuolated epithelium.

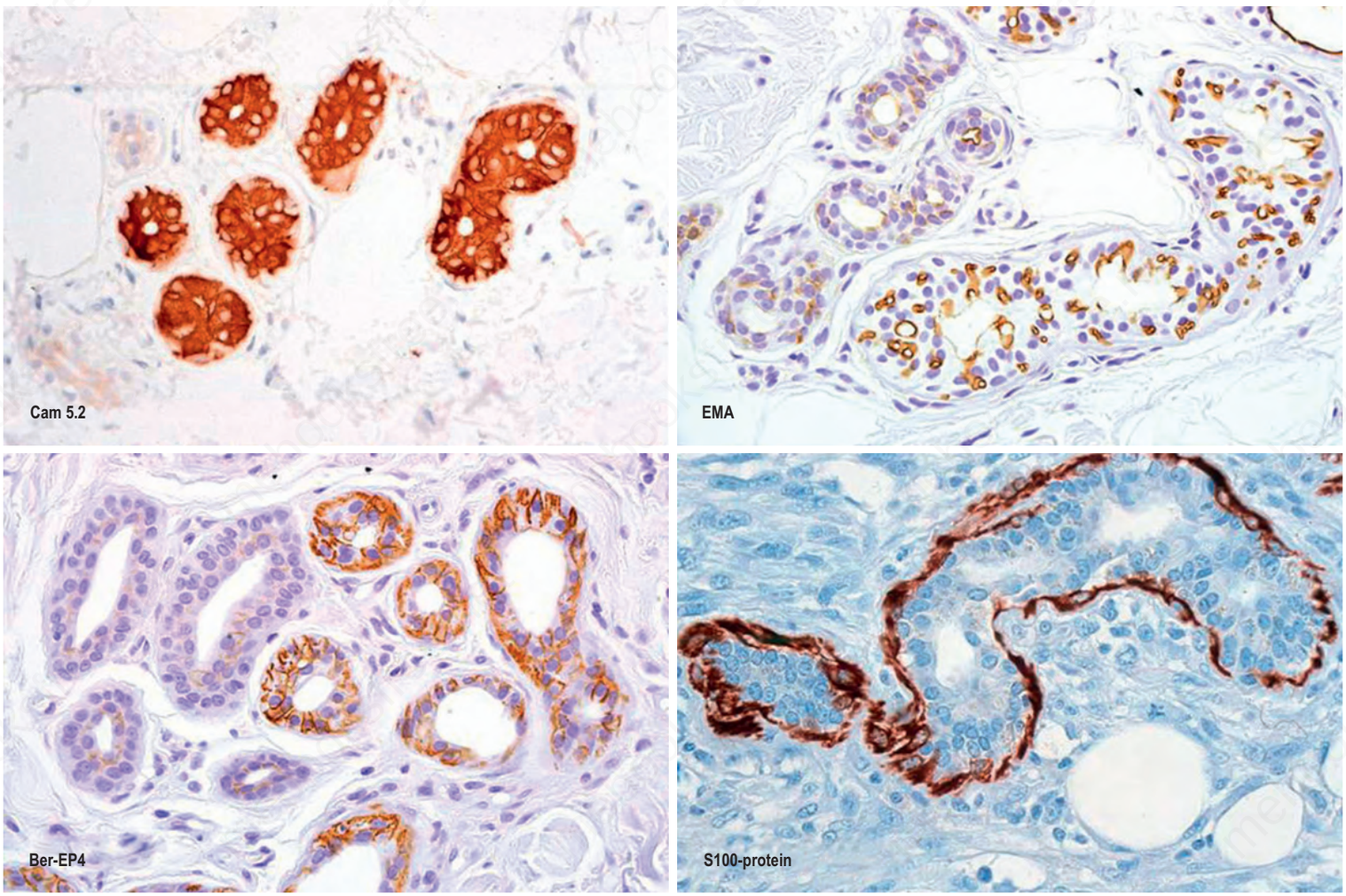

Fig. 1.63
Eccrine gland: immunohistochemistry.

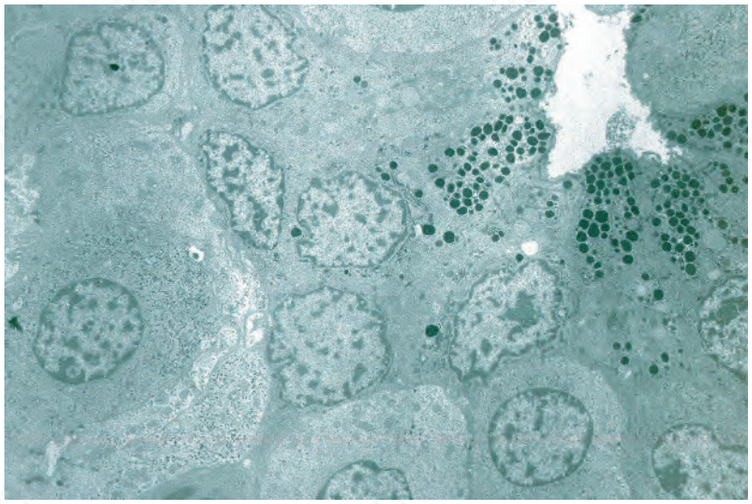

Fig. 1.64
Eccrine gland: low-power electron micrograph showing the lumen in the upper-right quadrant, granular mucous-secreting cells and serous cells.

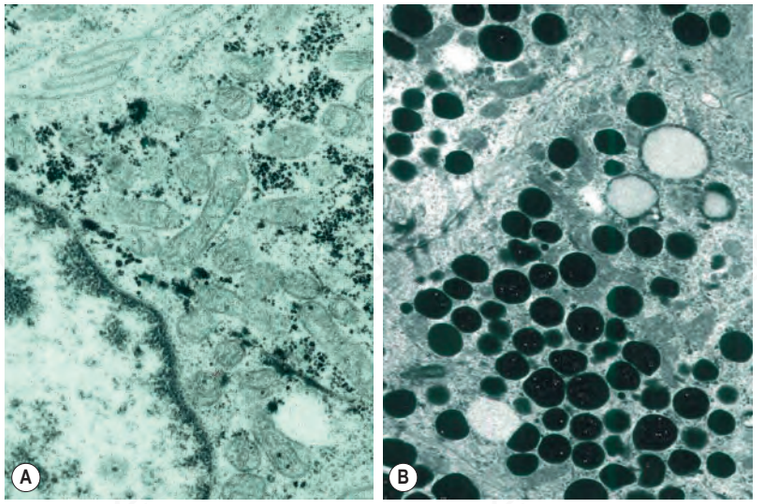

Fig. 1.65
Eccrine gland: (*left*) high-power view of clear cell showing conspicuous mitochondria and numerous electron-dense glycogen granules, (*right*) high-power view of secretory granules in a dark cell.

muscle actin. The eccrine glands show strong activity for the enzymes amylophosphorylase, leucine aminopeptidase, succinic dehydrogenase and cytochrome oxidase.[3] Weak or no activity is seen for Nicotinamide adenine dinucleotide (NADH) diaphorase, esterase and acid phosphatase.

With electron microscopy, the serous cells are characterized by abundant intracytoplasmic glycogen granules and numerous mitochondria (*Figs 1.64*, *1.65*). Adjacent cell membranes, which show marked interdigitations, may separate to form microvilli-lined intercellular canaliculi. The mucous cells contain numerous electron-dense lipid droplets and lysozymes. Myoepithelial cells are present at the periphery of the secretory coil within the eccrine basal lamina (lamina densa) and contain abundant myofilaments with characteristic dense bodies. The sweat duct lumen is bordered by conspicuous microvilli (*Fig. 1.66*). The cytoplasm contains numerous clear vesicles. Tonofilaments are characteristically orientated in a circumferential manner deep to the plasma membrane, the so-called cuticle of light microscopy. This is particularly well developed in the acrosyringium.

Human perspiration is classified into two types: insensible perspiration and active sweating. Insensible perspiration involves water loss from the respiratory passages, the skin, and gaseous exchanges in the lungs. Heat, exercise and carbon dioxide can all induce active sweating in human beings.

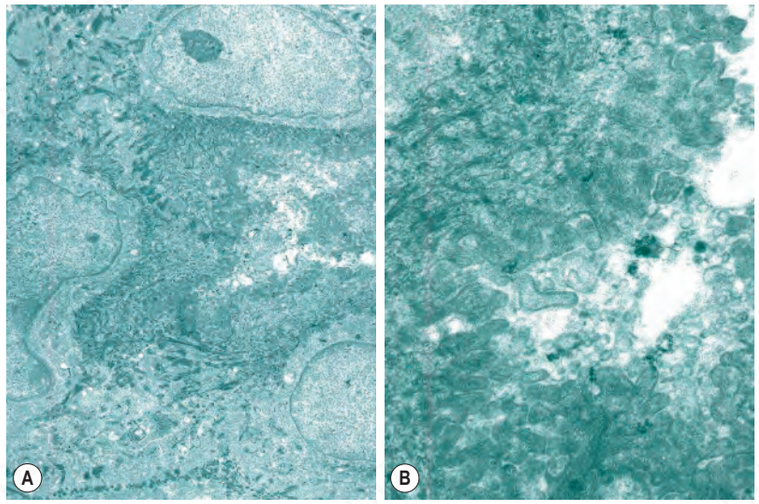

Fig. 1.66
Eccrine gland: (**A**) lumen of the eccrine dermal duct lined by conspicuous microvilli, (**B**) high-power view of eccrine dermal duct showing microvilli and circumferentially orientated tonofilaments.

Active sweating may be classified into two types: thermal and mental/emotional. Thermal sweating plays an important role in keeping the body's temperature constant and involves the whole body surface.[4] The secretory nerve fibers innervated in human sweat glands are sympathetic, which appear to be cholinergic in character as sweating is produced by pilocarpine and stopped by atropine.[5] VIP coexisting in the cholinergic nerve fibers has been suggested as a candidate neurotransmitter that may control the blood circulation of the sweat glands. Acetylcholine is the primary neurotransmitter released from cholinergic sudomotor nerves and binds to muscarinic receptors on the eccrine sweat gland, although sweating can also occur via exogenous administration of α- or β-adrenergic agonists. The initial fluid released from the secretory cells is isotonic and similar to plasma although it is devoid of proteins. As the fluid travels up the duct towards the surface of the skin, sodium and chloride are reabsorbed, resulting in sweat on the surface being hypotonic relative to plasma.[6] When the rate of sweat production increases, however, for example during exercise, ion reabsorption mechanisms can be overwhelmed due to the large quantity of sweat secreted into the duct, resulting in higher ion losses. The sodium content in sweat on the skin's surface, therefore, is greatly influenced by sweat rate.

Apocrine glands

Apart from eccrine glands, the skin also contains apocrine sweat glands.[1,2] Apocrine glands have a low secretory output, and hence no significant role in thermoregulation. Apocrine glands are found predominantly in the anogenital and axillary regions, but are also located in the external auditory meatus (ceruminous glands), the eyelid (Moll gland), and within the areola. They are derived from the epidermis, and develop as an outgrowth of the follicular epithelium. They first appear during the fourth to fifth month of gestation. Their function in humans is unknown, but in other mammals they are responsible for scent production and have importance in sexual attraction. As with sebaceous glands, they are smaller in childhood, becoming larger and functionally active at puberty. The secretions of the ceruminous glands are believed to lubricate, clean and protect the external ear from bacterial and fungal infections.

Apocrine glands include two distinct components: a complex secretory element situated in the lower reticular dermis or subcutaneous fat, and a tubular duct linking the gland with the pilosebaceous follicle at a site above the sebaceous duct. Microscopically, the secretory portion comprises an outer discontinuous layer of myoepithelial cells and an inner layer of cuboidal to columnar eosinophilic cells (*Figs 1.67*, *1.68*). Although a histologic artifact, secretory droplets, which appear to be pinched off from

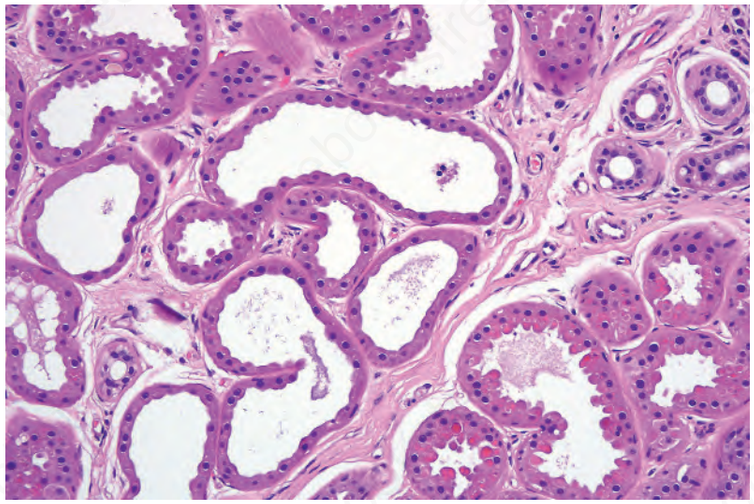

Fig. 1.67
Apocrine gland: this specimen from normal axillary skin shows apocrine secretory lobules in the subcutaneous fat. Ducts are present in the upper right of the field.

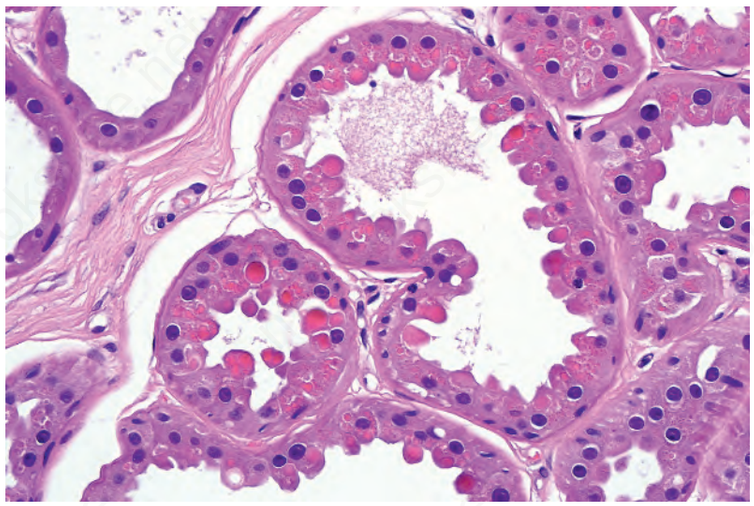

Fig. 1.68
Apocrine gland: lobules are lined by tall columnar cells with intensely eosinophilic cytoplasm. 'Decapitation secretion' is conspicuous.

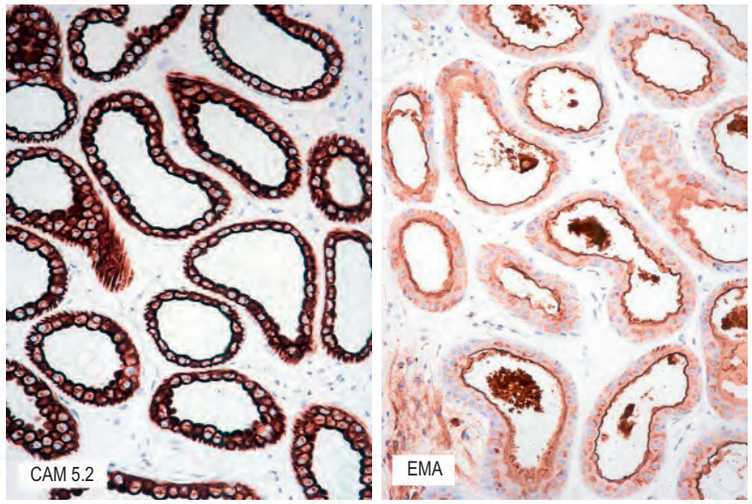

Fig. 1.69
Apocrine gland: immunohistochemistry (CAM 5.2 and EMA).

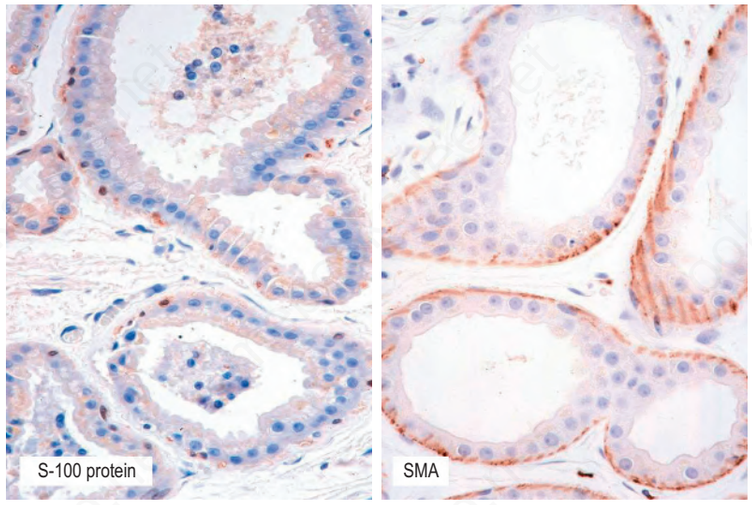

Fig. 1.70
Apocrine gland: immunohistochemistry (S100 protein and SMA).

the superficial aspect of the columnar cells (decapitation secretion), can be seen on light microscopy. The duct portion is formed by a double layer of cuboidal epithelium. It is morphologically indistinguishable from the eccrine duct. The inner layer of the secretory portion contains a single columnar secretory cell type containing numerous large dense granules located at the apical aspect, which contribute to the lipid-rich secretion produced. The inner layer is also surrounded by a fenestrated layer of myoepithelial cells but the lumen may be larger in diameter than that present in eccrine tissue. The apocrine excretory duct does not have any known reabsorptive function and consists of a double layer of cuboidal cells that merge distally with the epithelium of the hair follicle, resulting in emptying of the secretion into the hair follicle.

Immunohistochemically, the secretory unit shows very strong labeling with the antibody CAM 5.2 (both cytoplasmic and membranous), and there is luminal accentuation. The apocrine duct is negative (*Fig. 1.69*). EMA labels the cytoplasm of the secretory cells, and is accentuated along the luminal border. It is also present along the luminal aspect of the apocrine duct. With CEA, there is faint, focal staining of the secretory epithelium. The luminal aspect of the duct is strongly outlined. Cytoplasmic granules express epidermal growth factor. The myoepithelial cells of the secretory unit are reactive for S100 protein and smooth muscle actin (*Fig. 1.70*). The apocrine secretory epithelium strongly expresses the enzymes NADH diaphorase, esterase, acid phosphatase and β-glucuronidase. There is weak or absent reactivity for amylophosphorylase, leucine aminopeptidase, succinic dehydrogenase and cytochrome oxidase. The apocrine gland also can be stained with cationic colloidal gold at pH 2.0.[3]

Ultrastructure of the apocrine reveals cuboidal to columnar secretory cells containing numerous osmiophilic secretory vacuoles. Mitochondria are present in large numbers. While some show obvious double cristae, others are so electron dense that the internal structure is obscured. The Golgi is conspicuous. The luminal border is lined by prominent microvilli (*Fig. 1.71*).

The mechanism of apocrine secretion and control of apocrine glands is uncertain, but there is adrenergic sympathetic innervation, and secretion is provoked by external stimuli such as excitement or fear.[4] The unpleasant odor of apocrine secretion, which is odorless in itself, is due to breakdown products produced by cutaneous bacterial flora.

A third type of intermediate sweat gland, the apo-eccrine gland, has also been described in axillary skin but its existence is not universally accepted.

Dermal–epidermal junction

The interface between the lower part of epidermis and the top layer of dermis consists of a complex network of interacting macromolecules that form the cutaneous basement membrane zone (BMZ) (*Figs 1.72*, *1.73*).[1] Many of

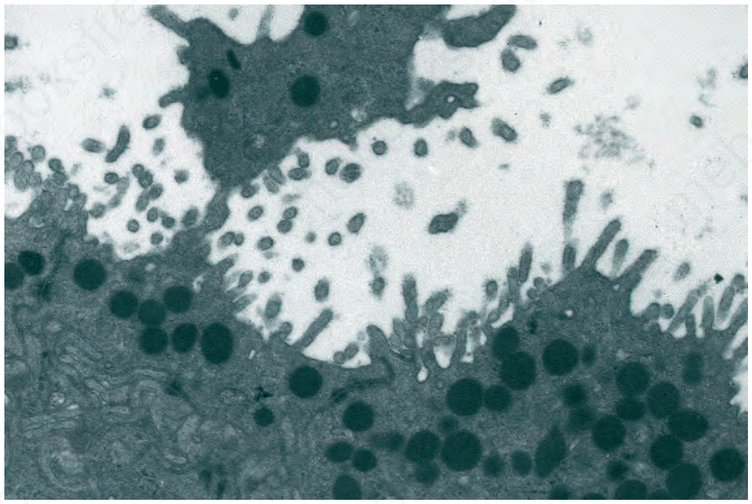

Fig. 1.71
Apocrine gland: close-up view showing microvilli and decapitation secretion.

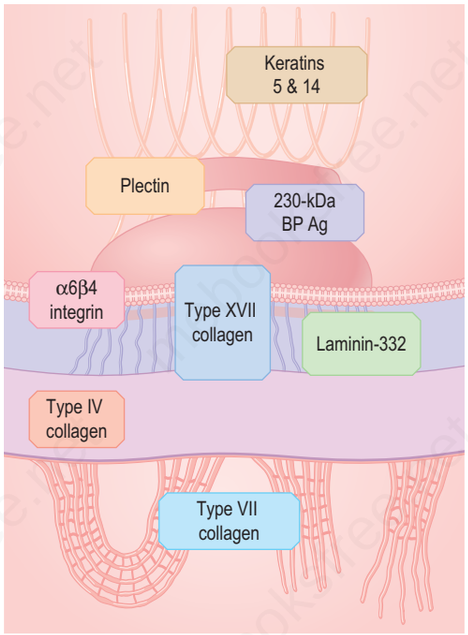

Fig. 1.72
The macromolecular components of the dermal–epidermal junction centered on a hemidesmosome-anchoring filament-anchoring fibril complex. Protein–protein interactions between these molecules secure adhesion between the epidermis and the subjacent dermis.

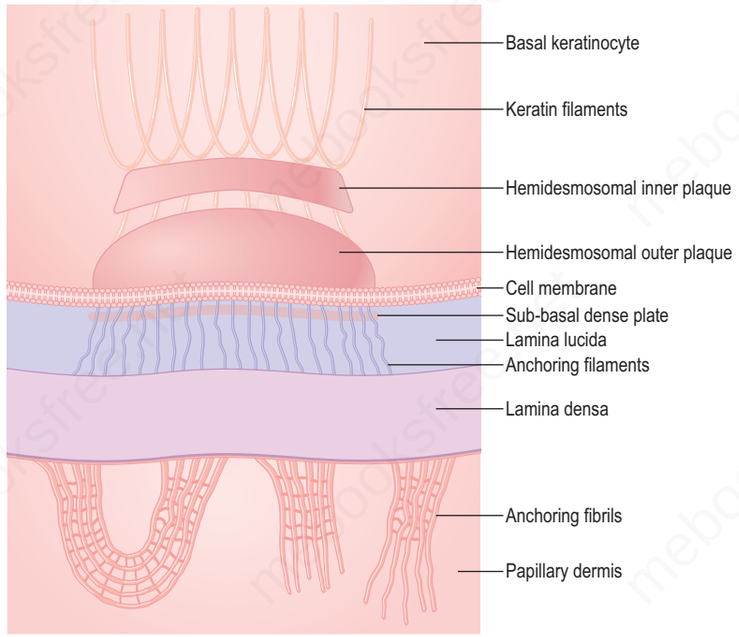

Fig. 1.73
Schematic representation of a hemidesmosome-anchoring filament-anchoring fibril complex at the dermal–epidermal junction. A continuum of adhesive proteins extends from the keratin tonofilaments within basal keratinocytes through to dermal collagen. This complex represents the main adhesion unit at the dermal–epidermal junction.

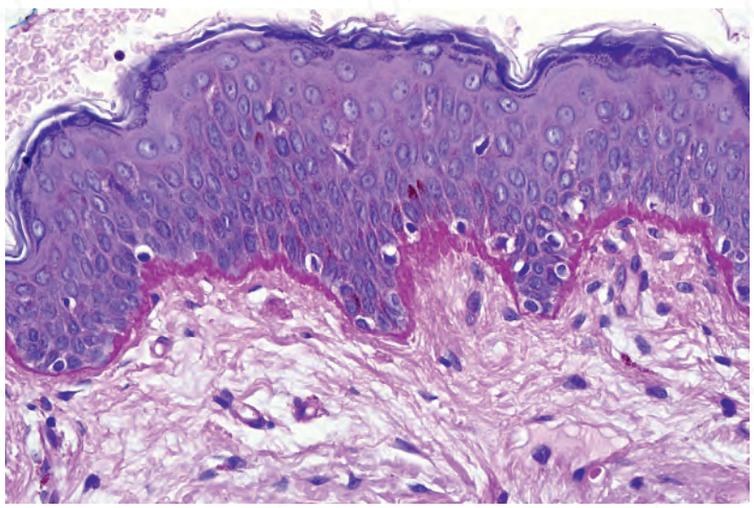

Fig. 1.74
The basement membrane region stains strongly with periodic acid-Schiff.

these components are glycoproteins and thus the BMZ can be recognized histologically as staining positive with PAS staining (*Fig. 1.74*). Ultrastructural examination of the BMZ by transmission electron microscopy shows two layers with different optical densities (*Fig. 1.75*).[2] The upper layer, the lamina lucida, is a low electron density region of 30–40 nm in breadth which is directly subjacent to the plasma membranes of basal keratinocytes. Below the lamina lucida is the lamina densa, an electron-dense region, 30–50 nm across, which interacts with the extracellular matrix of the upper dermis. Within the cutaneous BMZ distinct adhesion complexes are evident. Extending from inside the basal keratinocytes, through the lamina lucida and lamina densa, and into the superficial dermis are ultrastructurally recognizable attachment structures. The components of these adhesion units are the hemidesmosomes, anchoring filaments and anchoring fibrils.[3] The importance of these structural complexes in securing adhesion of the epidermis to the underlying dermis is highlighted by both inherited and acquired subepidermal blistering skin diseases (*Figs 1.76*, *1.77*). The precise role of individual proteins in adhesion is demonstrated by the group of inherited skin blistering diseases, epidermolysis bullosa, in which components in the hemidesmosomal structures, anchoring filaments, or anchoring fibrils are genetically defective or absent.[4] Other rare forms of epidermolysis bullosa can result from mutations in vesicle transport proteins (exophilin-5) or components of focal contacts at the dermal–epidermal junction (kindlin-1 or α3 integrin), as well as desmosomal proteins (plakophilin-1, desmoplakin, and plakoglobin) and during cornification (transglutaminase-5).[5] Collectively, these mutations lead to skin and sometimes mucous membrane fragility following minor trauma. The level of blistering in epidermolysis bullosa may vary from at or just above the dermal–epidermal junction to within the epidermis to above the granular cell layer, depending on the mutated protein.

The hemidesmosomes extend from the intracellular compartment of the basal keratinocytes to the cell membrane adjacent to the lamina lucida in the upper portion of the dermal–epidermal basement membrane. The inner plaques of hemidesmosomes serve as attachment sites for keratin filaments while the outer plaques associate with anchoring filaments that traverse the lamina lucida. Subjacent to the hemidesmosomal outer plaques in the lamina lucida are the sub-basal dense plates which contribute to the structural organization of the attachment complex. Intracellular hemidesmosomal proteins include the 230-kD bullous pemphigoid antigen 1 and the 500-kD plectin protein. Transmembranous hemidesmosomal proteins comprise the 180-kD bullous pemphigoid antigen (also known as type XVII collagen), and the α6 and β4 integrin molecules.[6] The hemidesmosomes are associated with anchoring filaments in the lamina lucida, thread-like structures 3–4 nm in diameter that span the lamina lucida to the lamina densa.

Located at the lamina lucida–lamina densa interface are the laminins. The major laminin within the cutaneous BMZ is laminin 332, previously known as laminin 5 (*Fig. 1.78*). In addition, laminin 111 (laminin 1), laminin 311 (laminin 6), laminin 321 (laminin 7) and laminin 511 (laminin 10) are also integral components of the dermal–epidermal junction.[7] The cruciform structure of laminins contains both globular and rodlike segments which contribute to interactions with other extracellular matrix molecules, as well as cell attachment and spreading, and cellular differentiation. The critical role of laminin 332 in providing integrity to the cutaneous BMZ is evident from findings that mutations in any of the three polypeptide subunits (the α3, β3, or γ2 chains) can result in junctional forms of epidermolysis bullosa.

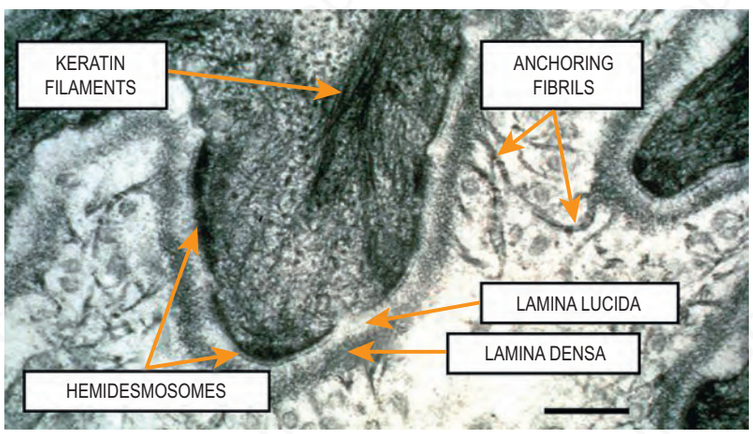

Fig. 1.75
Transmission electron microscopy of the dermal–epidermal junction. Bar = 200 nm.

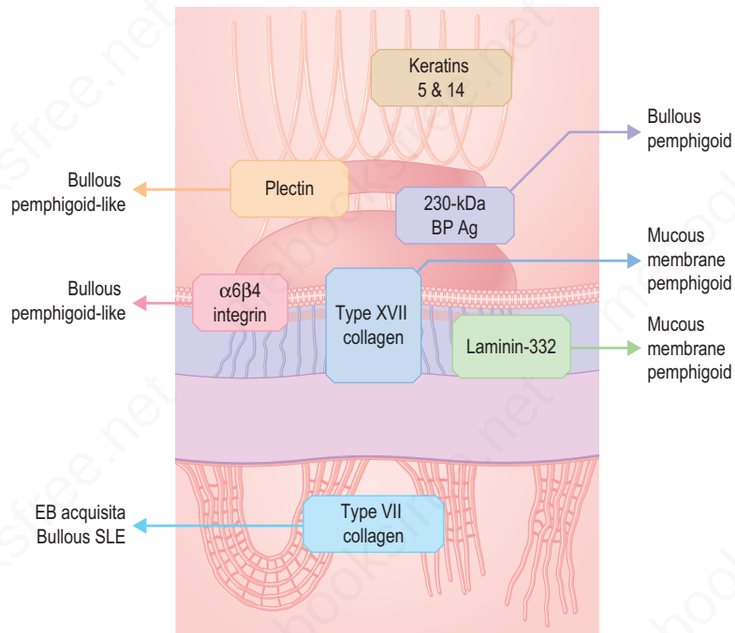

Fig. 1.77
Acquired disorders of hemidesmosomal proteins. Autoantibodies directed against components of the hemidesmosome-anchoring filament-anchoring fibril complex give rise to specific subepidermal autoimmune blistering diseases. *SLE,* systemic lupus erythematosus; *EB,* epidermolysis bullosa.

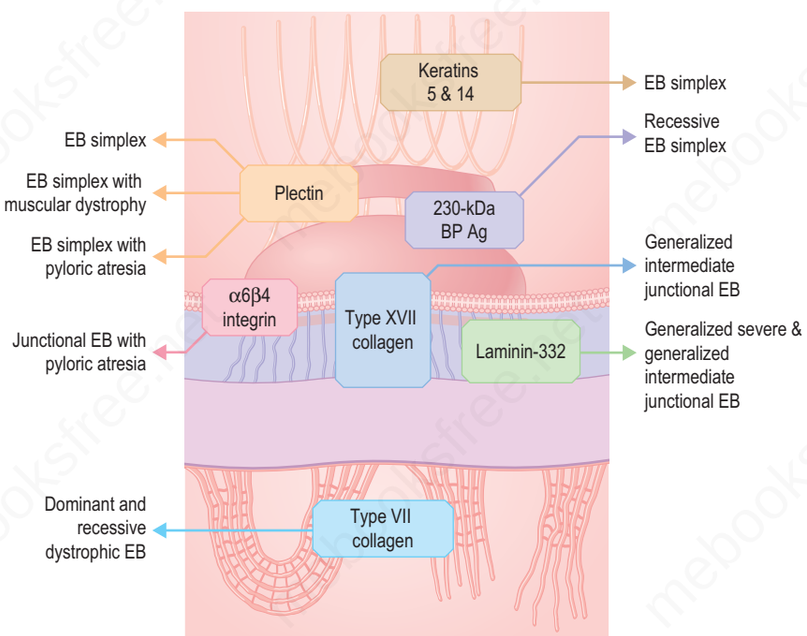

Fig. 1.76
Genetic disorders of hemidesmosomal proteins. Mutations in components of the hemidesmosome-anchoring filament-anchoring fibril network give rise to specific variants of epidermolysis bullosa (EB).

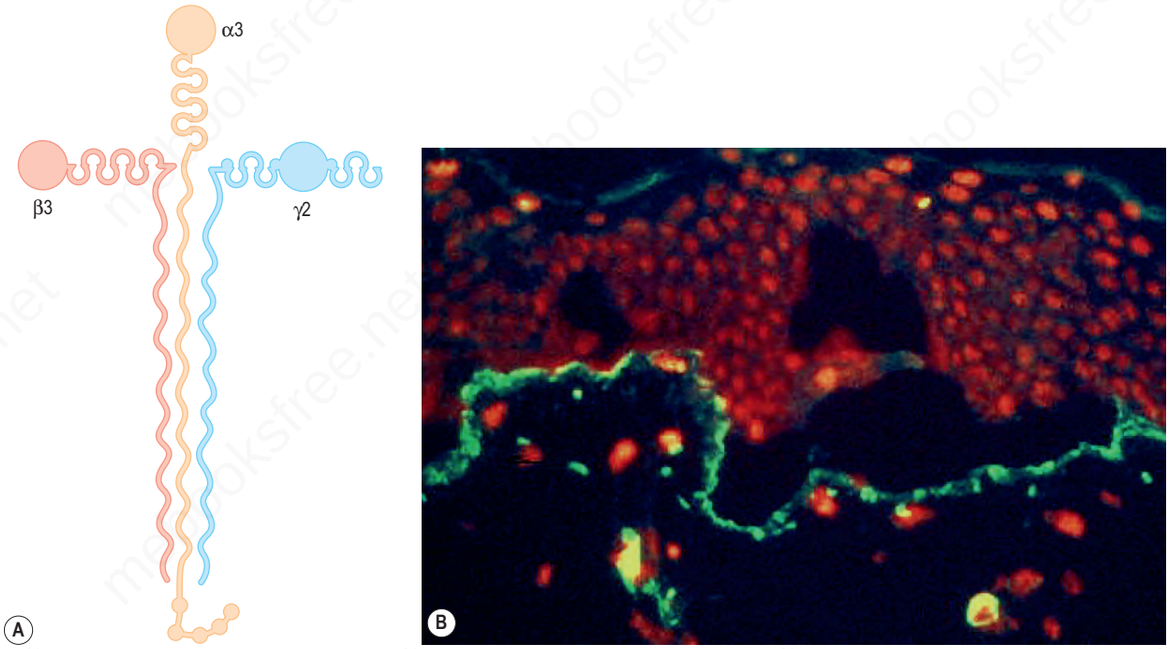

Fig. 1.78
Laminin-332 is a major adhesion protein at the dermal–epidermal junction: (**A**) the protein is composed of three polypeptide chains: α3, β3, and γ2; (**B**) Laminin-322 identified by immunofluorescence in a sample of split skin.

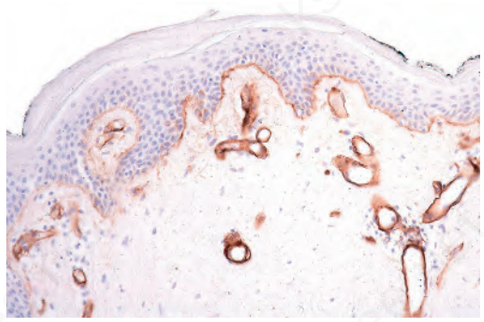

Fig. 1.79
Basement membrane: basement membrane staining with type IV collagen.

The major component of the lamina densa is type IV collagen, which in skin is mainly composed of the α1 and α2 chains.[8] Type IV collagen is assembled to form a complex hexagonal arrangement which allows high flexibility to the BMZ and facilitates interactions with other collagenous and noncollagenous proteins (*Fig. 1.79*). Other BMZ components at the dermal–epidermal junction include the glycoprotein nidogen (previously known as entactin) which interacts with type IV collagen either alone or as part of a laminin-nidogen complex. Also present are the heparan sulfate proteoglycans, which are highly negatively charged and hydrophilic and capable of interacting with a number of basement membrane components and thus contribute to the architectural organization of the BMZ.[9]

Anchoring fibrils are ultrastructurally recognizable fibrillar structures which extend from the lower part of lamina densa to the upper reticular dermis. The main component of anchoring fibrils is type VII collagen (*Fig. 1.80*).[10] Individual type VII collagen molecules are ≈450 nm long and by complexing as antiparallel dimmers and aggregating laterally, they form loops which are traversed by interstitial dermal collagens (mainly types I and III) to adhere the BMZ to the underlying dermis.[11] Type VII collagen is synthesized by both dermal fibroblasts and epidermal keratinocytes. Also inserting into the lamina densa at the dermal–epidermal junction are elastic microfibrils, containing proteins such as fibrillin. Fibrillin-containing

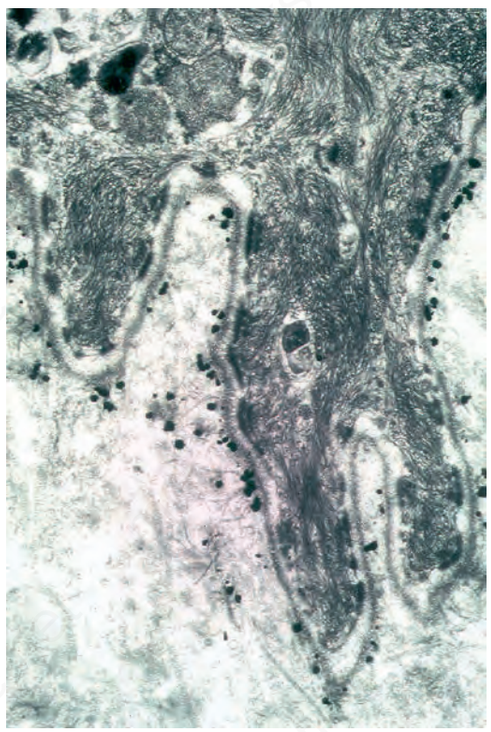

Fig. 1.80
Normal skin: the anchoring fibrils are composed predominantly of type VII collagen as shown in this pre-embedding immunogold electron microscopic preparation.

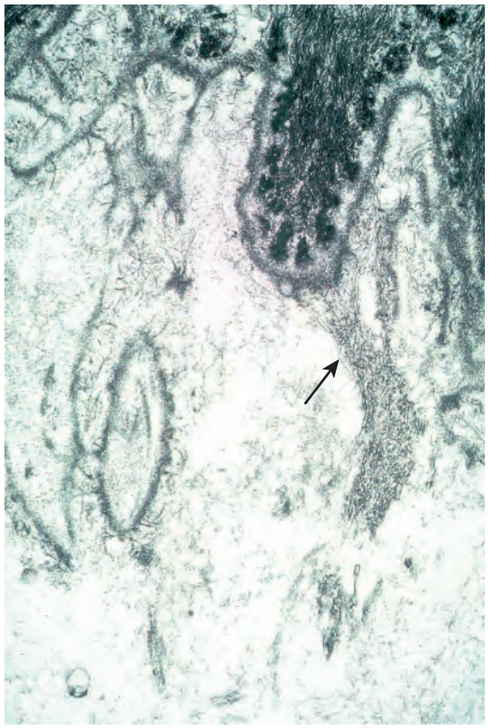

Fig. 1.81
Normal skin: this ultrastructural image shows a well-formed dermal microfibril bundle (*arrowed*).

microfibrils may exist as a fibrillar mantle surrounding an elastin core or be found independently as elastin-free microfibrils. The latter, located beneath the lamina densa, are known as the dermal microfibril bundles (*Fig. 1.81*).

Dermal collagen

The major extracellular matrix component in the dermis is collagen. Currently, 29 distinct collagens have been identified in vertebrate tissues and each is designated a Roman numeral in the chronological order of its discovery. At least eight different collagens are found in human skin. All collagen molecules consist of three subunit polypeptides which can either be identical in homotrimers or can consist of two or even three genetically different polypeptides in heterotrimeric molecules. Since the different subunits are all distinct gene products, there are well over 40 different genes in the human genome that encode the different subunit polypeptides.[1] Collagens demonstrate considerable tissue specificity and are synthesized by a number of different cell types, including dermal fibroblasts, keratinocytes, vascular endothelial cells, and smooth muscle cells. A characteristic feature of collagen is the presence of hydroxyproline and hydroxylysine residues, amino acids that are post-translationally synthesized by hydroxylation of proline and lysine residues, respectively. These hydroxylation reactions take place in the rough endoplasmic reticulum by prolyl and lysyl hydroxylases, respectively, enzymes that require ascorbic acid, molecular oxygen and ferrous iron as cofactors. The hydroxylation of prolyl residues is necessary for stabilization of the triple-helical conformation at physiologic temperatures, and hydroxylysyl residues are required for formation of stable covalent cross-links. In the rough endoplasmic reticulum, trimeric molecules are formed and following the prolyl hydroxylation reactions, triple helices are generated which are then secreted through Golgi vesicles into the extracellular space. Here, parts of the noncollagenous peptide extensions are cleaved by specific proteases, and the collagen molecules undergo supramolecular organization. To acquire fibrillar strength, the fibers are then covalently linked together by specific intra- and intermolecular cross-links. The most common forms of cross-links in type I collagen are derived from lysine and hydroxylysine residues, and in some collagens there are also cysteine-derived disulfide bonds. On the basis of their fiber architecture in tissues, collagens can be divided into different classes. Types I, II, III, V and IX align into large fibrils and are designated as fibril-forming collagens. Type IV is arranged in an interlacing network within the basement membranes, while type VI is a distinct microfibril-forming collagen and type VII collagen forms anchoring fibrils. Fibril-associated collagen with interrupted triple helix (FACIT) collagens (fibril-associated collagens with interrupted triple-helices), include types IX, XII, XIV, XIX, XX, and XXI.[2] Many of the FACIT collagens associate with larger collagen fibers and act as molecular bridges stabilizing the organization of the extracellular matrices.

Type I collagen, the most abundant form of collagen, is the predominant collagen in human dermis, accounting for approximately 80% of total collagen. Type I collagen associates with type III collagen to form broad, extracellular fibers in the dermis. Mutations in the type I and III collagens or in their processing enzymes can result in connective tissue abnormalities seen in different forms of the Ehlers-Danlos syndrome, and mutations in the type I collagen gene lead to osteogenesis imperfecta.[3]

Type III collagen accounts for about 10% of the total collagen in adult dermis, although it is the predominant dermal collagen in the fetus. It predominates in vascular connective tissues, the gastrointestinal tract, and the uterus, and mutations in the type III collagen gene occur in the vascular type of the Ehlers-Danlos syndrome.

Type V collagen is present in most connective tissues, including the dermis, where it represents less than 5% of the total collagen. Type V collagen is located on the surface of large collagen fibers in the dermis, and its function is to regulate their lateral growth. A lack of type V collagen leads to variable collagen fiber diameters and an irregular fiber contour in cross-section. Such fibers are seen in autosomal dominant forms of Ehlers-Danlos syndrome associated with mutations in the type V collagen gene.

Mature collagen fibers are relatively inert and can exist in tissues under normal physiologic conditions for long periods. However, there is some continuous turnover of collagen that involves a number of enzymes of the matrix metalloproteinases (MMP) family. These proteinase families include the collagenases, gelatinases, stromelysins, matrilysins, and the membrane-type MMPs.[4] The MMPs are synthesized and secreted as inert proenzymes which become activated proteolytically by removal of the propeptide. The MMPs are zinc metalloenzymes and require calcium for their activity. The MMPs also have specific small molecular weight peptide inhibitors, known as tissue inhibitors of metalloproteinases (TIMPs). These proteins stoichiometrically complex with MMPs to prevent collagen degradation. In normal human skin, a number of MMPs are synthesized and secreted by fibroblasts and keratinocytes. The expression of these enzymes is enhanced in various pathologic states, including invasion and metastasis of cutaneous malignancies, as well as during dermal wound healing.

Within the papillary dermis, collagen fibers are fine and often vertically orientated whereas reticular dermal collagen consists of broad, thick bundles generally arranged parallel to the surface epithelium (*Figs 1.82*, *1.83*). When longitudinal sections of collagen are examined by transmission electron microscopy they show cross-striations with a periodicity of approximately 64 nm (*Fig. 1.84*). The cross-striations are seen because of the longitudinal overlap of individual collagen molecules, which occurs during assembly of the mature fibril. Fibrous long-spacing collagen is a variant with a periodicity of 90–120 nm (*Fig. 1.85*). It is characteristically seen in peripheral nerve and central nervous system tumors. Collagen bundles exhibit anisotropy and are therefore birefringent when viewed with polarized light (*Fig. 1.86*).

Dermal elastic tissue

The elastic fiber network provides resilience and elasticity to the skin.[1] Elastic fibers are a relatively minor component in normal sun-protected adult skin, comprising less than 2–4% of the total dry weight of the dermis. The configuration of elastic fibers in the reticular dermis consists of horizontally orientated fibers which interconnect (*Fig. 1.87*).[2] Extending from these into the papillary dermis is a network of vertical extensions of relatively fine fibrils which consist either of bundles of microfibrils (oxytalan fibers) or of small amounts of cross-linked elastin (elaunin fibers) (*Fig. 1.88*).[3] Elastic

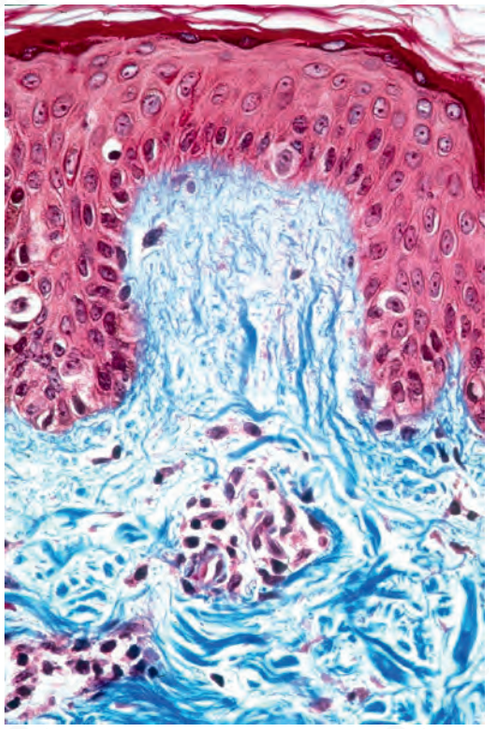

Fig. 1.82
Normal skin of forearm: in the papillary dermis the collagen fibers are fine and sometimes have a vertical orientation. Masson trichrome.

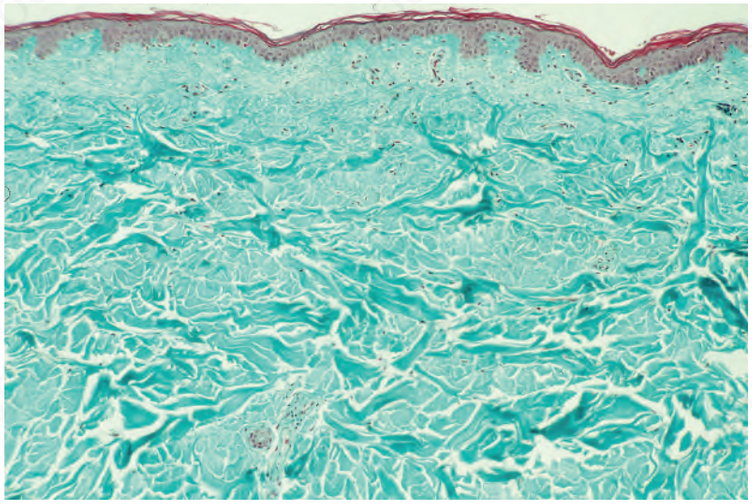

Fig. 1.83
Normal skin of back: broad bundles of collagen typify the reticular dermis. Masson trichrome.

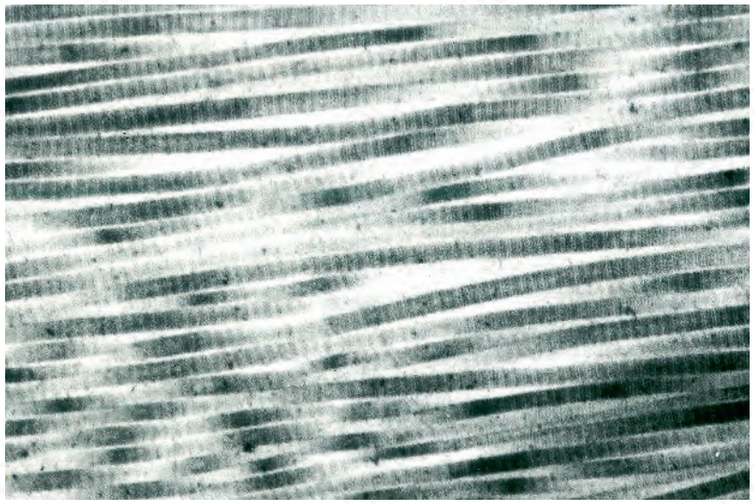

Fig. 1.84
Collagen: it is characterized by cross-striations with a periodicity of 64 nm.

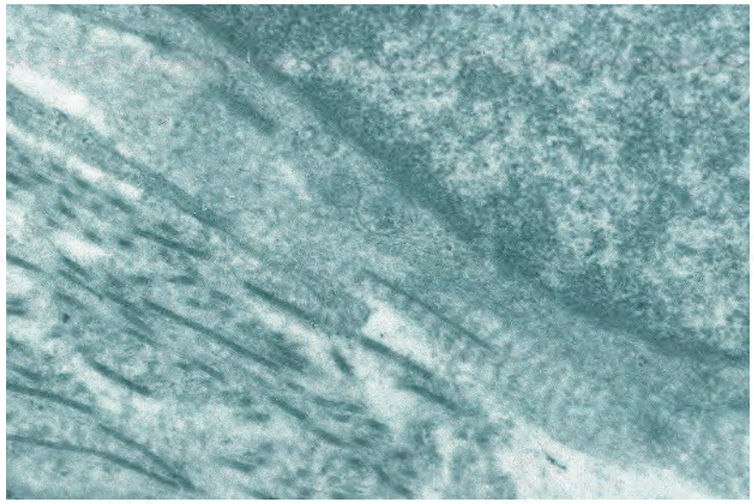

Fig. 1.85
Fibrous long-spacing collagen: compare with the adjacent conventional collagen fibers. There is a very different periodicity.

fibers have two principal components: elastin, which is a connective tissue protein that forms the core of the mature fibers, and the elastin-associated microfibrils which consist of a family of proteins. Examination by transmission electron microscopy reveals an elastin core that makes up over 90% of the elastic fiber and which is surrounded by more electron-dense microfibrillar structures (*Fig. 1.89*).

Elastin is initially synthesized as a precursor polypeptide, tropoelastin, which consists of approximately 700 amino acids with a molecular mass of ≈70 kD.[4] The amino acid composition of tropoelastin is similar to collagen in that about one-third of the total amino residues consist of glycine but the primary sequence is different, with domains rich in glycine, valine, and proline, alternating with lysine- and alanine-rich sequences: a characteristic sequence motif is the presence of two lysine residues separated by two or three alanine residues. The lysine residues in tropoelastin are critical for the formation of covalent cross-links between desmosine and its isomer, isodesmosine, which appear to be unique to elastin. The first step in formation of these elastin-specific cross-links is oxidative deamination of three lysine residues to formaldehydes, known as allysines. These aldehydes, with additional lysine, fuse to form a stable desmosine compound which covalently links two of the tropoelastin polypeptides. Addition of desmosines to other parts of the molecule progressively converts tropoelastin molecules into an insoluble fiber structure. The oxidative deamination of lysyl residues to corresponding aldehydes is catalyzed by a group of enzymes, lysyl oxidases, which require copper for their activity. Thus, copper deficiency can lead to reduced lysyl oxydase activity and synthesis of elastic fibers that are not stabilized by sufficient amounts of desmosines. In such a situation, the individual tropoelastin polypeptides remain soluble and susceptible to non-specific proteolysis, and the elastin-rich tissues are fragile. The metabolic turnover of elastin is slow, but is increased in some forms of cutis laxa and cutaneous aging. Elastic fibers are degraded by elastases and metalloelastases.

The elastin-associated microfibrils consist of tubular structures of ≈10–12 nm in diameter. These proteins include fibrillin, the latent transforming growth factor (TGF)-β binding family of proteins, and the fibulins. Other components comprise the families of microfibril-associated

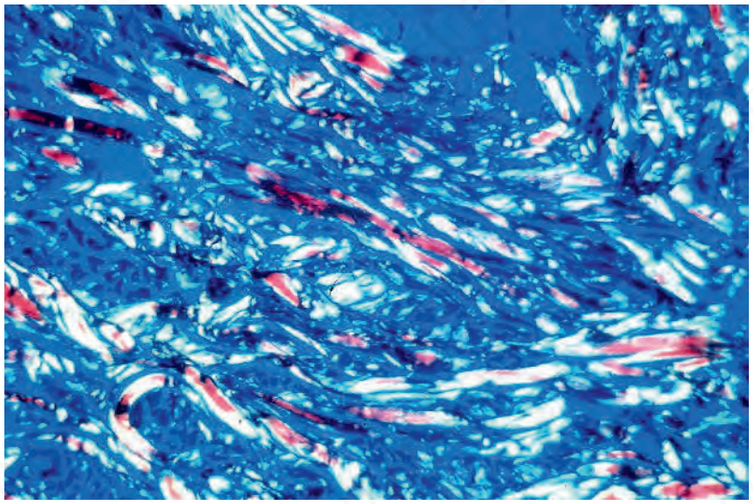

Fig. 1.86
Collagen of the reticular dermis: note the birefringence when viewed with polarized light. Masson trichrome.

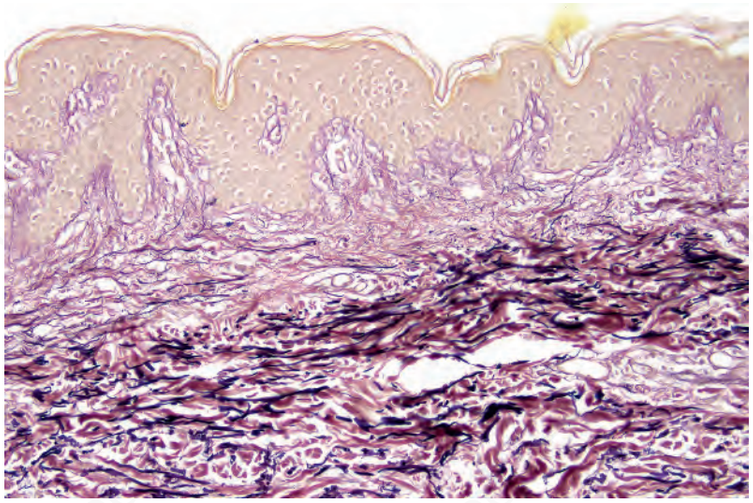

Fig. 1.87
Reticular dermis: the elastic fibers are long and fairly thick and tend to run parallel to the surface epithelium.

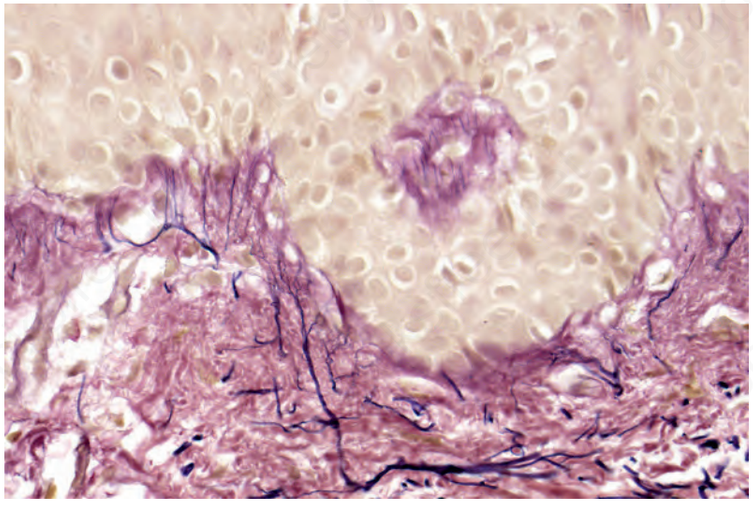

Fig. 1.88
Papillary dermis: the elastic fibers are delicate and orientated perpendicular to the epithelial surface. Weigert–van Gieson stain.

Fig. 1.89
Elastic fiber: this consists of microfibrils embedded in an electron-dense matrix called elastin.

glycoproteins and microfibril-associated proteins (MFAP), the emilins and certain lysyl oxidases. The importance of the fibrillin is illustrated by mutations resulting in Marfan syndrome with skeletal abnormalities, aortic dilatation, subluxation of the ocular lens, and cutaneous hyperextensibility.[5] Likewise, the significance of certain fibulins is evident from mutations resulting in cutis laxa, manifesting with loose and sagging skin and loss of elastic recoil.

Ground substance

Proteoglycans form a number of subfamilies defined by a core protein to which polymers of unbranched disaccharide units, glycosaminoglycans (GAGs), are linked.[1] The core proteins can be intracellular, reside on the cell surface, or be part of the extracellular matrix and the GAGs are highly charged polyanionic molecules that vary greatly in size. For example, dermal fibroblasts can synthesize versican which consists of a core protein with attachment sites for 12 to 15 GAG side chains. The GAGs in versican are primarily chondroitin sulfate or dermatan sulfate, but versican can also bind hyaluronic acid, resulting in formation of large aggregates. Proteoglycan/GAG complexes have multiple functions. For example, the proteoglycans containing heparan sulfate and dermatan sulfate have the ability to bind extracellular matrix components, including various collagens.[2] In addition, these proteoglycans bind several growth factors, cytokines, cell adhesion molecules, and growth factor binding proteins, thereby influencing the bioactivity of these molecules. They can also serve as antiproteases. In addition to binding to a number of extracellular molecules, proteoglycans also play a role in the adhesion of cells to the extracellular matrix. For example, syndecan-4, which is selectively enriched in dermal fibroblasts, facilitates the adherence of cells in conjunction with other extracellular matrix binding molecules, such as the integrins.[3] Proteoglycans also interact with other extracellular matrix molecules besides collagen; notably, chondroitin sulfate and dermatan sulfate bind fibronectin and laminin. The largest extracellular GAG, hyaluronic acid, plays an important role in providing physical and chemical properties to the skin, mediated in part by its hydrophilicity and viscosity in dilute solutions. Of particular note, hyaluronic acid has an expansive water-binding capacity, providing hydration to normal skin. Indeed, water makes up ≈60% of the weight of normal human skin in vivo. Other properties attributed to large proteoglycans complexes, such as those formed with the versican or basement membrane proteoglycans, include their ability to serve as ionic filters, regulate salt and water balance, and provide an elastic cushion.[1]

Except when present in very large amounts, ground substance cannot be easily detected by routine hematoxylin and eosin staining (*Fig. 1.90*).

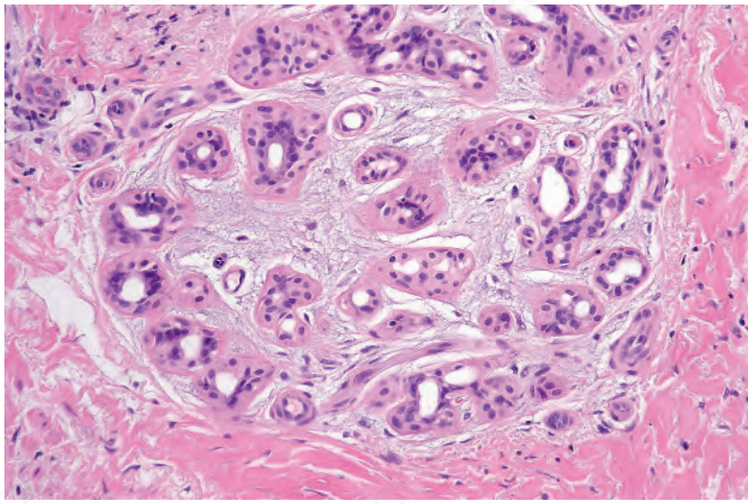

Fig. 1.90
Ground substance: an eccrine gland from the sole of the foot shows an abundance of glycosaminoglycans.

Cationic dyes, such as Alcian blue at appropriate pH and electrolyte concentration, are usually necessary for its demonstration.

Fibroblast biology

The main cell responsible for the synthesis of collagens, elastic tissue and proteoglycan/glycosaminoglycan macromolecules in the dermis is the fibroblast.[1] In the mid-dermis of postnatal skin, the number of fibroblasts ranges from 2100 to 4100 per mm^3, and the cells have a limited replicative capacity ranging from 50–100 cell divisions. Fibroblasts also play a significant role in epithelial–mesenchymal interactions, secreting various growth factors and cytokines that have a direct effect on epidermal proliferation, differentiation and formation of extracellular matrix. The term fibroblast refers to a fully differentiated, biosynthetically active cell, while the term fibrocyte refers to an inactive cell.

Myofibroblasts are a specialized form of fibroblast found in granulation tissue and are involved in wound contraction. They are functionally distinct from other fibroblasts with ultrastructural, biochemical and physical features of smooth muscle cells. Moreover, myofibroblasts are characterized by the presence of intracellular bundles of α smooth muscle actin, which is the actin isoform expressed by smooth muscle cells. Currently it is thought that the evolution of myofibroblasts involves a preceding form known as the protomyofibroblast, although the latter do not always become the fully differentiated myofibroblast. In contrast to myofibroblasts, protomyofibroblasts have stress fibers but no α smooth muscle actin filaments. A biosynthetically active fibroblast has an abundant cytoplasm, well-developed rough endoplasmic reticulum, and prominent ribosomes attached to the membrane surfaces.

Fibroblasts from different anatomical sites all have similar morphology but fibroblasts in different sites have their own gene-expression profiles and characteristic phenotypes, synthesizing extracellular matrix proteins and cytokines in a site-specific manner.[2] Moreover, embryologically fibroblasts in the papillary dermis appear to be distinct from those in the reticular dermis.[3] The former contribute to hair follicle growth, whereas the latter have more prominent roles in formation of adipocytes and in wound healing.

Dermal fibroblasts have numerous functions, not only in synthesizing and depositing extracellular matrix components, but also in proliferation and migration in response to chemotactic, mitogenic and modulatory cytokines, and also autocrine and paracrine interactions. Autocrine activity includes the TGF-β-induced synthesis and secretion of connective tissue growth factor which promotes collagen synthesis as well as fibroblast proliferation. Paracrine activity affects keratinocyte growth and differentiation, specifically through fibroblast secretion of keratinocyte growth factor (KGF), granulocyte-macrophage colony-stimulating factor (GM-CSF), interleukin (IL)-6 and fibroblast growth factor (FGF)-10. Fibroblasts also contribute to basement membrane formation partly by producing type IV collagen, type VII collagen, laminins and nidogen, but also through the secretion of cytokines, such as TGF-β, that stimulate keratinocytes to produce basement membrane components.

Neovascularization and lymphangiogenesis are also important processes for the maintenance of normal skin homeostasis and wound healing, for which fibroblasts have an important paracrine role. Members of the vascular endothelial growth factor (VEGF) family include VEGF-A, -B, -C, and -D, which are produced by normal human fibroblasts and are important in regulating vascular and lymphatic endothelial cell proliferation through specific receptors.

There is, however, considerable heterogeneity within fibroblast populations. For example, fibroblasts isolated from the papillary dermis compared to the reticular dermis have higher rate of synthesis of type III collagen and there can be as much as 30-fold differences in the level of fibronectin expression within individual cells. Fibroblasts from the papillary dermis appear smaller, grow faster and have a longer replicative lifespan.[4] When co-cultured with keratinocytes, papillary dermal fibroblasts produce a more differentiated and organized epidermis with complete formation of the dermal–epidermal junction. Papillary dermal fibroblasts also produce more GM-CSF and relatively less KGF than reticular dermal fibroblasts. In addition, there are differences in the synthesis of some extracellular matrix components, such as decorin. While fibroblasts demonstrate certain variability in their gene expression profiles they are considered fully differentiated cells with relatively little plasticity. Recent observations, however, suggest that fibroblasts can be induced to become pluripotent stem cells (iPS), essentially indistinguishable from the embryonic stem cells, by transduction of cultured fibroblasts with four transcription factors, Oct4, Sox2, Klf4, and c-myc.[5]

Cutaneous blood vessels and lymphatics

The skin receives a rich blood supply from perforating vessels within the skeletal muscle and subcutaneous fat.[1] Most of the blood flow is directed toward the more metabolically active constituents of the skin, namely the epidermis, hair papillae and the adnexal structures. While the dermal papillae are richly vascularized, no capillaries actually enter the epidermis, which receives its nutrition by diffusion. The subcutaneous vessels give rise to two vascular plexuses linked by intercommunicating vessels: the deep vascular plexus lies in the region of the interface between the dermis and subcutaneous fat, and the superficial vascular plexus lies in the superficial aspects of the reticular dermis and supplies the papillary dermis with a candelabra-like capillary loop system (*Fig. 1.91*). Each loop consists of an ascending arterial limb and a descending venous limb. The vessels of the dermal papillae comprise terminal arterioles, arterial and venous capillaries, and postcapillary venules, with the last predominating. Within the deep vascular plexus are small muscular arteries, which give rise to the arterioles that supply the superficial vascular plexus (*Fig. 1.92*).

The histology of these plexuses is similar, the difference being one of size rather than structure (arterioles have a diameter of less than 0.3 mm).[2] From the lumen outwards the arteriole consists of a very thin intima resting against a conspicuous internal elastic lamina. Next to this is the media, consisting of two layers of smooth muscle, which constitutes the bulk of the vessel. The adventitia surrounding the media is composed of loose connective tissue. In small muscular arteries (but not arterioles), the adventitia often contains elastic fibers constituting the external elastic lamina. Small arterioles have an endothelium surrounded by a single layer of smooth muscle. Capillaries consist of a single layer of endothelial cells, but may have adjacent pericytes, which have less well-developed dense bodies and fewer filaments than smooth muscle cells. Endothelial cells and pericytes form tight junctions. Venous capillaries have numerous pericytes and a multilayered basement membrane in contrast to arterial vessels where the basement membrane is solitary and homogeneous. Each dermal papilla is supplied by a single capillary loop. Endothelial cells contain vimentin filaments,

Weibel-Palade bodies measuring approximately 0.1 × 3.0 µm (containing factor VIII) and numerous pinocytotic vesicles (*Figs 1.93*, *1.94*). Postcapillary venules are larger, but have the same basic structure as capillaries. Their wall is devoid of smooth muscle. The small muscular venules into which the postcapillary venules drain have an intima made up of flattened endothelial cells surrounded by a smooth muscle layer one or two cells thick. They are therefore similar to small arterioles, but with much wider lumina. Veins are composed of an endothelium surrounded by a muscle coat several layers thick. Typically, an internal elastic lamina is poorly represented. There is usually a thick connective tissue adventitia, but elastic fibers are absent; only very large muscular veins have elastic tissue (*Fig. 1.95*).

Also present in the dermis are veil cells, which surround all the microvessels and separate them from the adjacent connective tissue. Veil cells are long, thin cells with an attenuated cytoplasm, and they more closely resemble fibroblasts than pericytes. They do not have a basement membrane investment and are located outside the vessel wall.

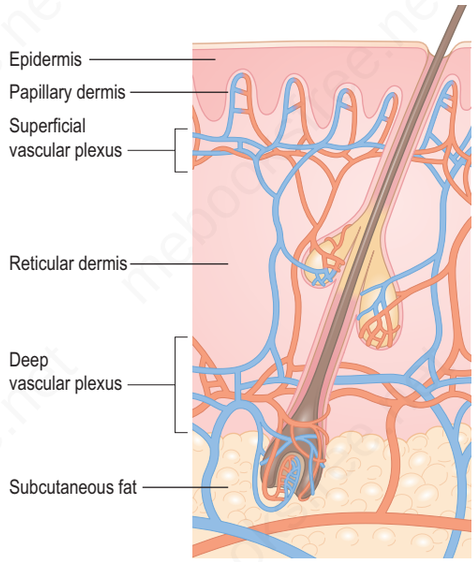

Fig. 1.91
Relationship of the superficial and deep vascular plexuses.

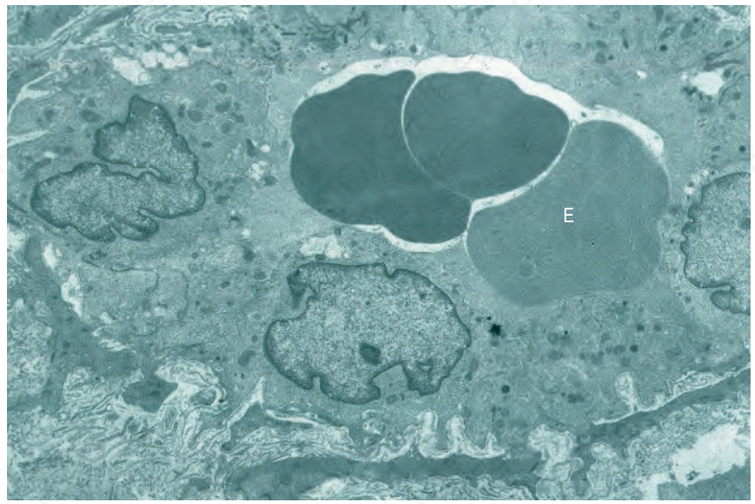

Fig. 1.93
Normal dermal capillary: note the lining of endothelial cells surrounded by a pericyte cell process and adjacent basal lamina. The lumen contains erythrocytes (*E*).

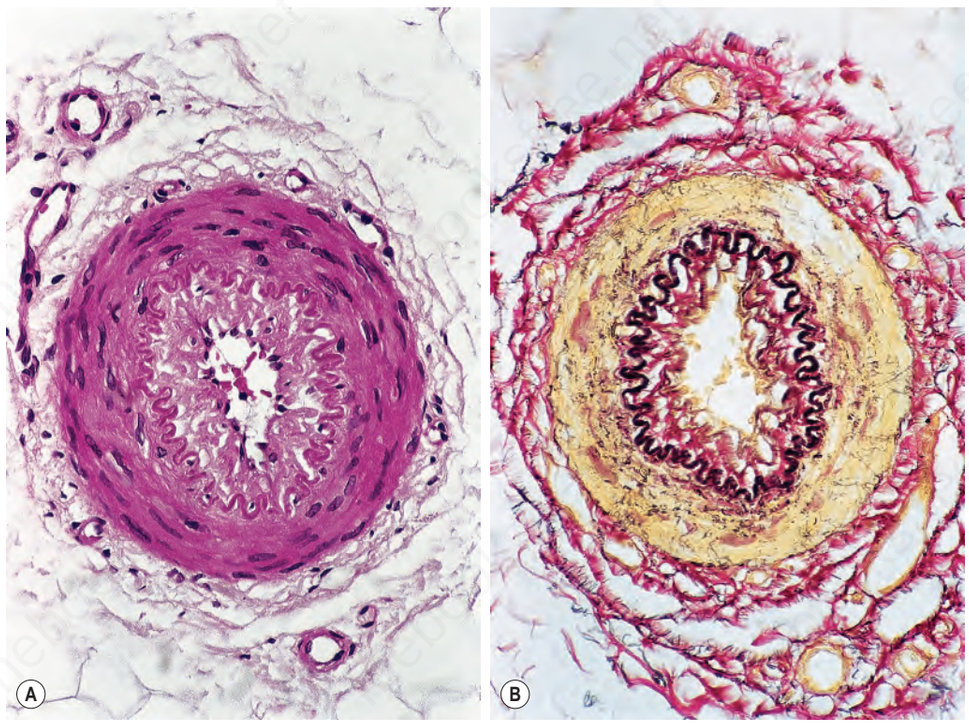

Fig. 1.92
Small muscular artery from the deep vascular plexus from the lower leg of an elderly man with endarteritis (intimal thickening): note the thick muscle coat and conspicuous internal elastic lamina, the latter accentuated by the Weigert–van Gieson reaction. (**A**) Hematoxylin and eosin; (**B**) Weigert–van Gieson.

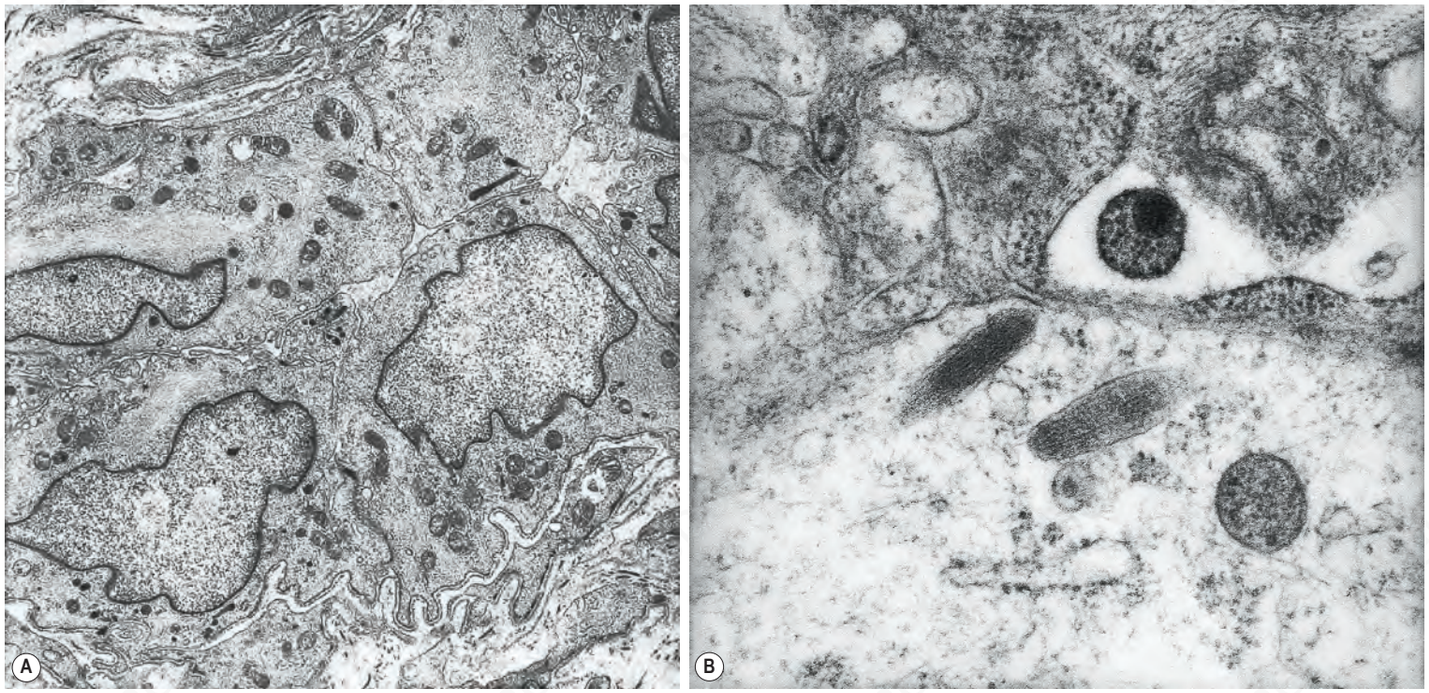

Fig. 1.94
(**A**) Small dermal arteriole: the lumen is compressed to a narrow slitlike space; (**B**) high-power view of typical Weibel-Palade bodies. These are characteristic of blood vessel endothelium.

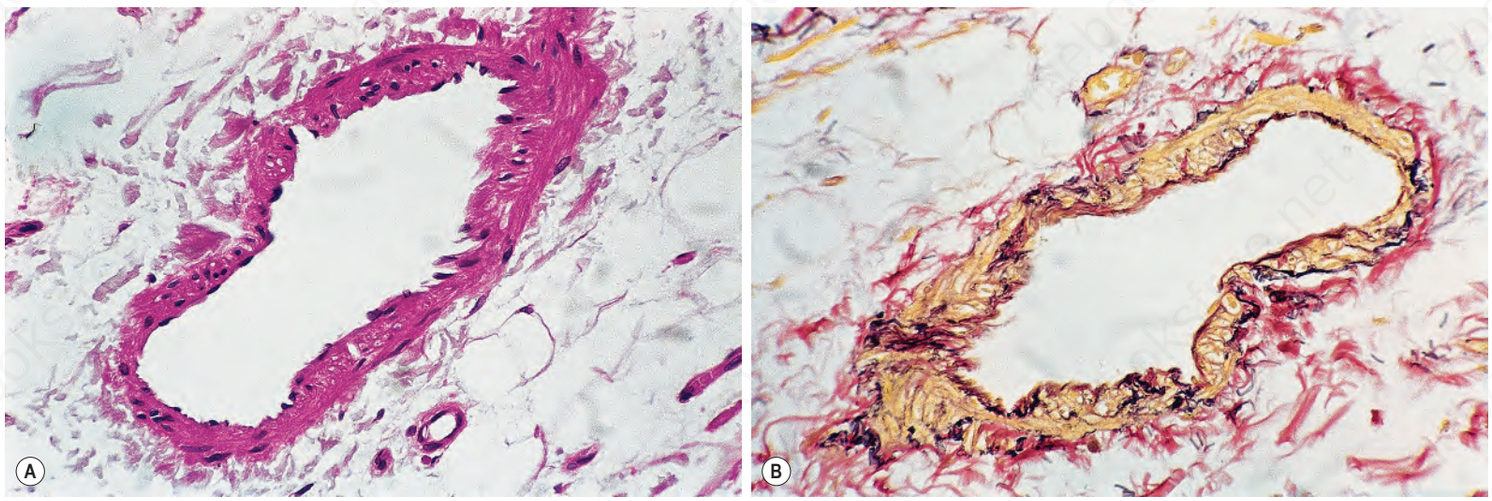

Fig. 1.95
Companion vein to *Fig. 1.92*: note the wide diameter of the lumen in comparison to the relatively thin muscle coat. There is a little elastic tissue but no discernible internal elastic lamina. (**A**) Hematoxylin and eosin; (**B**) Weigert–van Gieson.

The capillary loop in the dermal papilla has an ascending arterial component and an intrapapillary segment, which is characterized by a hairpin turn and a descending venous capillary segment. Capillary loops run perpendicular to the skin surface, except in the nail where they have a parallel orientation.

The dermis is richly supplied with arteriovenous anastomoses. Specialized shunts (glomus bodies), found primarily in the dermis of the fingertips, consist of an arterial segment (Sucquet-Hoyer canal), which connects directly to the venous limb (*Fig. 1.96*). The canal is surrounded by several layers of modified smooth muscle cells (glomus cells) with a particularly rich nerve supply. Glomus bodies function as sphincters, allowing the capillaries of the superficial dermis to be bypassed, therefore increasing the venous return from the extremities.

Cutaneous blood flow (under hypothalamic control) is of extreme importance in thermoregulation. Mediated by the autonomic nervous system, heat loss can be increased or decreased by varying the blood flow to the superficial vascular plexuses. If the environmental temperature exceeds that of the body, then the blood flow to the papillary dermis increases. A concomitant increase in eccrine sweat gland secretion, evaporation of which cools the outer parts of the body, lowers the temperature of the circulating blood and maintains a stable core temperature. Temperature control therefore depends on a delicate interplay between both vascular and sweat gland functions.

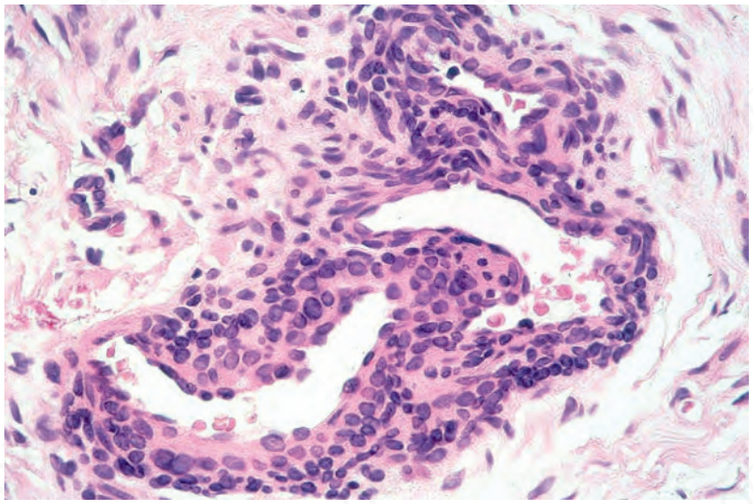

Fig. 1.96
Glomus body: note the arterial and venous limbs connected by a vascular channel rich in glomus cells.

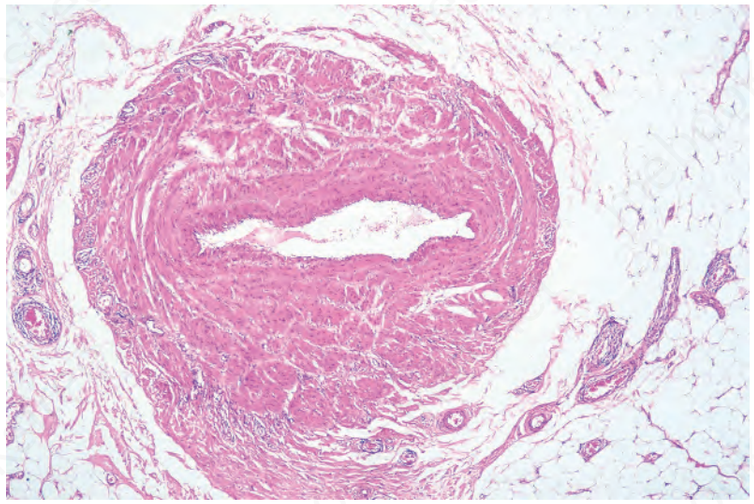

Fig. 1.98
Skin of lower leg: muscular lymphatic trunks can be readily mistaken for arteries. An internal elastic lamina is characteristically absent.

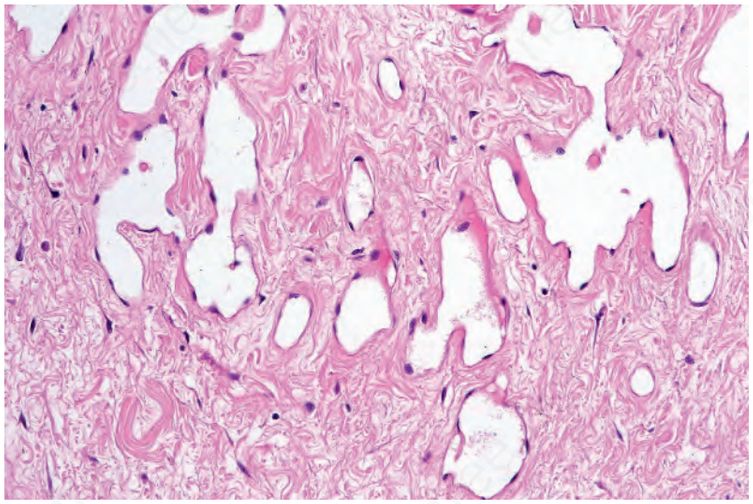

Fig. 1.97
Lymphatics: these exceedingly thin-walled channels are normally not visible in the dermis. They become readily apparent, however, when obstructed, as in this patient with lymphedema.

The dermis also contains an extensive lymphatic system, which is closely associated with the vascular plexuses.[3] Although largely disregarded except for their role in tumor spread, lymphatics are of major importance in removing the debris of daily wear and tear including fluid, cells and macromolecules (*Fig. 1.97*). They also represent the primary disposal mechanism for contaminating microorganisms. Lymphatics have been shown to supply the major route for epidermal Langerhans cells to reach the regional lymph node following antigen stimulation. Under normal circumstances these delicate vessels are collapsed and are difficult to detect. They are supported by delicate elastic tissue scaffolding and consist of a large thin-walled collapsed vessel lined by attenuated endothelium and characterized by the presence of multiple valves. Their presence is much more obvious in obstructive situations (e.g., lymphedema or due to the presence of metastases). Dermal lymphatics are loosely aggregated into a superficial and deep plexus, which drain into muscularized lymphatic trunks.[4] In the lower limbs the lymphatic trunks are very thick and muscular and can be confused with an artery (*Fig. 1.98*). The absence of an internal elastic lamina readily allows their distinction. Vascular endothelial cells may be identified by the monoclonal antibodies CD31 and avian v-ets erythroblastosis virus E26 oncogene homolog (ERG) or by an anti-von Willebrand factor antibody. Lymphatic vessel endothelial hyaluronan receptor 1 (LYVE-1), Prox-1 and podoplanin may be useful immunohistochemical markers.[5] Recent genetic insights have demonstrated that lymphatic dysfunction is not a passive bystander in disease but in fact actively contributes to the pathophysiology of infection and immunity, malignancy, obesity and cardiovascular disease.[6]

Nervous system of the skin

The skin may be innervated with around one million afferent nerve fibers. Most terminate in the face and extremities; relatively few supply the back. The cutaneous nerves contain axons with cell bodies in the dorsal root ganglia. Their diameters range from 0.2 to 20.0 µm. The main nerve trunks entering the subdermal fatty tissue each divide into smaller bundles. Groups of myelinated fibers fan out in a horizontal plane to form a branching network from which fibers ascend, usually accompanying blood vessels, to form a web of interlacing nerves in the superficial dermis. The cutaneous nerves supply the skin appendages and form prominent plexuses around the hair bulbs and the papillary dermis. The afferent receptors consist of free nerve endings, nerve endings in relation to hair, and encapsulated nerve endings. Free nerve endings, of both myelinated and nonmyelinated types and with a low conduction speed, are mainly responsible for the appreciation of temperature, itch and pain. Hair follicles are supplied by an intricate network of myelinated fibers, some of which ramify as free nerve endings in the periadnexal fibrous tissue sheath, while others enter the epidermis to terminate as expansions in intimate association with Merkel cells in the external root sheath. The hair disc is a complex structure consisting of basally situated Merkel cells and an associated myelinated peripheral nerve fiber. Despite the name, it has an inconstant association with hair follicles. Hair discs are slowly adapting mechanoreceptors. Throughout their course the axons of cutaneous nerves are enveloped in Schwann cells but, as they track peripherally, an increasing number lack myelin sheaths. Most end in the dermis; some penetrate the basement membrane, but do not travel far into the epidermis.

Sensory endings are of two main kinds: corpuscular, which embrace non-nervous elements; and 'free', which do not. Corpuscular endings can, in turn, be subdivided into encapsulated receptors, of which a range occurs in the dermis, and nonencapsulated, exemplified by the Merkel 'touch spot', which is epidermal.

The most striking of the encapsulated receptors is the Pacinian corpuscle. It is an ovoid structure about 1 mm in length, which is lamellated in cross-section like an onion, and is innervated by a myelinated sensory axon,

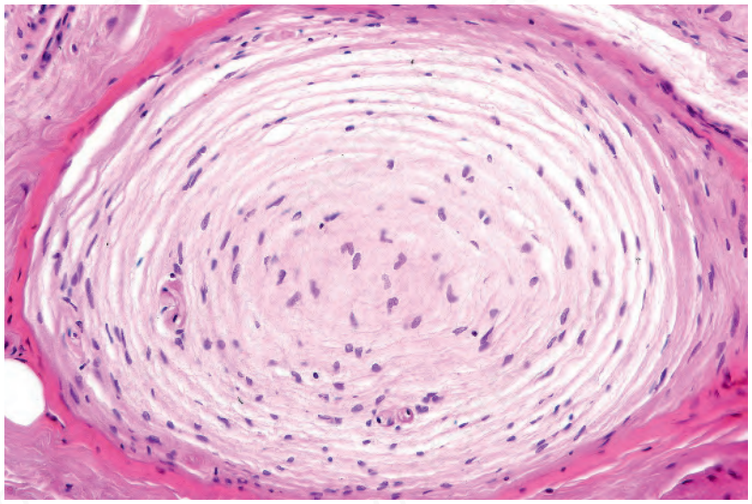

Fig. 1.99
Pacinian corpuscle: note the characteristic lamellar internal structure.

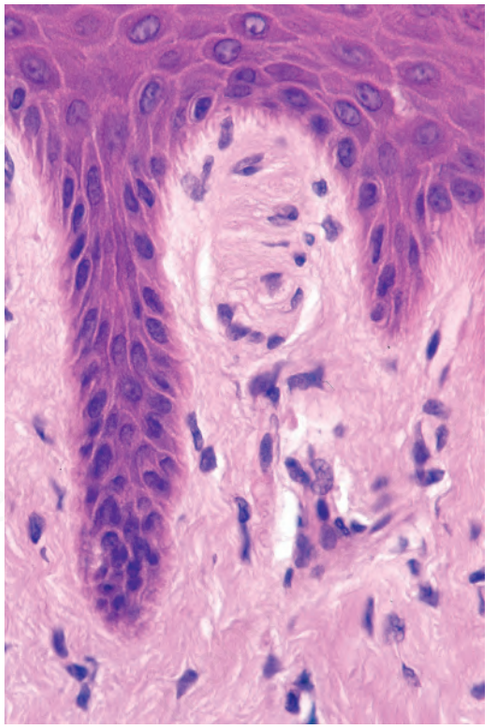

Fig. 1.100
Meissner corpuscle within a dermal papilla: with hematoxylin and eosin staining it appears as perpendicularly orientated lamellae of Schwann cells.

which loses its sheath as it traverses the core (*Fig. 1.99*). Pacinian corpuscles are responsible for the appreciation of deep pressure and vibration and are found predominantly in the subcutaneous fat of the palms and soles, dorsal surfaces of the digits, around the genitalia, and in ligaments and joint capsules.

The Golgi-Mazzoni corpuscle found in the subcutaneous tissue of the human finger is similarly laminate but of much simpler organization. Another classical receptor is the Krause end bulb, an encapsulated swelling on myelinated fibers situated in the superficial layers of the dermis.

Meissner corpuscles are characteristic of the papillary ridges of glabrous skin in primates. They have a thick, lamellated capsule, 20–40 µm in diameter and up to 150 µm long (*Fig. 1.100*).[1] Meissner corpuscles are involved in the appreciation of touch sensation (rapidly adapting mechanoreceptors) and are found predominantly in the dermal papillae of the hands and feet, the lips, and on the front of the forearm. They comprise a perineural-derived lamellated capsule surrounding a core of cells and nerve fibers, and are supplied by myelinated and nonmyelinated nerve fibers. They make intimate contact with the basal keratinocytes. Meissner corpuscles have a multiple nerve supply and each nerve may also supply multiple corpuscles. Of somewhat different structure are the terminals first described by Ruffini in human digits, in which several expanded endings branch from a single, myelinated afferent fiber. The endings are directly related to collagen fibrils. 'Free nerve-endings', which appear to be derived from nonmyelinated fibers, occur in the superficial dermis and in the overlying epidermis.[2] Those in the dermis are arranged in a tuftlike manner and have thus been designated penicillate nerve endings.

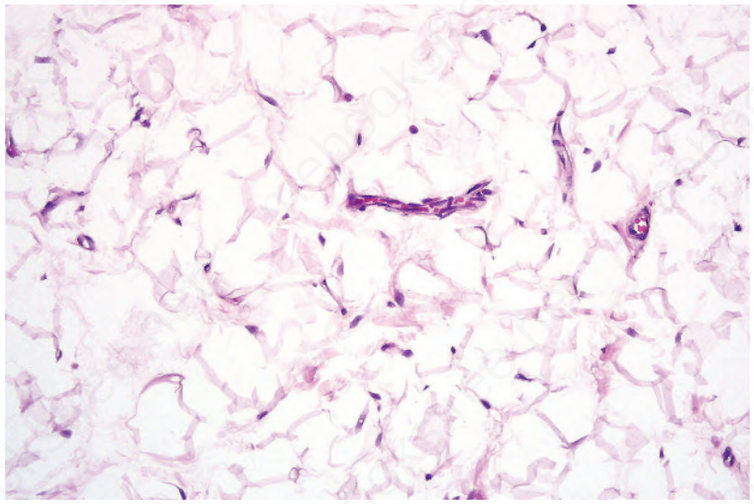

Fig. 1.101
The lipid contents of fat cells are dissolved during processing using conventional (paraffin-embedding) techniques. The cells therefore appear empty and have peripheral compressed nuclei.

Subcutaneous fat

Fat is a major component of the human body. In nonobese males, 10–12% of body weight is fat, while in females the figure is 15–20%. Eighty percent of fat is under the skin; the rest surrounds internal organs. Fat comprises white and brown adipose tissue, the latter being more common in infants and children and is characterized by different mitochondrial properties and increased heat production.[1] Historically, fat has been thought to provide insulation, mechanical cushioning and an energy store but recent data suggest that it also has an endocrine function, communicating with the brain via secreted molecules such as leptin to alter energy turnover in the body.[2] Adipocytes also have important signaling roles in osteogenesis and angiogenesis. Indeed, multipotent stem cells have been identified in human fat which are capable of developing into adipocytes, osteoblasts, myoblasts and chondroblasts. Biological clues to genes, proteins, hormones and other molecules that influence fat deposition and distribution are gradually being realized, from both research on rare inherited disorders (such as the lipodystrophies or obesity syndromes) as well as population studies on more common forms of obesity.[3]

The subcutaneous fat is divided into lobules by vascular fibrous septa, and its cells are characterized by the presence of a large single globule of lipid, which compresses the cytoplasm and nucleus against the plasma membrane (*Fig. 1.101*). The adipocyte is large, measuring up to 100 µm in diameter. The cytoplasm contains numerous mitochondria. Smooth endoplasmic reticulum is prominent and a Golgi is often conspicuous. Processing

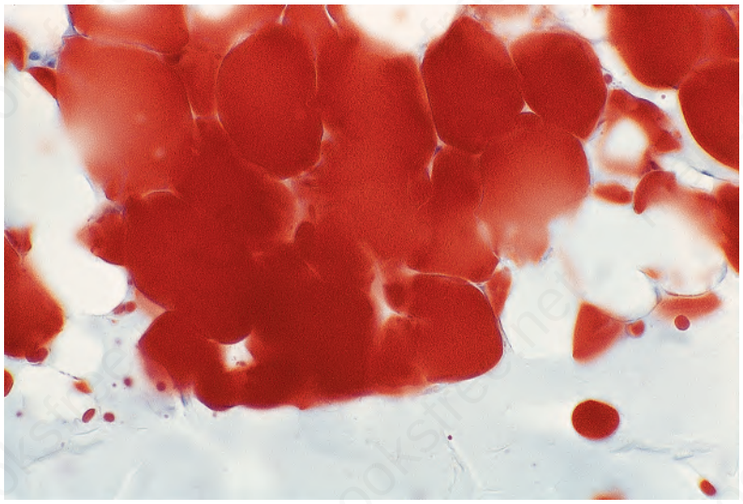

Fig. 1.102
Adult fat in frozen section stained by the Sudan IV technique.

for routine histologic preparation dissolves the lipid, but the use of special stains on frozen sections will reveal its presence (*Fig. 1.102*). The subcutaneous fat may contain large numbers of mast cells.

Deposits of brown fat may be seen in the newborn and occasionally in adults, particularly in the interscapular region, the back, thorax and mediastinum. The brown coloration is due to the high cytochrome content. The brown fat cytoplasm contains numerous, somewhat pleomorphic, mitochondria. Endoplasmic reticulum and a Golgi apparatus are not usually visible. The adipocytes have a bubbly appearance with the nucleus located towards the center of the cell (*Fig. 1.103*).

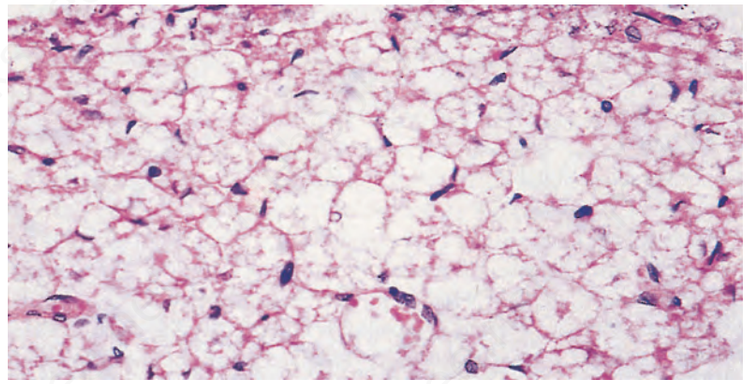

Fig. 1.103
Typical brown fat showing pink granular cytoplasm.

Access **ExpertConsult.com** for the complete list of references

REFERENCES

Normal epidermal histology

1. Toker C. Clear cells of the nipple epidermis. *Cancer*. 1970;25:601–610.
2. Lundquist K, Kohler S, Rouse RV. Intraepidermal cytokeratin 7 expression is not restricted to Paget cells but is also seen in Toker cells and Merkel cells. *Am J Surg Pathol*. 1999;23:212–219.
3. Van der Putte SC, Toonstra J, Hennipman A. Mammary Paget's disease confined to the areola and associated with multifocal Toker cell hyperplasia. *Am J Dermatopathol*. 1995;17:487–493.
4. Di Tommaso L, Franchi G, Destro A, et al. Toker cells of the breast. Morphological and immunohistochemical characterization of 40 cases. *Hum Pathol*. 2008;39:1295–1300.

Skin development

1. Schmidt-Ullrich R, Paus R. Molecular principles of hair follicle induction and morphogenesis. *Bioessays*. 2005;27:247–261.
2. Fuchs E. Scratching the surface of skin development. *Nature*. 2007;445:834–842.
3. Botchkarev VA, Flores ER. p53/p65/p73 in the epidermis in health. *Cold Spring Harb Perspect Med*. 2014;4:2–14, pii:a015248.
4. Loomis CA. Development and morphogenesis of the skin. *Adv Dermatol*. 2001;17:183–210.
5. Olivera-Martine I, Thelu J, et al. Molecular mechanisms controlling dorsal dermis generation from the somite dermoyotome. *Int J Dev Biol*. 2004;48:93–101.

Keratinocyte biology

1. Schweizer J, Bowden PE, Coulombe PA, et al. New consensus nomenclature for mammalian keratins. *J Cell Biol*. 2006;174:169–174.
2. Magin TM, Vijayaraj P, Leube RE. Structural and regulatory functions of keratins. *Exp Cell Res*. 2007;313:2031–2032.
3. Toivola DM, Boor P, Alam C, et al. Keratins in health and disease. *Curr Opin Cell Biol*. 2015;32:73–81.
4. Szeverenyi I, Cassidy AJ, Chung CW, et al. The Human Intermediate Filament Database: comprehensive information on a gene family involved in many human diseases. *Hum Mutat*. 2008;29:351–360.
5. Knobel M, O'Toole EA, Smith FJ. Keratins and skin diseases. *Cell Tissue Res*. 2015;360:583–589.

Epidermal stem cells

1. Braun KM, Prowse DM. Distinct epidermal stem cell compartments are maintained by independent niche microenvironments. *Stem Cell Rev*. 2006;2:221–231.
2. Fuchs E. Skin stem cells: rising to the surface. *J Cell Biol*. 2008;180:273–284.
3. Tumbar T, Guasch G, Greco V, et al. Defining the epithelial stem cell niche in skin. *Science*. 2004;303:359–363.
4. Potten CS. The epidermal proliferative unit: the possible role of the central basal cell. *Cell Tissue Kinet*. 1974;7:77–88.
5. Lechler T, Fuchs E. Asymmetric cell divisions promote stratification and differentiation of mammalian skin. *Nature*. 2005;437:275–280.
6. Hsu YC, Li L, Fuchs E. Emerging interactions between skin stem cells and their niches. *Nat Med*. 2014;20:847–856.
7. Toma JG, McKenzie IA, Bagli D, et al. Isolation and characterization of multipotent skin derived precursors from human skin. *Stem Cells*. 2005;23:727–737.
8. Chen FG, Zhang WJ, Bi D, et al. Clonal analysis of nestin (–) vimentin (+) multipotent fibroblasts isolated from human dermis. *J Cell Sci*. 2007;120:2875–2883.
9. Tamai K, Yamazaki T, Chino T, et al. PDGFRalpha-positive cells in bone marrow are mobilized by high mobility group box 1 (HMGB1) to regenerate injured epithelia. *Proc Natl Acad Sci USA*. 2011;16:6609–6614.

Skin barrier

1. Candi E, Schmidt R, Melino G. The cornified envelope: a model of cell death in the skin. *Nat Rev Mol Cell Biol*. 2005;6:328–340.
2. Ishida-Yamamoto A, Tanaka H, Nakane H, et al. Programmed cell death in normal epidermis and loricrin keratoderma. Multiple functions of profilaggrin in keratinization. *J Investig Dermatol Symp Proc*. 1999;4:145–149.
3. Bikle DD, Oda Y, Xie Z. Calcium and 1,25(OH)2D: interacting drivers of epidermal differentiation. *J Steroid Biochem Mol Biol*. 2004;89-90:355–360.
4. Elias PM, Williams ML, Holleran WM, et al. Thematic review series: skin lipids. Pathogenesis of permeability barrier abnormalities in the ichthyoses: inherited disorders of lipid metabolism. *J Lipid Res*. 2008;49:697–714.
5. Brown SJ, McLean WH. One remarkable molecule: filaggrin. *J Invest Dermatol*. 2012;132:751–762.
6. Ishida-Yamamoto A, Igawa S. The biology and regulation of corneodesmosomes. *Cell Tissue Res*. 2015;360:477–482.

Skin immunity

1. Sanford JA, Gallo RL. Functions of the skin microbiota in health and disease. *Semin Immunol*. 2013;25:370–377.
2. Goodarzi H, Trowbridge J, Gallo RL. Innate immunity: a cutaneous perpective. *Clin Rev Allergy Immunol*. 2007;33:15–26.
3. Lee KC, Eckert RL. S100A7 (Psoriasin) - mechanism of antibacterial action in wounds. *J Invest Dermatol*. 2007;127:945–957.
4. Harder J, Schroder JM. RNase 7, a novel innate immune defense antimicrobial protein of healthy human skin. *J Biol Chem*. 2002;277:46779–46784.
5. Schroder JM, Harder J. Human beta-defensin-2. *Int J Biochem Cell Biol*. 1999;31:645–651.
6. Schauber J, Gallo RL. Antimicrobial peptides and the skin immune defense system. *J Allergy Clin Immunol*. 2008;122:261–266.
7. Oppenheim JJ, Tewary P, de la Rosa G, et al. Alarmins initiate host defense. *Adv Exp Med Biol*. 2007;601:185–194.
8. Nishibu A, Ward BR, Jester JV, et al. Behavioral responses of epidermal Langerhans cells in situ to local pathological stimuli. *J Invest Dermatol*. 2006;126:787–796.
9. Leon B, Lopez-Bravo M, Ardavin C. Monocyte-derived dendritic cells. *Semin Immunol*. 2005;17:313–318.
10. Nestle FO, Nickoloff BJ. Deepening our understanding of immune sentinels in the skin. *J Clin Invest*. 2007;117:2382–2385.

Melanocytes

1. Carlson JA, Linette GP, Aplin A, et al. Melanocyte receptors: clinical implications and therapeutic relevance. *Dermatol Clin*. 2007;25:541–557.
2. Murisier F, Beermann F. Genetics of pigment cells: lessons from the tyrosinase gene family. *Histol Histopathol*. 2006;21:567–578.
3. Schouwey K, Beermann F. The Notch pathway: hair graying and pigment cell homeostasis. *Histol Histopathol*. 2008;23:609–619.
4. Ginger RS, Askew SE, Ogborne RM, et al. SLC24A5 encodes a trans-golgi network protein with potassium-dependent sodium-calcium exchange activity that regulates human epidermal melanogenesis. *J Biol Chem*. 2008;283:5486–5495.

Merkel cells

1. Boulais N, Misery L. Merkel cells. *J Am Acad Dermatol*. 2007;57:147–165.
2. Moll I, Bladt U, Jung EG. Presence of Merkel cells in sun-exposed and not sun-exposed skin: a quantitative study. *Arch Dermatol Res*. 1990;282:213–216.
3. Merot Y, Mooy A. Merkel cell hyperplasia in hypertrophic varieties of actinic keratoses. *Dermatologica*. 1989;178:189–193.
4. Hartschuh W, Weihe E, Yanaihara N, et al. Immunohistochemical localization of vasoactive intestinal polypeptide (VIP) in Merkel cells of various mammals: evidence for a neuromodulator function of the Merkel cell. *J Invest Dermatol*. 1983;81:361–364.
5. Ortonne JP, Petchot-Bacque JP, Verrando P, et al. Normal Merkel cells express a synaptophysin-like immunoreactivity. *Dermatologica*. 1988;177:1–10.
6. Garcia-Caballero TGR, Gallego E, Rosón M, et al. Calcitonin gene-related peptide (CGRP) in the neuroendocrine Merkel cells and nerve fibers of pig and human skin. *Histochemistry*. 1989;92:127–132.
7. Ortonne JP, Darmon M. Merkel cells express desmosomal proteins and cytokeratins. *Acta Derm Venereol*. 1985;65:161–164.
8. Gallego R, Garcia-Caballero M, Fraga A, et al. Neural cell adhesion molecule in Merkel cells and Merkel cell tumors. *Virchows Arch*. 1995;426:317–321.
9. Narisawa Y, Hashimoto K, Nihei Y, et al. Biological significance of dermal Merkel cells in the development of cutaneous nerves in human fetal skin. *J Histochem Cytochem*. 1992;40:65–71.
10. Beiras A, Garcia-Caballero T, Espinosa J, et al. Staining of Merkel cells of pig snout epidermis using the uranaffin reaction: morphometric analysis of neuroendocrine granules. *Differentiation*. 1986;28:136–154.

11. Moll I, Roessler M, Brandner JM, et al. Human Merkel cells - aspects of cell biology, distribution and functions. *Eur J Cell Biol*. 2005;84:259–271.
12. Lucarz A, Brand G. Current considerations about Merkel cells. *Eur J Cell Biol*. 2007;86:243–251.
13. Woo SH, Lumpkin EA, Patapoutian A. Merkel cells and neurons keep in touch. *Trends Cell Biol*. 2015;25:74–81.
14. Szrder V, Grim M, Halata Z, et al. Neural crest origin of mammalian Merkel cells. *Dev Biol*. 2003;253:258–263.
15. Sidhu GS, Chandra P, Cassai ND. Merkel cells, normal and neoplastic. *Ultrastruct Pathol*. 2005;29:287–294.

Intercellular junctions

1. Kowalczyk AP, Green KJ. Structure, function, and regulation of desmosomes. *Prog Mol Biol Transl Sci*. 2013;116:95–118.
2. Harmon RM, Green KJ. Structural and functional diversity of desmosomes. *Cell Commun Adhes*. 2013;20:171–187.
3. Samuelov L, Sprecher E. Inherited desmosomal disorders. *Cell Tissue Res*. 2015;360:457–475.
4. Bazzi H, Christiano AM. Broken hearts, woolly hair, and tattered skin: when desmosomal adhesion goes awry. *Curr Opin Cell Biol*. 2007;19:515–520.
5. Petrof G, Mellerio JE, McGrath JA. Desmosomal genodermatoses. *Br J Dermatol*. 2012;166:36–45.
6. Chan LS. Epitope spreading in paraneoplastic pemphigus: autoimmune indiction in antibody-mediated blistering diseases. *Arch Dermatol*. 2000;136:663–664.
7. Amagai M, Stanley JR. Desmoglein as a target in skin diseases and beyond. *J Invest Dermatol*. 2012;132:776–784.
8. Niessen CM. Tight/adherens junctions: basic structure and function. *J Invest Dermatol*. 2007;127:2525–2532.
9. Irie K, Shimizu K, Sasikawa T, et al. Roles and modes of action of nectins in cell-cell adhesion. *Semin Cell Dev Biol*. 2004;15:643–656.
10. Niessen MT, Iden S, Niessen CM. The in vivo function of mammalian cell and tissue polarity regulators – how to shape and maintain the epidermal barrier. *J Cell Sci*. 2012;125:3501–3510.
11. Sprecher E, Bergman R, Richard G, et al. Hypotrichosis with juvenile macular dystrophy is caused by a mutation in *CDH3*, encoding P-cadherin. *Nat Genet*. 2001;29:134–136.
12. Kjaer KW, Hansen L, Schwabe GC, et al. Distinct CDH3 mutations cause ectodermal dysplasia, ectrodacytly, macular dystrophy (EEM) syndrome. *J Med Genet*. 2005;42:292–298.
13. Mese G, Richard G, White TW. Gap junctions: basic structure and function. *J Invest Dermatol*. 2007;127:2516–2524.
14. Kelsell DP, Dunlop J, Hodgkins MB. Human diseases: clues to cracking the connexin code? *Trends Cell Biol*. 2001;11:2–6.
15. Lilly E, Sellitto C, Milstone LM, et al. Connexin channels in congenital skin disorders. *Semin Cell Dev Biol*. 2016;50:4–12.
16. Morita K, Miyachi Y. Tight junctions in the skin. *J Dermatol Sci*. 2003;31:81–89.
17. Brander JM, Kief S, Wladykowski E, et al. Tight junction proteins in the skin. *Skin Pharmacol Physiol*. 2006;19:71–77.
18. Hadj-Rabia S, Baala L, Vabres P, et al. Claudin-1 mutations in neonatal sclerosing cholangitis associated with ichthyosis: a tight junction disease. *Gastroenterology*. 2004;127:1386–1390.
19. Kirchmeier P, Sayer E, Hotz A, et al. Novel mutation in the *CLDN1* gene in a Turkish family with neonatal ichthyosis sclerosing cholangitis (NISCH) syndrome. *Br J Dermatol*. 2014;170:976–978.

Pilosebaceous unit

1. Schlake T. Determination of hair structure and shape. *Semin Cell Dev Biol*. 2007;18:267–273.
2. Schweizer J, Langbein L, Rogers MA, et al. Hair follicle-specific keratins and their diseases. *Exp Cell Res*. 2007;313:2010–2020.
3. Schweizer J, Bowden PE, Coulombe PA, et al. New consensus nomenclature for mammalian keratins. *J Cell Biol*. 2006;174:169–174.
4. Gong H, Zhou H, McKenzie GW, et al. An updated nomenclature for keratin-associated proteins (KAPs). *Int J Biol Sci*. 2012;8:258–264.
5. Thibaut S, Barbarat P, Leroy F, et al. Human hair keratin network and curvature. *Int J Dermatol*. 2007;1(suppl 46):7–10.

Eccrine gland

1. Wollina U, Abdel-Naser MB, Ganceviciene R, et al. Receptors of eccrine, apocrine, and holocrine skin glands. *Dermatol Clin*. 2007;25:577–588.
2. Hurley HJ. The eccrine sweat glands: structure and function. In: Freinkel RK, Woodley DT, eds. *The biology of the skin*. New York: Parthenon Publishing; 2001:47–76.
3. Saga K, Morimoto Y. The localization of alkaline phosphatase activity in human eccrine and apocrine sweat glands. *J Histochem Cytochem*. 1995;43:927–932.
4. Morimoto T, Itoh T. Thermoregulation and body fluid osmolality. *J Basic Clin Physiol Pharmacol*. 1998;9:51–72.
5. Shibasaki M, Wilson TE, Crandall CG. Neural control and mechanisms of eccrine sweating during heat stress and exercise. *J Appl Physiol*. 2006;100:1692–1701.
6. Quinton PM. Cystic fibrosis: lessons from the sweat gland. *Physiology (Bethesda)*. 2007;22:212–225.

Apocrine glands

1. Scrivener Y, Cribier B. Morphology of sweat glands. *Morphologie*. 2002;86:5–17.
2. Lonsdale-Eccles A, Leonard N, Lawrence C. Axillary hyperhidrosis: eccrine or apocrine. *Clin Exp Dermatol*. 2003;28:2–7.
3. Saga K. Histochemical and immunohistochemical markers for human eccrine and apocrine sweat glands: an aid for histopathologic differentiation of sweat gland tumors. *J Invest Dermatol Symp Proc*. 2001;6:49–53.
4. Farkas R. Apocrine secretion: new insights into an old phenomenon. *Biochim Biophys Acta*. **1850**;2015:1740–1750.

Dermal–epidermal junction

1. Uitto J, Pulkkinen L. Molecular complexity of the cutaneous basement membrane zone. *Mol Biol Rep*. 1996;23:35–46.
2. Bruckner-Tuderman L, Has C. Disorders of the cutaneous basement membrane zone–the paradigm of epidermolysis bullosa. *Matrix Biol*. 2014;33:29–34.
3. Has C, Bruckner-Tuderman L. The genetics of skin fragility. *Annu Rev Genomics Hum Genet*. 2014;15:245–268.
4. Uitto J, Bruckner-Tuderman L, Christiano AM, et al. Progress toward treatment and cure of epidermolysis bullosa: summary of the DEBRA International research symposium EB2015. *J Invest Dermatol*. 2016;136:352–358.
5. McGrath JA. Recently identified forms of epidermolysis bullosa. *Ann Dermatol*. 2015;27:658–666.
6. Koster J, Geerts D, Favre B, et al. Analysis of the interactions between BP180, BP230, plectin and the integrin α6ß4 important for hemidesmosome assembly. *J Cell Sci*. 2003;116:387–399.
7. Aumailley M, Bruckner-Tuderman L, Carter WG, et al. A simplified laminin nomenclature. *Matrix Biol*. 2005;24:326–332.
8. Khoshnoodi J, Pedchenko V, Hudson BG. Mammalian collagen IV. *Microsc Res Tech*. 2008;71:357–370.
9. Iozzo RV. Basement membrane proteoglycans: from cellar to ceiling. *Nat Rev Mol Cell Biol*. 2005;6:646–656.
10. Burgeson RE. Type VII collagen, anchoring fibrils, and epidermolysis bullosa. *J Invest Dermatol*. 1993;101:252.
11. Shimizu H, Ishiko A, Masunaga T, et al. Most anchoring fibrils in human skin originate and terminate in the lamina densa. *Lab Invest*. 1997;76:753.

Dermal collagen

1. Myllyharju J, Kivirikko KI. Collagens, modifying enzymes and their mutations in humans, flies and worms. *Trends Genet*. 2004;20:33–43.
2. Shaw LM, Olsen BR. FACIT collagens: Diverse molecular bridges in extracellular matrices. *Trends Biochem Sci*. 1991;16:191.
3. Kuivaniemi H, Tromp G, Prockop DJ. Mutations in fibrillar collagens (types I, II, III, and XI), fibril-associated collagen (type IX), and network-forming collagen (type X) cause a spectrum of diseases of bone, cartilage, and blood vessels. *Hum Mutat*. 1997;9:300–315.
4. Lemaitre V, D'Armiento J. Matrix metalloproteinases in development and disease. *Birth Defects Res C Embryo Today*. 2006;78:1–10.

Dermal elastic tissue

1. Kielty CM. Elastic fibres in health and disease. *Expert Rev Mol Med*. 2006;8:1–23.
2. Midwood KS, Schwarzbauer JE. Elastic fibers: Building bridges between cells and their matrix. *Curr Biol*. 2002;12:R279.
3. Ramirez F, Sakai LY, Dietz HC, et al. Fibrillin microfibrils: multipurpose extracellular networks in organismal physiology. *Physiol Genomics*. 2004;19:151–154.
4. Wise SG, Weiss AS. Tropoelastin. *Int J Biochem Cell Biol*. 2008.
5. Robinson PN, Arteaga-Solis E, Baldock C, et al. The molecular genetics of Marfan syndrome and related disorders. *J Med Genet*. 2006;43:769–787.

Ground substance

1. Iozzo RV. Basement membrane proteoglycans: from cellar to ceiling. *Nat Rev Mol Cell Biol*. 2005;6:646–656.
2. Esko JD, Lindahl U. Molecular diversity of heparan sulfate. *J Clin Invest*. 2001;108:169.
3. Gallo RL, Kim C, Kokenyesi R, et al. Syndecans-1 and -4 are induced during wound repair of neonatal but not fetal skin. *J Invest Dermatol*. 1996;107:667.

Fibroblast biology

1. Wong T, McGrath JA, Navsaria H. The role of fibroblasts in tissue engineering and regeneration. *Br J Dermatol*. 2007;156:1149–1155.
2. Chang HY, Chi JT, Dudoit S, et al. Diversity, topographic differentiation, and positional memory in human fibroblasts. *Proc Natl Acad Sci USA*. 2002;99:12877–12882.
3. Driskell RR, Lichtenberger BM, Hoste E, et al. Distinct fibroblast lineages determine dermal srchitecture in skin development and repair. *Nature*. 2013;504:277–281.
4. Sorrell JM, Baber MA, Caplan AI. Clonal characterization of fibroblasts in the superficial layer of the adult human dermis. *Cell Tissue Res*. 2007;327:499–510.
5. Park IH, Zhao R, West JA, et al. Reprogramming of human somatic cells to pluripotency with defined factors. *Nature*. 2008;451:141–146.

Cutaneous blood vessels and lymphatics

1. Higgins JC, Eady RAJ. Human dermal vasculature. I. Its segmental differentiation. Light and electron microscopic study. *Br J Dermatol*. 1981;104:116–130.
2. Braverman IM. Ultrastructure and organization of the cutaneous microvasculature in normal and pathologic states. *J Invest Dermatol*. 1989;93:2S–9S.
3. Ryan TJ. Structure and function of lymphatics. *J Invest Dermatol*. 1989;93:18S–24S.
4. Jurisic G, Detmar M. Lymphatic endothelium in health and disease. *Cell Tissue Res*. 2008.
5. Hosking B, Mäkinen T. Lymphatic vasculature: a molecular perspective. *Bioessays*. 2007;29:1192–1202.
6. Mortimer PS, Rockson SG. New developments in clinical aspects of lymphatic disease. *J Clin Invest*. 2014;124:915–921.

Nervous system of the skin

1. Hashimoto K. Fine structure of the Meissner corpuscle of human palmar skin. *J Invest Dermatol*. 1973;60:20–28.
2. Cauna N. The free penicillate nerve endings of the human hairy skin. *J Anat*. 1973;115:277–288.

Subcutaneous fat

1. Wehrli NE, Bural G, Houseni M, et al. Determination of age-related changes in structure and function of skin, adipose tissue, and skeletal muscle with computed tomography, magnetic resonance imaging, and positron emission tomography. *Semin Nucl Med*. 2007;37:195–205.
2. Farooqi IS, O'Rahilly S. Mutations in ligands and receptors of the leptin-melanocortin pathway that lead to obesity. *Nat Clin Pract Endocrinol Metab*. 2008;4:569–577.
3. Bessesen DH. Update on obesity. *J Clin Endocrinol Metab*. 2008;93:2027–2034.

See www.expertconsult.com for references and additional material

Specialized techniques in dermatopathology

Pratistadevi K. Ramdial, Boris C. Bastian, Jeffrey P. North, John Goodlad, John A. McGrath and Alexander J. Lazar

CHAPTER 2

Specimen fixation, grossing/put-through, processing, embedding and sectioning 35
Routine and 'special' stains 35
Immunohistochemical techniques 37
Immunohistochemical techniques and trouble shooting 39
Immunofluorescence 40
Electron microscopy 41
Frozen section examination of skin specimens 41
Diagnostic cytopathological techniques in dermatopathology 42
Diagnosis of inherited skin diseases 42
Molecular techniques 44
Chromosomal karyotyping 44
Allelic imbalance 44
Fluorescence in situ hybridization (FISH) 44
Comparative genomic hybridization (CGH) 47
Polymerase chain reaction (PCR) 48
Next-Generation Sequencing (NGS) 49
Diagnosis of lymphomas 50
PCR analysis of cutaneous lymphoid infiltrates 50
T-cell receptor gene rearrangement in cutaneous lymphoproliferations 51
IG gene rearrangement in cutaneous lymphoproliferations 51

Specimen fixation, grossing/put-through, processing, embedding and sectioning

The aim of fixation is to maintain clear and consistent lesional features and to preserve tissue in an optimal state suitable for a range of staining and ancillary histopathological techniques.[1,2] Most fixation methods employed during tissue processing depend on chemical fixation of tissue in liquid reagents.[3] Tissue fixation may also be accomplished by physical (heat, microwave, freeze-drying, and freeze substitution) and/or chemical (coagulant and cross-linking) methods.[4] The most commonly used fixative is 10% neutral-buffered formalin solution with a pH between 7.2–7.4. It prevents the formation of formalin pigment in tissue sections. The quality of fixation is affected by:

- the size of the specimen,
- duration and temperature of fixation,
- pH,
- concentration,
- osmolality,
- ionic composition of fixatives and additives contained in the fixative.[5]

Formalin fixation occurs at an approximate rate of 1 mm per hour.[4,6,7] The volume of the fixative should ideally be at least 10 times the volume of the specimen.[7] Large specimens, such as tumors, may require sectioning into 5-mm thick slices, covering with fixative-soaked gauze or cloth and fixation overnight.[5,7]

Diagnostic dermatological biopsies may be:

- small incisional (shave, core, punch),
- excisional specimens.[8]

Prior to put-through, excisional specimens that require an appraisal of margins should be inked. If localization sutures have been inserted by surgeons then four-quadrant, four-color painting or two-color painted halves (*Fig. 2.1*) is usually appropriate. Shave biopsies are used to sample or remove lesions and, if of appropriate size, may be divided into sections, bisected or trisected and embedded on edge. Edge embedding is critical in a shave excision of a lesion such as a small melanoma so that both the width and depth of invasion can be quantified.[8,9] The main purpose of core or punch biopsies, which generally measure 2–8 mm in diameter, is for diagnostic sampling of larger lesions. Biopsies larger than 4 mm in size should be bisected and the specimens embedded with the cut surfaces down. The bisectioning and embedding cut surface down ensures that the lesion is not missed. Biopsies less than 4 mm are put through *in toto*.[9,10]

Tissue processing refers to a series of steps that effect the removal of extractable water from biopsies to ensure sections of optimal diagnostic quality.[9] These include fixation, dehydration, clearing, infiltration, and embedding in a support matrix. Use of manual and automated tissue processing achieves this goal, including:

- carousel-type processors,
- self-contained vacuum infiltration tissue processors (*Fig. 2.2*),
- microwave tissue processing.

In most laboratories, overnight processing runs are the norm.[9] However, microwave-assisted tissue processing facilitates shorter processing times of 1–2 hours. Dehydrating reagents promote the removal of unbound water and aqueous fixatives from the tissue. Clearing reagents serve as an intermediary between the dehydrating and infiltrating solutions, being miscible with both. Paraffin is the most popular infiltration and embedding medium, being suitable for the majority of routine and special stains. The important principle to be adhered to during embedding of skin biopsies is that the orientation of the skin sample should offer the least resistance to the blade during microtomy (*Fig. 2.3*). Skin biopsies are usually cut in a plane at right angles to the epidermis so as to minimize its compression and distortion.

Suboptimally processed tissue may result in incomplete tissue sections and expansion or disintegration of sections in the water bath. Incorrectly embedded tissue may result in poorly orientated incomplete sections. Faulty microtome mechanisms; loose, dull, or damaged blades; and inaccurate clearance angles may be the causes for:

- thick and thin sections,
- folds (*Fig. 2.4*),
- holes (*Fig. 2.5*),
- scores (*Fig. 2.6*),
- chatter.[10]

The presence of calcified areas and suture in skin tissue and nicks in the blade may result in chatter or splitting of sections at right angles to the knife edge.

Routine and 'special' stains

With the advent of immunohistochemistry, special stains are less commonly employed, but can still play an important role in highlighting certain tissue characteristics or for detection of infectious organisms.

Diagnostic sections are usually stained with hematoxylin and eosin (H&E), the most widely used routine stain.[1] The hematoxylin component

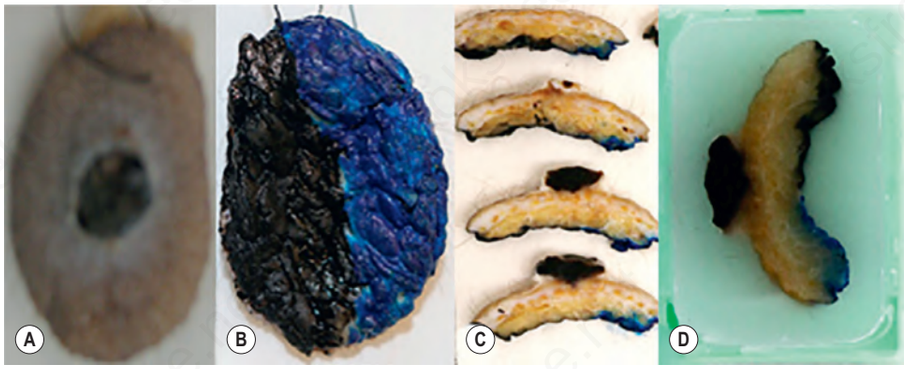

Fig. 2.1
Gross representation of pyogenic granuloma (**A**), with two-color painting of the inferior surface (**B**). 2-mm–thick gross sections demonstrating the black and blue painting at put-through (**C**) and in paraffin blocks (**D**). By courtesy of K. Nargan and K. Lumamba, Africa Health Research Institute, Durban, South Africa.

Fig. 2.2
A self-contained vacuum infiltration tissue processor of fluid-transfer type.

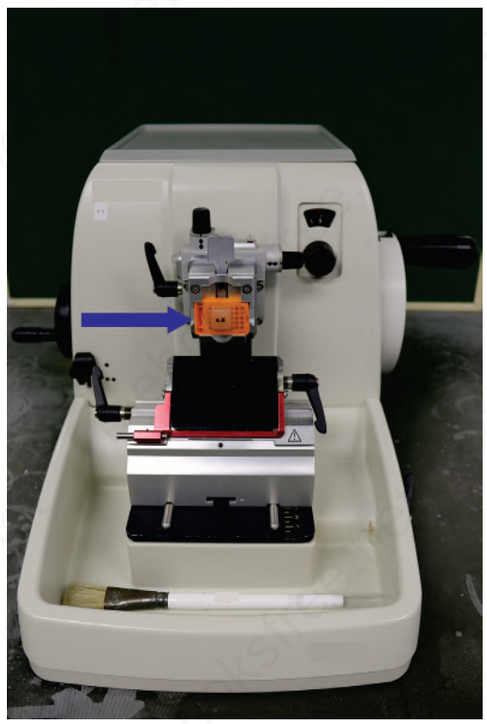

Fig. 2.3
Paraffin block containing skin tissue (arrow) on microtome.

is positively charged and thus acts as a basic dye staining the negatively charged DNA in the nucleus blue-black. Eosin is anionic and thus acts as an acidic stain of the positively charged proteins comprising the cytoplasmic compartment and connective tissue resulting in variable shades and intensity of pink, orange, and red. The periodic acid-Schiff (PAS) technique is used widely to demonstrate:

- glycogen,
- starch,
- sialomucin,
- neutral mucin,
- basement membranes,
- α1-antitrypsin,
- reticulin,
- Russell bodies of plasma cells,
- fungi.[2]

The PAS technique is employed to demonstrate basement membrane thickening in lupus erythematosus, porphyria cutanea tarda, and in some tumors. Glycogen is digested by diastase, while neutral mucopolysaccharides are not—thus these PAS-positive components can be distinguished. Mucicarmine demonstrates acidic epithelial mucins.[2] It is useful for the diagnosis of adenocarcinomas and the mucoid *Cryptococcus neoformans* capsule. Alcian blue highlights acidic mucopolysaccharides, staining the mucinous components of dermal mucinoses, granuloma annulare, scleredema of Bushke, lupus erythematosus, and metastatic adenocarcinomas among others. Alcian blue demonstrates heterogeneity of staining that is pH based: are demonstrated at pH 2.5 and sulfamucins at pH 1.0.[3]

While colloidal iron, initially described by Hale for the identification of acid mucopolysaccharides, is as sensitive as Alcian blue for this purpose, its specificity and selectivity are debatable and background staining can be problematic.[4] However, reduction of pH of the colloidal iron solution and

Fig. 2.4
Technical artifact: folds in tissue sections because of poor bath floating technique.

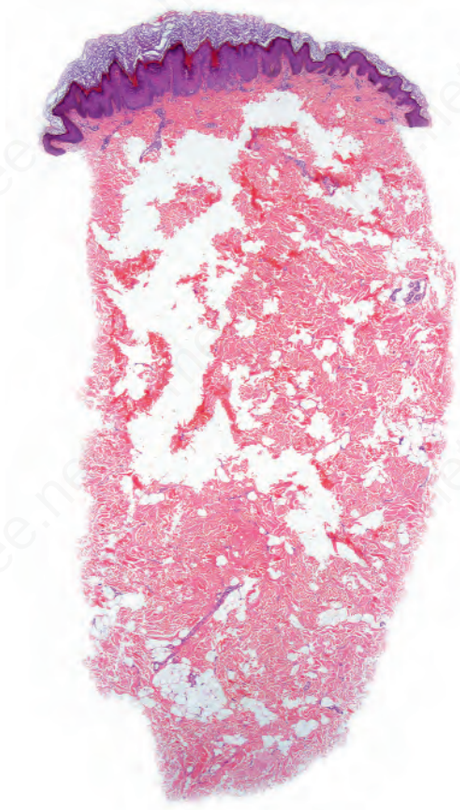

Fig. 2.5
Technical artifact: holes in tissue sections caused by excessively thin sectioning.

inclusion of acetic acid washes may reduce this artifact.[3–5] The high iron diamine stain, in contrast to colloidal iron, stains highly acidic sulfamucins but does not stain sialomucins or hyaluronic acid.[5–7] Connective tissue stains highlight collagen, elastic and reticulin fibers. The trichrome stain, a combination of three dyes, is employed for the differential demonstration of muscle, collagen fibers, fibrin, and erythrocytes.[8] Elastic fibers usually stain with eosin, phloxine, Congo red, and PAS stains but are demonstrated well and differentially with the Verhöeff method in the diagnosis of conditions like scleroderma, anetoderma, and pseudoxanthoma elasticum. Silver stains are useful to demonstrate reticulin fibers, melanin, and the identification of infective agents. While methenamine silver and Gomori-Grocott methenamine silver stains highlight fungi and bacteria, Warthin-Starry, Dieterle,

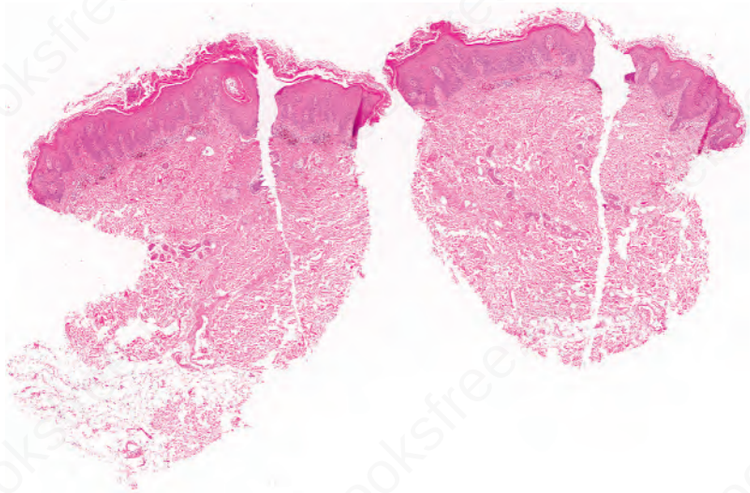

Fig. 2.6
Technical artifact: vertical scores in tissue sections caused by a damaged microtome blade. By courtesy of K. Nargan, Africa Health Research Institute, Durban, South Africa.

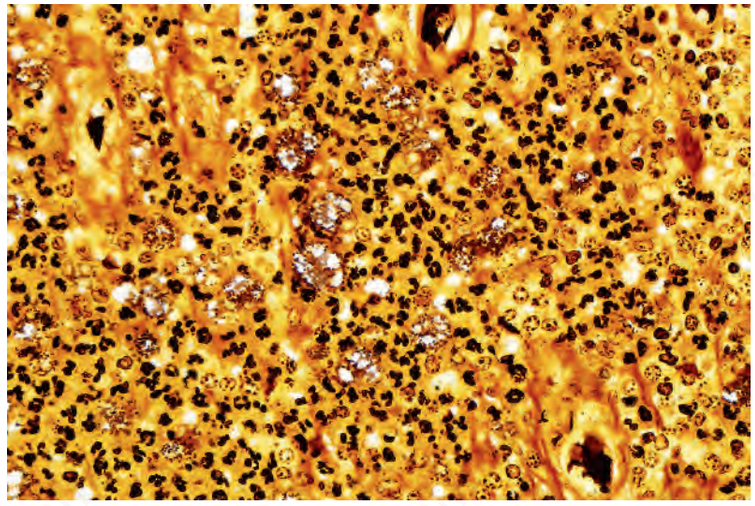

Fig. 2.7
Special stains: Warthin-Starry silver stain demonstrating Donovan bodies.

and Steiner silver stains are particularly useful in the demonstration of spirochetes, *Bartonella* species and Donovan bodies (*Fig. 2.7*). Masson-Fontana silver staining is pivotal to the staining of the cell wall of *C. neoformans*, especially in the identification of capsule-deficient *C. neoformans*. The role of the more commonly used special stains is summarized in *Table 2.1*.

Immunohistochemical techniques

Since the first practical application of antibodies using the peroxidase-labeled antibody method on paraffin-embedded tissues in 1968, immunohistochemistry (IHC) has emerged as a powerful supplementary investigation to histomorphological assessment.[1–3] IHC has widespread dermatopathological diagnostic, prognostic, therapeutic, and pathogenetic applications, not only in a range of neoplastic (*Table 2.2*), immunobullous, and infective disease, but also in the distinction between reactive and neoplastic disorders.[4–14] Immunohistological techniques can be performed manually or in automated platforms (*Fig. 2.8*). While automation allows enhanced quality and reproducibility of staining; detailed, exact IHC protocols are critical in the many laboratories that still perform manual IHC, to achieve optimal, reproducible results.

Table 2.1
Commonly used histochemical stains

	Stain	Component	Outcome
A.	**Routine**		
	Hematoxylin-eosin	Cells, connective tissue	Nuclei: blue Cytoplasm: pink/red Extracellular matrix: red/pink
B.	**Carbohydrates & glycoconjugates**		
	Periodic acid-Schiff (PAS)	Neutral mucins, glycogen	Magenta
	PAS-diastase	Glycogen, proteoglycans, HA resistant sialomucin	Resistant to diastase digestion
	Alcian blue, pH 2.5	Labile sialomucin	Blue
	Alcian blue, pH 1.0	Sulfomucin, resistant sialomucin	Blue
	Mucicarmine	Sialomucin, sulfomucin	Pink
	Colloidal iron	Sialomucin, sulfomucin HA, proteoglycans	Blue
	High iron diamine	Proteoglycans, sulfomucin	Blue
	Toluidine blue	Sulfomucin	Blue
	Hyaluronidase	HA	Sensitive to HA
C.	**Connective tissue fibers**		
	Masson trichrome	Collagen Muscle, nerve	Blue or green Red
	Verhöeff-van Gieson	Elastic fibers	Black
	Pinkus acid orcein	Elastic	Dark brown
	Silver nitrate	Reticulum fibers	Black
D.	**Infective stains**		
	Ziehl Neelsen	Acid fast bacilli	Red
	Fite-Faraco	(weakly) acid fast bacilli	Red
	PAS	Fungi, parasites	Magenta
	Mucicarmine	*Cryptococcus* sp	Red
	Giemsa	*Leishmania* sp, Donovan bodies	Red Metachromatically purple
	Methenamine silver	Fungi, bacteria	Black
	Grocott methenamine silver	Fungi	Black
	Warthin Starry silver	Spirochetes, bacteria	Black
	Dieterle and Steiner silver	Spirochetes, bacteria	Black
E.	**Other**		
	Perl potassium ferrocyanide	Hemosiderin	Blue
	Oil red O	Lipids	Red
	Scarlet red	Lipids	Red
	Von Kossa	Phosphate (often as calcium phosphate)	Black Black
	Alizarin red S	Calcium	Orange-red
	Alkaline Congo red	Amyloid	Apple green birefringence
	Chloro-acetate esterase	Myeloid series	Red granules

HA, Hyaluronic acid.

Table 2.2
Some diagnostic immunohistochemical applications for cutaneous tumors[4–13]

Stain	Application
	Epidermal and appendageal neoplasms
AE1/AE3	Pan-keratin. Confirms epithelial lineage
CAM 5.2	CKs 8,18. Confirm epithelial lineage. Useful to confirm glandular neoplasms
MNF 116	CKs 5, 6, 8, 17, 19. Useful in diagnosis of SCC with single cell infiltration
BerEP4	Positive in BCC. Negative in SCC
CK 7	Confirmation of mammary and extramammary Paget disease
p63	Distinguish primary cutaneous spindle SCC from mesenchymal spindle cell tumors & primary cutaneous adnexal from metastatic adenocarcinomas
CD10	Trichoepithelioma: positive in stroma and papillae, negative in epithelium. BCC: positive in epithelium, negative in stroma
bcl2	Positive in BCC, negative in SCC
	Vascular proliferations
ERG	Nuclear staining in endothelial cells. High specificity and specificity for endothelial tumors (better than CD31)
CD31	High specificity and good sensitivity for endothelial tumors
CD34	High sensitivity but low specificity for endothelial tumors
Fli-1	Nuclear staining of endothelial cells
GLUT 1	Positive in endothelial cells of all juvenile hemangiomas. Usually negative in congenital hemangiomas (rapidly involuting congenital hemangioma and noninvoluting congenital hemangioma)
	Melanocytic tumors
S100 protein	Most widely used melanocytic marker. It is highly sensitive but not as specific as other melanocytic markers
Sox-10	Newly introduced melanocytic marker also positive in neural tumors. Very useful in spindle cell melanomas including desmoplastic melanoma and in the evaluation of intraepidermal melanocytic proliferations as lentigo maligna (nuclear staining)
MITF-1	Low specificity but useful in the evaluation of intraepidermal melanocytic proliferations (nuclear staining)
HMB 45	Good specificity but relatively low sensitivity. Tends to be negative in spindle cell melanoma. Also positive in PEComa
Melan A/ Mart 1	Similar specificity to HMB45. Tends to be negative in spindle cell melanomas
Ki-67	Higher proliferation index in melanoma (13–35%) than in nevi (<5%). Useful in the evaluation of some melanocytic tumors, mainly nevoid melanoma
	Neuroectodermal and neural tumors
S100 protein	Positive in neuroectodermal, neuronal, nerve sheath, chondroid tumors, some sweat gland tumors, and myoepithelioma
NSE	Merkel cell carcinoma
CK 20	Merkel cell carcinoma
Neurofilament	Merkel cell carcinoma
Chromogranin	Merkel cell carcinoma
Synaptophysin	Merkel cell carcinoma
TTF1	Negative in most Merkel cell carcinoma
	Myogenic/myofibroblastic differentiation
MSA	Tumors of muscle origin
Desmin	Tumors of muscle origin (smooth muscle and skeletal muscle, rarely and focally in myofibroblastic tumors)
Myogenin	Positive in rhabdomyosarcoma
SMA	Positive in smooth muscle tumors, glomus tumor, myopericytoma, dermatomyofibroma

BCC, Basal cell carcinoma; *CK*, cytokeratin; *MSA*, muscle specific actin; *PEComa*, perivascular epithelioid cell tumor; *SCC*, squamous cell carcinoma; *SMA*, anti-smooth muscle actin.

Immunohistochemical techniques and trouble shooting

In many centers, IHC is now the most commonly utilized ancillary test for clinical tissue samples.

Historically, the introduction of enzymes as labels in IHC overcame difficulties associated with immunofluorescence, including the inability to assess histomorphology with the latter.[1] The peroxidase-antiperoxidase (PAP) technique was replaced by alkaline phosphatase-antialkaline phosphatase (APAAP) techniques and avidin-biotin complex (ABC) labeling.[1,2] Although the streptavidin-biotin labeling system gained popularity, the endogenous biotin-associated background staining under certain circumstances has resulted in increasing use of labeled polymer-based detection systems, suitable for manual and automated IHC platforms (*Fig. 2.9*).[3]

Fig. 2.8
Autostainer used for automated immunohistochemical testing.

The direct conjugation of the primary antibody to the label formed the principle of the initial, traditional direct technique, in which the labeled antibody reacted directly with the tissue antigen.[1] In the two-step indirect technique, labeled secondary antibody directed against the immunoglobulin of the animal from which the primary antibody was obtained to visualize the unlabeled primary antibody.[4] The labeled streptavidin-biotin (LSAB) method is a three-step technique. An unconjugated primary monoclonal or polyclonal antibody attached to the tissue antigen forms the first layer, creating an antigen-antibody complex. The second layer is formed by a biotinylated secondary antibody raised against the same species of the primary animal.[1] The secondary antibody binds to the primary antibody with the biotinylated end being available for binding to a third layer. This layer may bind either to enzyme-labeled streptavidin or to a complex of enzyme-labeled biotin and streptavidin. The enzyme may be horseradish peroxidase or alkaline phosphatase. An appropriate chromogen is used for detection. In the peroxidase method, peroxidase-oriented chromogens such as diaminobenzidine or 3-amino-9 ethylcarbazole are appropriate. Indole reagents (red), naphthol fast red (red), or NBT/BCIP (blue) are the chromogens used in the alkaline phosphatase-streptavidin method.[1,4]

The presence of endogenous biotin and resultant background staining led to the introduction of the increasingly popular polymer-based immunohistochemical methods. In the new direct enhanced polymer one-step (EPOS) technique, approximately 70 enzyme molecules and 10 primary antibodies are conjugated to a dextran 'backbone.' While the entire IHC procedure is completed in one step, the method is limited to highly select manufacturer-specific primary antibodies. Other newer polymer detection systems with a dextran backbone to which multiple enzyme molecules may attach are available for manual and automated IHC. These quick, reliable, and reproducible techniques are also characterized by greater sensitivity. Single-, dual-, triple-, and multi-color staining with different chromogens is possible.[1,2,4,5]

Background staining is a common difficulty that has multiple predisposing causes.[6] While monoclonal antibodies reduce non-specific background staining, not only must antibody concentrates and prediluted preparations be optimized for usage at the correct dilution in different laboratories (*Figs 2.10* and *2.11*), diluent pH is also critical in ensuring the absence of antibody degeneration and resultant background staining. Avidin-biotin detection systems and horseradish peroxidase systems may require biotin blocking and endogenous peroxidase quenching steps to decrease unnecessary background staining. Polymer-based detection systems can effectively

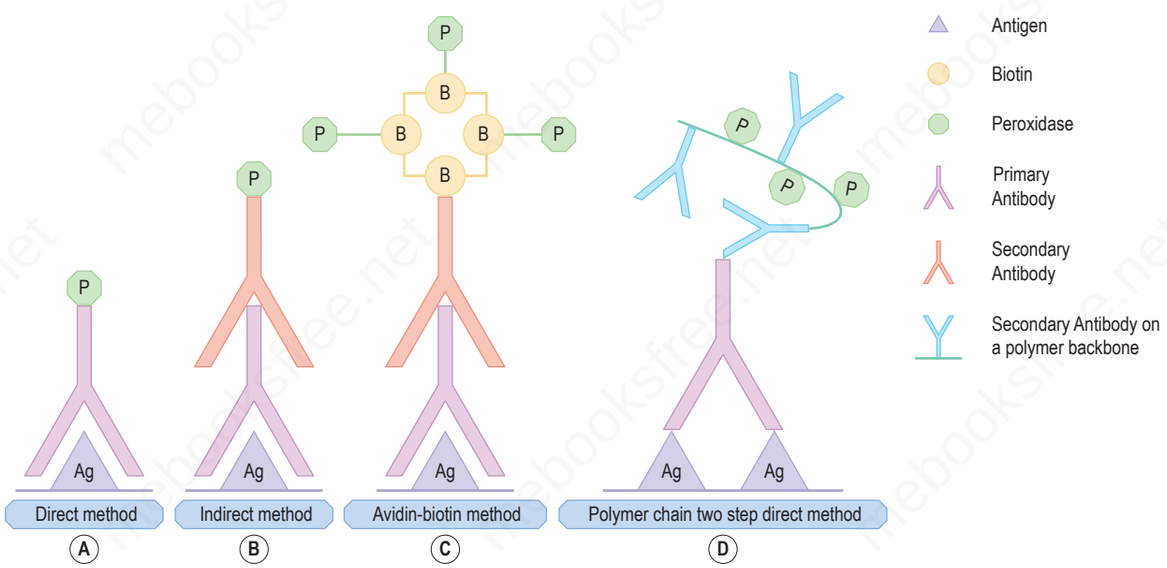

Fig. 2.9
Immunohistochemical techniques (**A**) direct, (**B**) indirect, (**C**) streptavidin biotin, (**D**) polymer chain. By courtesy of K Lumamba, Africa Health Research Institute, Durban, South Africa.

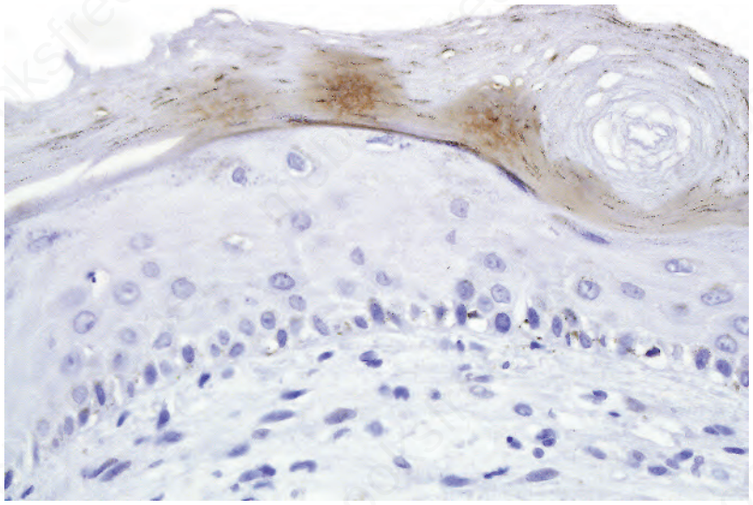

Fig. 2.10
Technical artifact: HHV8-stained sections demonstrating chromogen entrapment in stratum corneum.

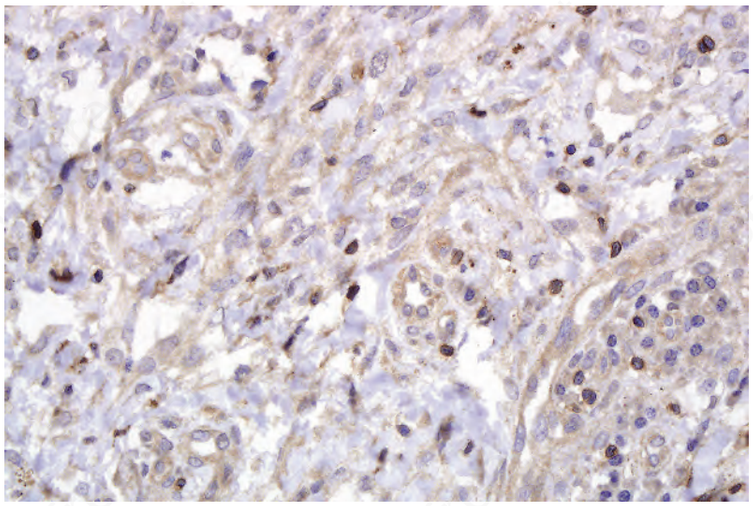

Fig. 2.11
Technical artifact: suboptimal antibody concentration of CD3 antibody resulting in background staining.

Fig. 2.12
Technical artifact: poor tissue fixation resulting in incomplete sections, fragmentation, and suboptimal AE1/AE3-stained sections.

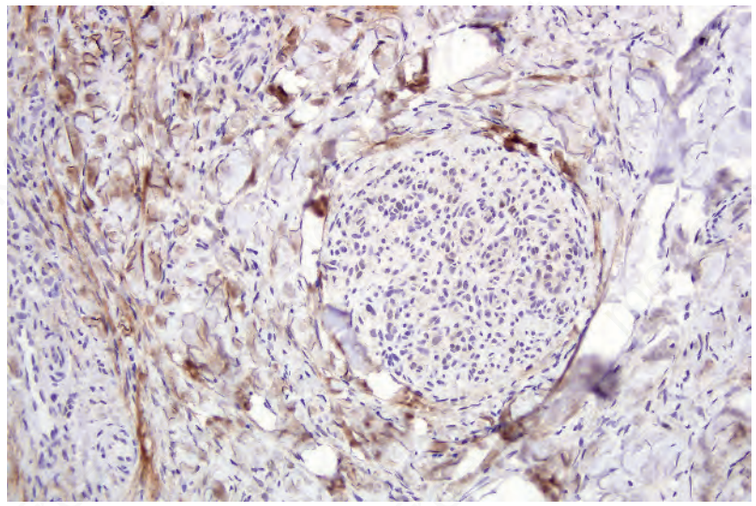

Fig. 2.13
Technical artifact p53 stain: wrinkling and background staining of tissue sections because of erroneously high temperature heat-assisted microwave antigen retrieval exposure of sections in EDTA buffer (pH 8.0).

eliminate biotin-induced false-positive staining. While antigen retrieval techniques are critical for antigen unmasking, optimal results require control of the pH and temperature of retrieval solutions and controlled enzymatic digestion.[7–10] The latter may cause variable tissue loss (*Fig. 2.12*), excessive background staining when sections are exposed to increased digestion time, inappropriate high temperature and inadequate rinsing, causing protein diffusion into or deposition in skin sections and background staining.

Chromogen entrapment, precipitation, and contaminants may lead to false-positive interpretation of an IHC test. Depletion of peroxidase or alkaline phosphatase chromogenic activity, a consequence of the breakdown of chromogens because of the sensitivity to light and heat, results in a background blush. A similar effect is seen when there is inadequate chromogen rinsing or prolonged chromogen time. Filtering of the chromogen is effective in preventing chromogen precipitation. Chatter, tears, folds and wrinkles and poor adhesion of sections to slides causes entrapment and suboptimal rinsing of chromogen (*Fig. 2.13*). Skin sections with a thick stratum corneum, dermal calcification, or sclerosis may be prone to these artifacts, requiring meticulous microtomy to prevent its occurrence. The improper handling of water baths, tissue sections, and slides with ungloved hands may cause contamination of sections with squames.[1]

False-negative immunostaining may also compromise IHC interpretation. Incomplete deparaffinization causes suboptimal or incomplete staining because of incomplete tissue penetration by the antibody. Overdigestion of tissue sections by proteolytic enzymes can destroy the tissue sections with attendant loss of antigen for antibody binding. Other causes of false-negative immunostaining include:

- incorrect temperature of reagents, including retrieval solutions,
- expired antibodies,
- inappropriate dilutions,
- suboptimal storage of antibodies.[1,3]

Immunofluorescence

Immunofluorescent techniques have the potential to define antigen-antibody interactions at a subcellular level.[1] This interaction requires the irreversible binding of a readily identifiable label for its recognition.[1,2] Fluorochromes such as rhodamine or fluorescein are labels that can absorb radiation in the form of ultraviolet or visible light.[1–5] Direct and indirect immunofluorescence (IMF) techniques demonstrate a range of tissue antigens of

dermatopathological importance, including the diagnosis of infectious and autoimmune blistering disorders.[3] In the direct IMF technique, antibody is conjugated directly with a fluorochrome and is used to detect an antigen in a tissue section using ultraviolet light microscopy.[1–3] In the indirect IMF technique, patient serum (containing the antibodies) interacts with a tissue section containing the antigen. Antibody to a human immunoglobulin, conjugated to a fluorochrome, is applied thereafter.[1–7] The successful demonstration of the antigen requires the antigen to remain sufficiently insoluble *in situ*. Skin biopsies for direct immunofluorescence can be transported fresh on saline-soaked gauze in a container on ice, or in a transport medium such as Michel medium.[8] The transport medium must be maintained at a pH of 7.0–7.2.[1,3,5] The main uses for IMF in dermatopathology are in the interpretation of the autoimmune blistering diseases, lupus erythematosus, and vasculitis.[6,7] In general, immunofluorescence has the following advantages over immunohistochemistry:

- more sensitive detection of antigen.
- use of special fixation that preserves 'difficult' antigens.

Fading of immunofluorescence sections can be overcome by the use of anti-fading mountants.

Electron microscopy

Electron microscopy is much less utilized than in the past. Immunohistochemical approaches are preferred in those instances where they are a reasonable substitute.

Transmission electron microscopy offers much better resolution than light microscopy.[1] To optimize this, tissue has to be embedded in extremely rigid material to allow ultrathin sectioning at 80 nm. In most circumstances, hydrophobic epoxy resins are preferred. When a specimen requires ultrastructural examination, the portion to be examined must be treated in a suitable fixative immediately. The volume of the fixative should be 10 times the sample size. The final specimen is cubed to 1 mm portions.[1] Fixation is affected by:

- pH,
- osmolarity,
- ionic composition of buffer,
- fixative concentration,
- temperature,
- duration of fixation.

Primary fixation in an aldehyde, usually glutaraldehyde, and secondary fixation in osmium tetroxide are standard procedures. Advances in immunohistochemistry have decreased the dependence on electron microscopy for ultrastructural confirmation of cell lineage. Notwithstanding, dermatologic ultrastructural investigations are important in the diagnosis of:

- undifferentiated tumors,
- immunobullous disease,
- cerebral autosomal dominant arteriopathy with subcortical infarcts and leukoencephalopathy (CADASIL),
- amyloidosis,
- metabolic storage diseases.[2–7]

Intercellular junctions, Weibel-Palade bodies, melanosomes, and premelanosomes may help in the diagnosis of carcinomas, endothelial tumors, and melanocytic tumors, respectively.[3] In CADASIL, extracellular, electron-dense granular material is present in an indentation in vascular smooth muscle cells.[5,6] Amyloid is identifiable as randomly arranged, extracellular, nonbranching fibrils of indeterminate length and 7–10 nm diameter.[7] Transmission electron microscopy remains a valuable tool in the ongoing evaluation of the structure of normal and pathological human cell and tissue components and infective agents.[8–10] Technological advancements have enabled electronic capture of ultrastructural images (*Fig. 2.14*).

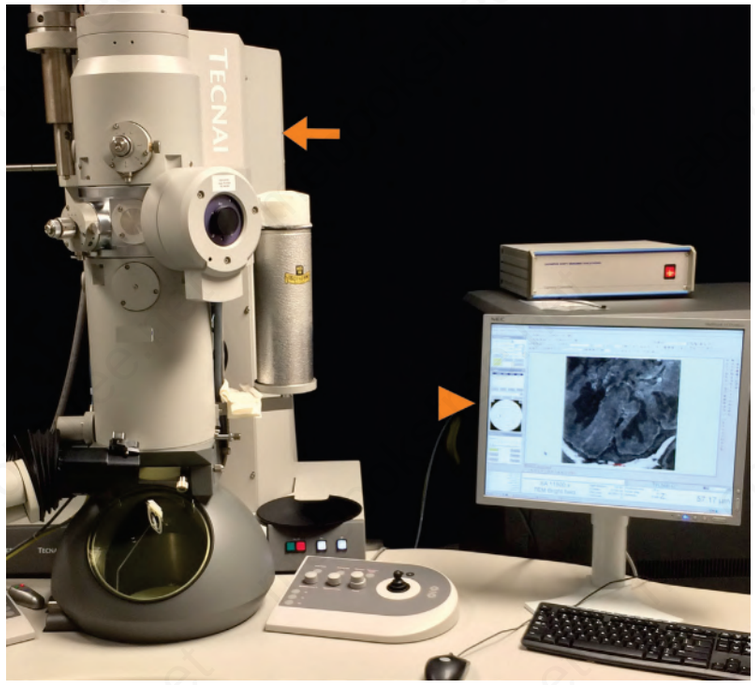

Fig. 2.14
Transmission electron microscope (*arrow*) with electronic image capture (*arrowhead*).

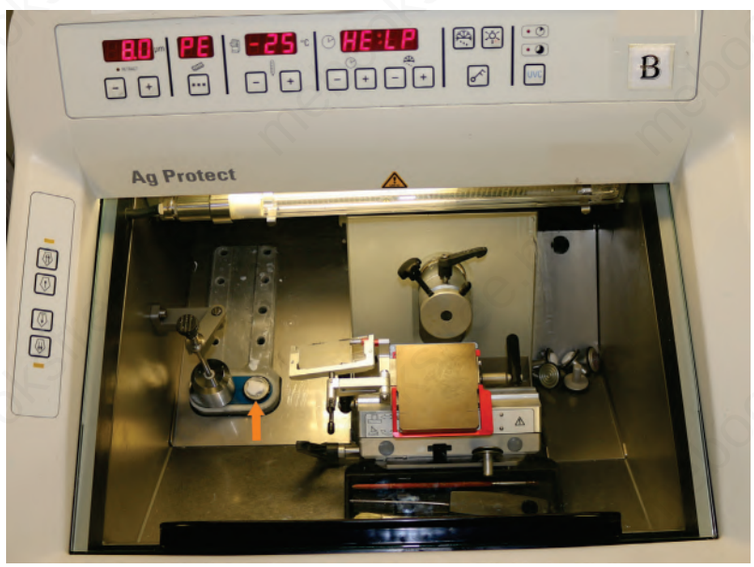

Fig. 2.15
Cryostat with tissue on freezing stage (*arrow*).

Frozen section examination of skin specimens

Although frozen section appraisal of the skin is undertaken mainly for assessment of excision margins of cutaneous tumors, it may also be used for primary diagnosis of cutaneous lesions. Frozen section evaluation of incisional (punch, shave) or excisional biopsies can be performed.[1] Frozen section specimen processing and sectioning is undertaken in a cryostat ('cryo' referring to cold and 'stat' referring to stationary) (*Fig. 2.15*), a refrigerated steel cabinet with a holding temperature of –5 to –30°C, containing a microtome and an anti-fogging air circulating system.[2] Commercially available freezing mixtures, e.g., optimum cooling temperature (OCT) mixture, enables rapid fixation of the skin sample on a freezing stage. Evaluation of tumor margins by conventional or Mohs micrographic surgery is expensive and time consuming; hence cases for frozen section assessment must be selected carefully.[3] Indications for frozen section evaluation include lesions with poorly defined clinical margins, infiltrative growth patterns, and long-standing and/or recurrent lesions, especially those in locations where skin preservation is necessary.

Diagnostic cytopathological techniques in dermatopathology

Cytopathological investigation of selected skin lesions has excellent outcomes in dermatopathological practice if used appropriately.[1,2] Cytodiagnostic skin testing, introduced in the previous century by way of the Tzanck test, currently encompasses exfoliative and aspirational sampling methods.[3–5] The exfoliative technique involves touch imprints or gentle scraping of a skin lesion with a straight scalpel and smearing of the scraped contents onto a slide, air drying, and staining with hematoxylin and eosin, May-Grünwald-Giemsa, or Papanicolaou stains.[6] The main indications for exfoliative cytology in dermatological practice includes autoimmune bullous disease infections and genodermatoses.[5–8] Fine-needle aspiration cytology may be used for the initial diagnosis of some superficial, palpable nodular, tumoral lesions inclusive of basal cell carcinomas, Langerhans cell histiocytosis, mast cell diseases, and adnexal tumors and infections but limitations of the technique include technical training of aspirators, poor cellular yields, and lack of assessment of tumor patterns and excision margins.[6,9] Issues related to tumor patterns and excision margins may be overcome by various cell block techniques that may be undertaken when small aspirated tissue fragments are unsuitable for cytological preparation and for processing of residual cell sediments after smear preparation.[2,5,10,11] Cell block preparations have evolved from simple sedimentation techniques to sample centrifugation and the addition of a range of cellular adjuvants for cell cohesion.[10] The fundamental steps in cell block preparation encompass fixation, centrifugation and cell pellet hardening and transfer for paraffin embedding.[10] The most popular adjuvants for manual pellet hardening include plasma thrombin and agar techniques.[10] Recent technological advances have introduced automated cell block preparation that are claimed to have shorter processing times, maintain crisp and clear cellular architecture, maximized cellularity, reduced cross-contamination risk, and minimal operator-associated result inconsistency.[12]

Diagnosis of inherited skin diseases

An efficient approach to genetic testing often relies on initial traditional histologic characterization of skin biopsies.

Recent advances in molecular genetics and gene sequencing have led to many inherited skin diseases being diagnosed or confirmed by clinical molecular biologists rather than dermatopathologists. Analysis of skin biopsies still remains vital for the accurate diagnosis of several genodermatoses, and often provides a guide for subsequent molecular analyses. Examination of the skin biopsy informs the selection of additional molecular testing. Communication between the dermatopathologist and molecular laboratory is absolutely critical for efficient use of molecular techniques.

Analysis of the inherited skin blistering disorder known collectively as epidermolysis bullosa (EB) discussed in detail in Chapter 4 demonstrates the complex, multifaceted approach to diagnosis required in such cases. EB has been shown to result from mutations in at least 18 different genes encoding different structural proteins at or close to the dermal-epidermal junction or within the epidermis (*Fig. 2.16*).[1,2] Clinically, the different types of EB are characterized by widely differing prognoses, from death in early infancy to blistering that may become milder in later life.[3] The clinical presentation in neonates, however, can be confusing to dermatologists and pediatricians because of the overlapping features (*Fig. 2.17*). In these circumstances, skin biopsy, usually a superficial shave biopsy since the key region is usually the dermal-epidermal junction, can provide critical diagnostic and prognostic information. Typically, non-blistered skin is sampled; clinicians should be discouraged from biopsying established blisters however because of the potential artifact associated with re-epithelization and misrepresentation of the true plane of cleavage. Just before the biopsy is taken, the non-blistered skin is rubbed gently in an attempt to induce fresh microsplits in the skin to facilitate the microscopic subtyping of EB (*Fig. 2.18*).

The most informative investigation is immunolabeling of the dermal-epidermal junction (and keratinocyte junctional proteins for more

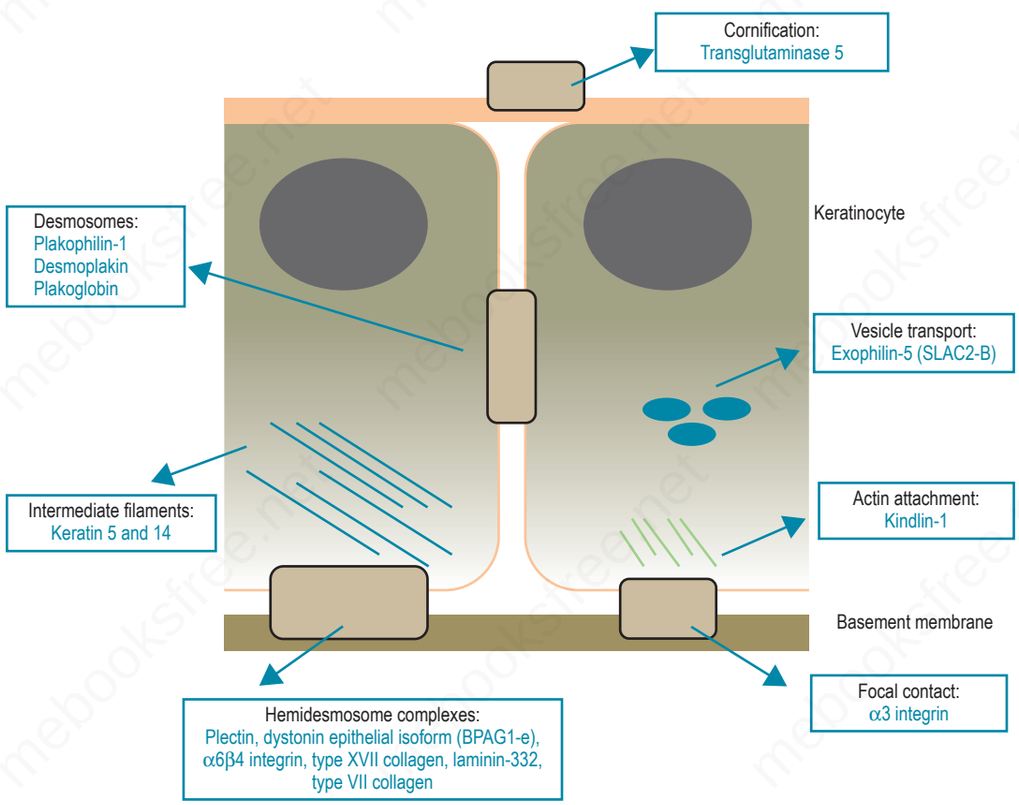

Fig. 2.16
Basement membrane region: protein components at the dermal-epidermal junction and the subtypes of EB that result from mutations in the genes encoding these proteins.

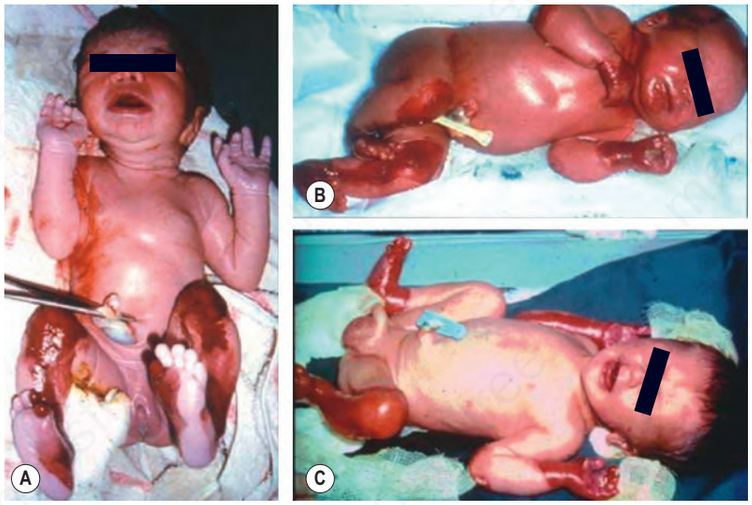

Fig. 2.17
Clinical appearances of neonates with different forms of inherited EB. All three cases have similar blisters and erosions but their respective prognoses differ considerably. (**A**) Severe, generalized recessive dystrophic EB; (**B**) Dowling-Meara EB simplex; (**C**) Herlitz junctional EB. Skin biopsy is fundamental to establishing the subtype of severe forms of EB.

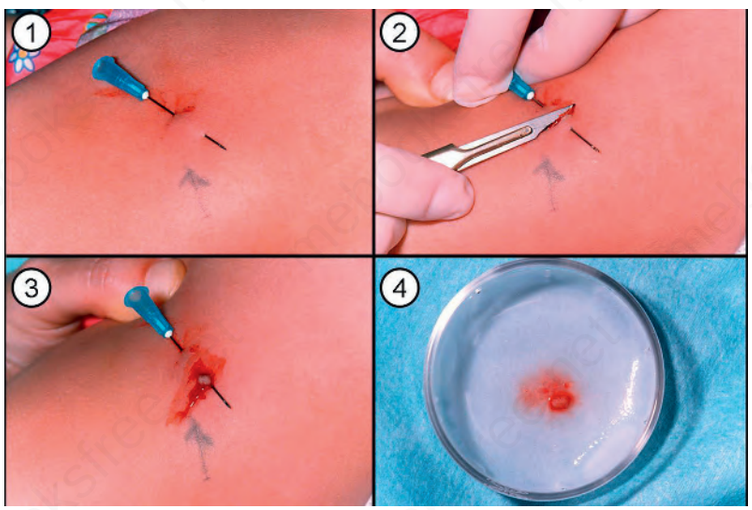

Fig. 2.18
Optimal skin biopsy for diagnosing EB: following local anesthesia, the normal-appearing skin is gently rubbed, and then a superficial shave biopsy is taken. The skin sample can then be subdivided for immunolabeling of frozen sections as well as being processed for transmission electron microscopy.

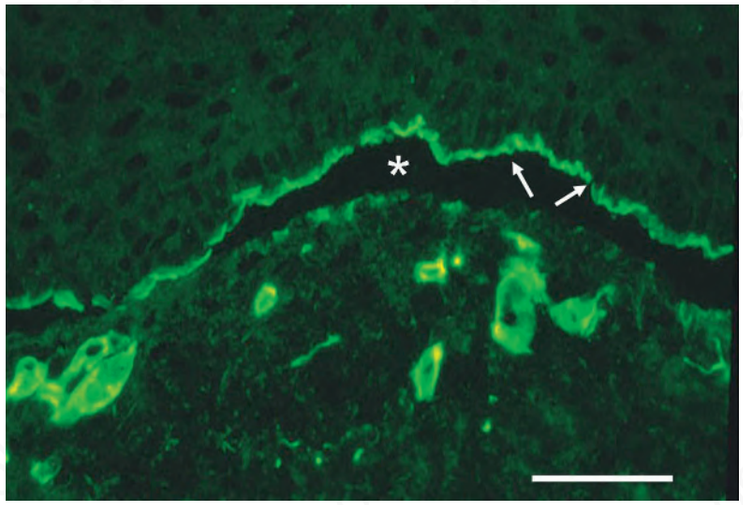

Fig. 2.19
Antigen mapping to diagnose the subtype of inherited EB: this picture shows immunolabeling of rubbed skin from an individual with EB (case illustrated in *Fig. 2.17A*) with an anti-type IV collagen antibody. Rubbing the skin induces microsplits at the dermal–epidermal junction (*asterisk*). The type IV collagen reactivity maps to the roof of the dermal–epidermal junction (*arrows*). This indicates a sublamina densa plane of cleavage and establishes a diagnosis of dystrophic EB. (Bar = 25 μm.)

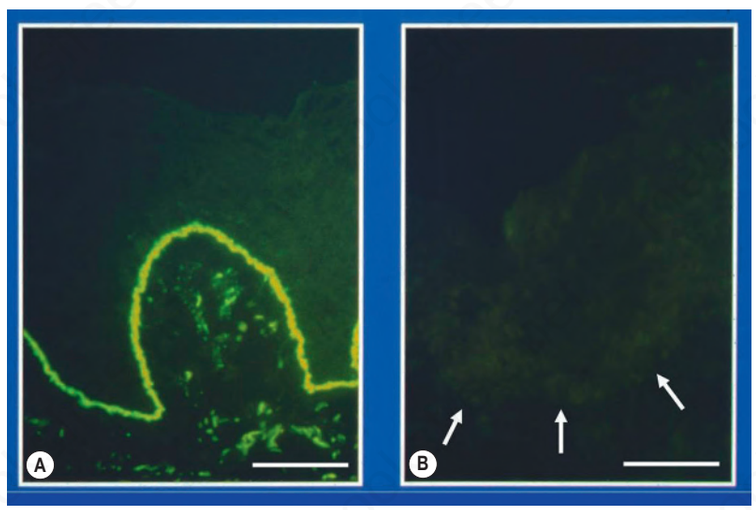

Fig. 2.20
Specific antibody probes to subtype inherited EB: (**A**) immunostaining of normal control skin with an antibody to type VII collagen shows bright linear labeling at the dermal–epidermal junction; (**B**) in contrast, the complete absence of labeling in skin from an individual with EB (case illustrated in *Fig. 2.17A*) indicates a diagnosis of severe, generalized recessive dystrophic EB. (Bar = 50 μm.)

superficial forms of EB, if necessary) using a panel of basement membrane or desmosomal antibodies. Skin biopsies can be transported in Michel medium to a diagnostic laboratory at ambient temperature: this fixative is extremely useful since basement membrane zone and desmosome immunoreactivity is maintained for at least 6 months.[4] For the immunolabeling, frozen skin sections are used rather than formalin-fixed paraffin-embedded material because the antigenic epitopes of several transmembranous proteins may be lost in routine skin processing. The antibodies can be used either to determine the level of cleavage in the skin (antigen mapping) or to see if there is a reduction or absence of immunostaining for a particular antigen.[5] *Fig. 2.19*, for example, demonstrates labeling using an antibody against type IV collagen in skin from the neonate illustrated in *Fig. 2.17A*. In this example, labeling maps to the roof of the split. This indicates that the lamina densa is in the blister roof and that there is a sublamina densa plane of blister formation. These findings support a diagnosis of dystrophic EB. This diagnosis can be refined by immunolabeling with an antibody to type VII collagen, as shown in (*Fig. 2.20*). In normal skin there is bright, linear labeling at the dermal-epidermal junction; however, in the skin from the neonate shown in *Fig. 2.17A*, there is a complete absence of type VII collagen immunoreactivity. All other antibodies show normal reactivity at the dermal-epidermal junction. These findings therefore establish a diagnosis of generalized severe recessive dystrophic EB. Reduced or absent immunolabeling with specific basement membrane antibodies is an extremely useful and rapid means of diagnosing recessive forms of EB. For example, skin from the neonate shown in *Fig. 2.17C* demonstrated a lack of reactivity against laminin-332 but normal immunostaining for all other antibodies. These findings establish a diagnosis of generalized severe junctional EB.

The development of a panel of antibodies for the target proteins implicated in the different forms of EB, most of which are commercially available,

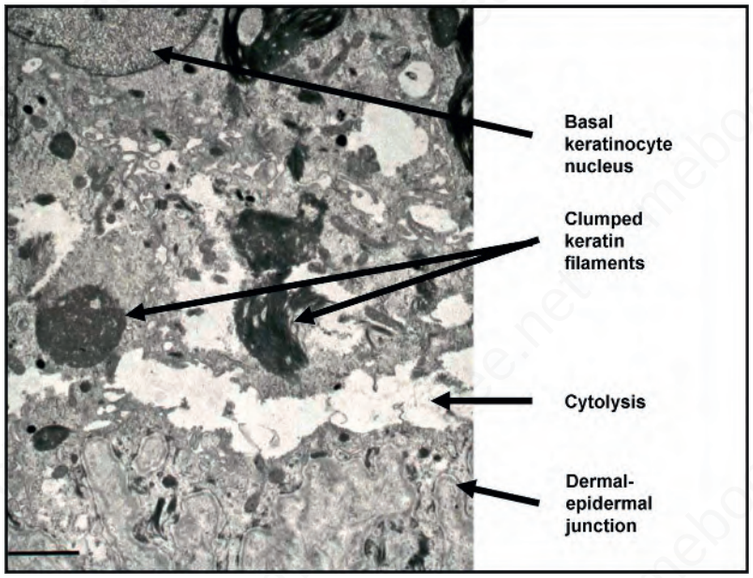

Fig. 2.21
Transmission electron microscopy of skin in Dowling-Meara EB simplex (case illustrated in *Fig. 2.17B*): within the basal keratinocyte cytoplasm the keratin filaments are condensed and form clumps and there is cytolysis that occurs just above the dermal–epidermal junction. (Bar = 1 μm.)

has led to decreased emphasis on transmission electron microscopy as a diagnostic tool in EB.[6] Ultrastructural analysis, however, can be useful in confirming the plane of cleavage and in establishing the diagnosis of certain dominant forms of EB. Skin from the neonate illustrated in *Fig. 2.17B*, for example, shows normal intensity basement membrane zone reactivity for all diagnostic probes but transmission electron microscopy (*Fig. 2.21*) identifies discrete clumps of tonofilament and basal keratinocyte cytolysis, characteristic of the generalized severe variant of autosomal dominant EB simplex. For recessive forms of EB, however, skin immunolabeling has become the most important diagnostic approach.[7] Reduced or absent staining for a particular protein provides a rapid diagnosis as well as a means of identifying the encoding gene (or genes) in which the underlying pathogenic mutations are present. Thus the skin biopsy findings, both histologic and immunohistochemical, provide a direct guide to molecular screening tests, most of which are PCR-based or next-generation sequencing (NGS)–based, as discussed below. For dominant forms of EB, however, skin immunohistochemistry of patient skin may be indistinguishable from normal control skin and therefore Sanger sequencing of DNA is often preferred to skin biopsy analysis as the initial diagnostic investigation.[6] Indeed, DNA sequencing is the optimal method for diagnosing the most common form of EB, localized EB simplex (blisters mainly on the hands and feet, which accounts for >70% of all cases of EB). Furthermore, the diagnosis of EB is increasingly embracing NGS technologies, including whole exome sequencing and selected gene panels, as primary diagnostic tools.[7] This molecular information can then be used for genetic counseling, carrier screening, and DNA-based prenatal testing, if indicated. Nevertheless, a clear advantage of skin biopsy diagnostics for EB is time to diagnosis: skin immunohistochemistry can be completed within 2 days and thus skin biopsy is likely to remain a key part of EB diagnostics, particularly in the diagnosis of neonates with EB, for the foreseeable future.

Molecular techniques

Chromosomal karyotyping

This technique can be used as an initial screen to demonstrate gross chromosomal aberrations associated with certain tumors. Most skin tumors are small and thus tissue is generally not set aside for karyotype analysis.

Chromosomal karyotyping is the historical gold standard for detecting chromosomal aberrations in neoplastic tissue (*Fig. 2.22*), though many other excellent techniques now exist as well. Fresh tumor tissue is required to grow the cells and the cytogenetic preparations and interpretation require skilled personnel. Nonetheless, this technique provides an open, unbiased look at all of the chromosomes of a particular tumor. Total chromosomal gains and losses and also translocations between chromosomes can be demonstrated. Some of these chromosomal translocations are virtually diagnostic of certain tumors, particularly soft tissue and hematopoietic tumors.[1,2] Other chromosomal changes can be suggestive of certain tumor types. While most translocations are now confirmed by the other molecular methods described below, traditional chromosomal karyotyping retains a minor role as an initial examination of the chromosomal complement of a neoplasm and an important tool for discovery of new chromosomal aberrations.[3] Historically, the discovery of chromosomal translocations within specific tumor types is proportional to the number of cases karyotyped.[4] More recently, this discovery modality has been supplanted by massively parallel sequencing techniques (NGS), in particular RNA sequencing discussed further below. The interpretation of complex karyotypes can be informed by additional methodologies discussed below such as spectral karyotyping (SKY) or multiplexed fluorescence in situ hybridization (mFISH).

Allelic imbalance

Gains or losses of specific regions of DNA, often containing particular genes of interest, can provide diagnostic insight.

An allele is a variant of a particular genetic locus or region of DNA such as a gene. Detection of allelic imbalance or loss of heterozygosity (LOH) is a method that can detect the presence of deletions or gains of specific alleles in paraffin-embedded material.[5] This usually corresponds to regions of a particular gene(s) of interest. For this approach, PCR is used to amplify small genomic fragments that carry common polymorphisms and thus have a high likelihood of being present in two different variants (alleles) in an individual. Ideally, these variants are of different size so that they can easily be detected on an electrophoretic gel; DNA sequencing can be used if this is not possible. Only if two different alleles in the normal tissue of a patient are present is this technique informative. Imbalance (loss of one allele) is implied if one detects only one of the alleles in the tumor tissue, or more commonly a vast excess of one allele since normal tissue is present with the tumor cells. More detailed analysis can distinguish those that are true losses. Sites of recurrent losses are typically areas that harbor tumor suppressor genes. This method can detect losses that would not be demonstrated in a traditional chromosomal karyotype analysis and can be readily adapted to formalin-fixed, paraffin-embedded (FFPE) tissue. The limitations of LOH analysis include that it is sensitive to contamination by normal (stromal) cells that with increasing amounts can make it difficult to decide whether an allele is lost. Another drawback is its inability to determine whether the imbalance is caused by the loss of one marker or by a copy number increase of the other marker.

Fluorescence in situ hybridization (FISH)

FISH uses specific probes to determine the number of copies of a specific region of DNA that are present or whether a particular locus has been rearranged as part of a chromosomal translocation.

FISH utilizes fluorescently labeled probes that are complementary to and thus specifically hybridize a specific region of genomic DNA, allowing it to be visualized.[6,7] The labeled probe and the target genomic DNA, which can be metaphase spreads, interphase nuclei (*Fig. 2.23*), or nuclei in formalin-fixed, paraffin-embedded tissue sections (*Fig. 2.24*), are denatured and brought into contact for several hours to days. Given appropriate hybridization conditions, the labeled probes will anneal with the corresponding sequence in the target DNA. This is easiest if probes are targeted to chromosomal regions that are rich in repetitive sequences such as the centromeres. In these regions the probe can hybridize multiple times, resulting in hybridization signals that are large and easy to detect. However, these regions typically do not contain any functional genes, and while increases in chromosome copy number can be recognized, no direct information on the copy number of a specific cancer gene or locus can be obtained. Human cancers, including

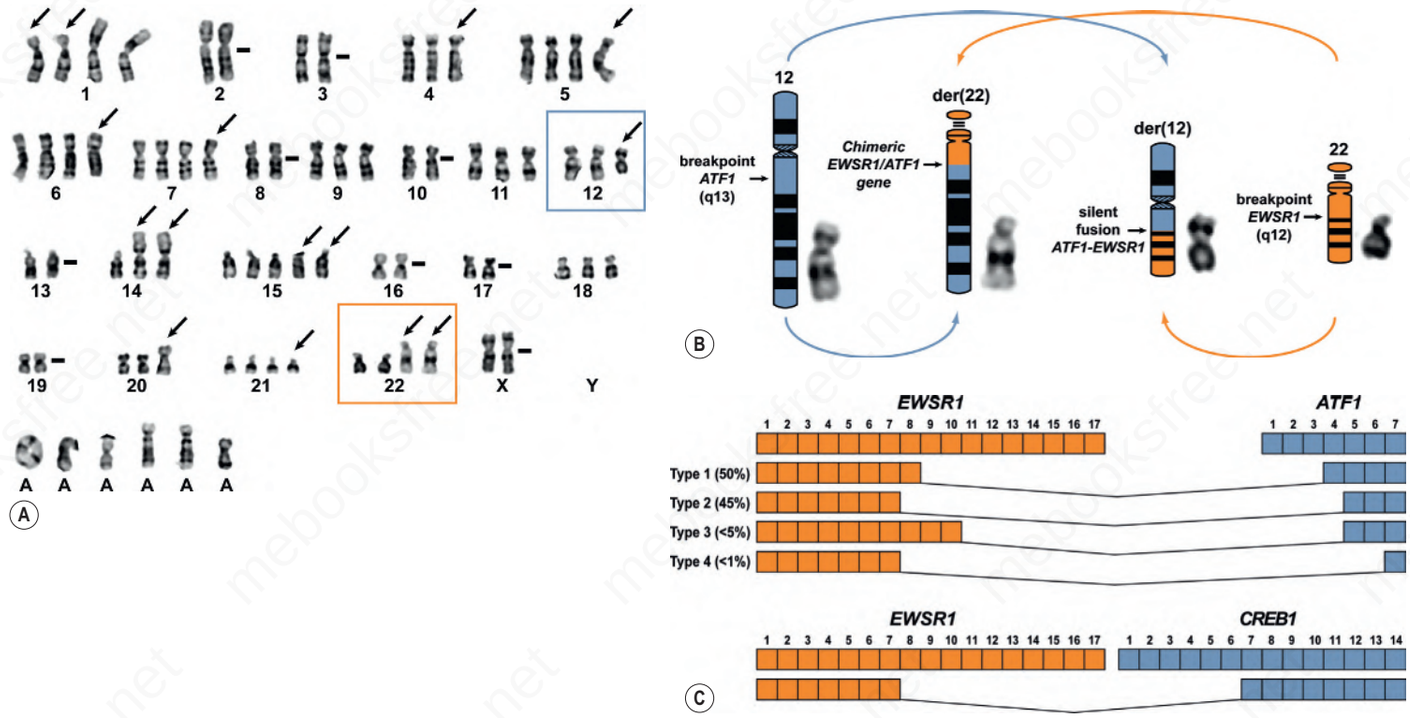

Fig. 2.22

Genetics of clear cell sarcoma: (**A**) this complicated karyotype shows derivative chromosomes 12 (*blue box*) and 22 (*orange box*). While recurrent translocation-associated karyotypes are initially simple, they can become more complex with tumor progression. (**B**) The mechanism of chromosomal translocation involves breaks in chromosomes 12 and 22 that recombine to produce novel derivative chromosomes 12 and 22. The active fusion gene (*EWSR1-ATF1*) is produced on der(22). The fusion genes can be produced by a variety of breakpoints within the introns of the involved genes making multiple exon combinations (**C**). This complicates the design of PCR-based detection methods, as does substitution of the *CREB1* gene for *ATF1* on occasion.

melanoma, frequently have aberrations that involve only fragments of the chromosome. The detection of these types of aberrations requires probes targeted to unique, i.e., nonrepetitive, sequences of DNA. Unique sequence probes give smaller hybridization signals and can be more difficult to detect. However, by using larger probe sizes of 100–300 kb, detection of unique sequences is possible in paraffin sections (see *Fig. 2.22*). The advantage of FISH is that it can detect cells with aberrations in the presence of significant numbers of normal cells, provided that the neoplastic cells can be morphologically identified in the hybridized section. Combinations of FISH and immunofluorescence have been developed to assist in the identification of the target cell population, but the compromises that have to be made to accommodate antigen preservation while maintaining acceptable hybridization efficiency restrict its application for routine use in paraffin-embedded tissue. Detection of heterozygous deletions is more difficult with FISH in tissue sections, because truncation of nuclei in tissue sections cut at normal thickness results in random loss of hybridization signals. Similarly, increased ploidy of the neoplastic tumor cell population can simulate a gain of the target locus. These problems can be compensated spatially by simultaneously hybridizing multiple, differentially labeled, probes to several loci in the genome and statistically by analyzing a larger number of cells. Comparing a probed locus to a centromeric probe on the same chromosome in an alternate color can control for cell aneuploidy. A common example of this technique is comparison of the hybridization signals for the *HER2* locus on 17q with centromere 17. This allows one to detect and distinguish both increased copy number of chromosome 17 and specific amplification of the *HER2* locus.

FISH using probes that flank a potential breakpoint associated with a chromosomal translocation can be used to demonstrate rearrangement of that locus (*Fig. 2.25*). This can be diagnostically helpful in certain hematopoietic malignancies with recurrent translocations, e.g., large cell anaplastic lymphoma and some soft tissue tumors that can involve the skin.[8,9] In this method, the flanking probes are fluorescently labeled in two different colors such as green and red, and when they are in close proximity in an intact chromosome, the spectral overlap leads to two yellow signals, one for each normal chromosome. In a cell with a rearrangement of a gene such as *EWSR1* at 22q12 in clear cell sarcoma, nuclei are seen with one intact chromosome 22 with *EWSR1* producing a yellow signal. In addition, the centromeric probe is retained on the derivative (rearranged) 22 chromosome while the telomeric probe is transferred to the recipient chromosome (12 in the case of clear cell sarcoma) leading to separate red and green signals in the nucleus. This method only indicates that a locus is rearranged, not the identity of the chromosomal partner and gene. Thus caution must be used in interpretation as different translocations seen in different neoplasms can be associated with the same probed locus. For instance, *EWSR1* is rearranged in clear cell sarcoma, Ewing sarcoma, extraskeletal myxoid chondrosarcoma, angiomatoid fibrous histiocytoma, and some cases of myxoid liposarcoma (*Fig. 2.26*). Careful correlation with the clinical and histologic features can help avoid confusion in these situations.

The disadvantage of FISH is that it can only look at a few loci at a time, and that analysis is time-consuming because signals in a large number of nuclei have to be counted. The latter restriction has been partially overcome by the development of computer-based counting algorithms.[10]

In situ hybridization can also employ chromogenic probes such that light microscopy can be used to visualize signals (termed CISH). This method is useful for detecting amplification of a genetic locus and technically can be utilized in a break-apart probe strategy to detect translocations, but in practice this latter application can be very difficult to interpret. Probably the most common use for CISH is in direct detection of nucleic acids associated with infections in cells such as human papillomavirus (HPV) or Epstein-Barr virus. In HPV, this technique can be used to type the virus and determine

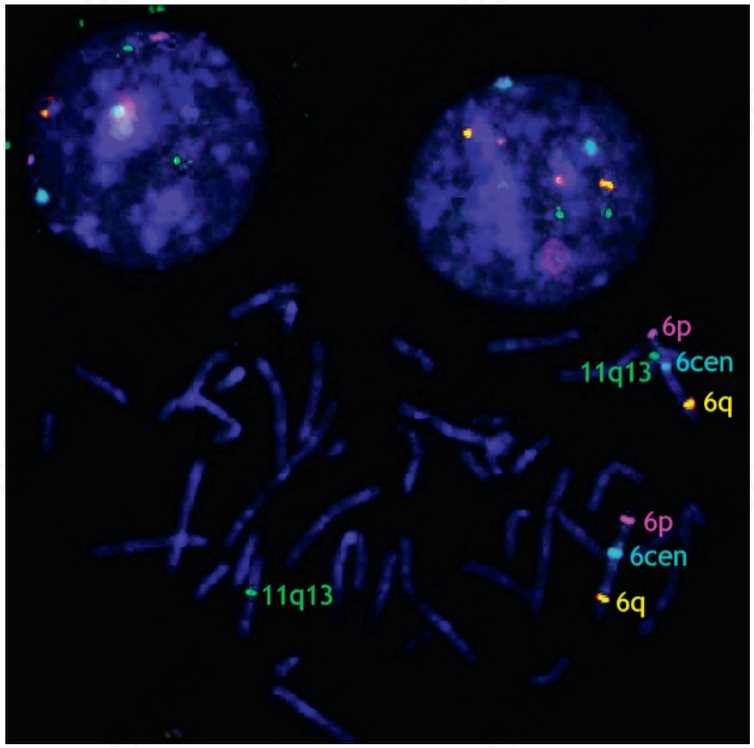

Fig. 2.23
Four-color FISH to two interface nuclei and metaphase chromosomes: the upper portion shows two interface nuclei with the hybridization signals for the four colors detectable as discrete spots. In the metaphase spread underneath, the hybridization signals can be seen to map to chromosome 6p (*purple*), 6 centromere (*light blue*), 6q (*yellow*), and chromosome 11q13 (*green*).

whether it is high risk (e.g., 16 and 18) or low risk (6 and 11). In this application, ISH is used to demonstrate the presence of viral DNA that is not present in a cell until infection occurs. Modifications of this technique can be used to detect messenger RNA in tissue sections as well.

In situ hybridization, fluorescent or chromogenic, is best used to demonstrate:

- amplification of a specific gene,
- rearrangement of a specific gene,
- presence of 'foreign' (infection-related) DNA or RNA.

Modifications of the FISH technique termed multiplex FISH, spectral karyotyping, or whole chromosomal painting can be used to individual color each chromosome allowing for more ready karyotyping and quickly identifying fusion or derivative chromosomes.[11] Such techniques can be very helpful in

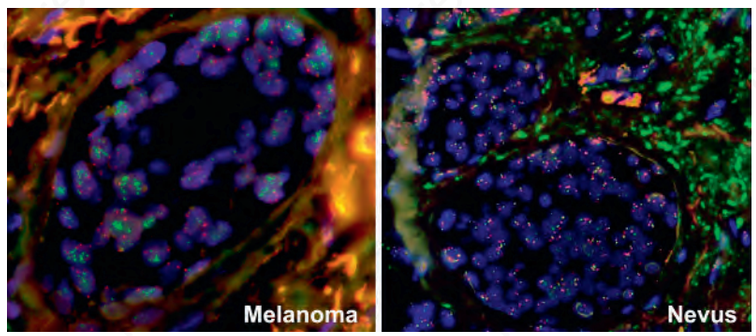

Fig. 2.24
FISH to tissue sections of a melanoma (*left panel*) and nevus (*right panel*): the panels show 400-fold magnifications of two nests of melanocytes with the nuclei stained in blue. The green probe for chromosome 11q13 shows amplification in the melanoma as evident by a marked copy number increase compared to the purple signals representing chromosome 6p. By contrast, the melanocytes of the nevus in the right panel do not show significant differences for these two loci.

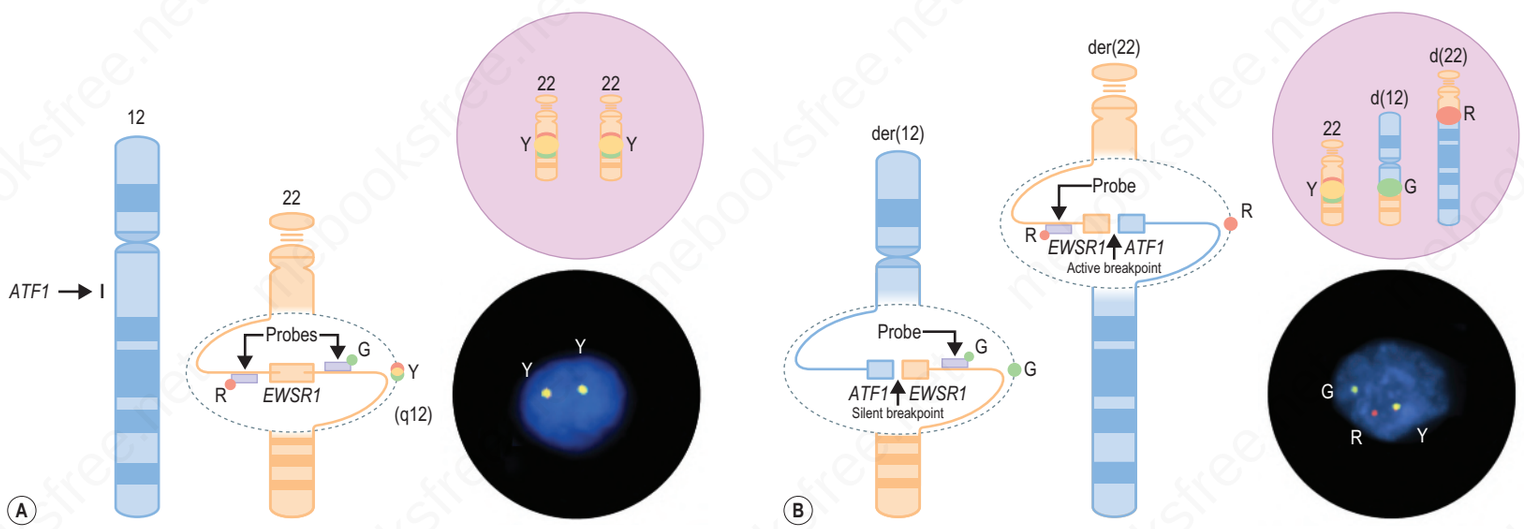

Fig. 2.25
Break-apart FISH technique: the 12;22 translocation associated with clear cell sarcoma is depicted. (**A**) When the *EWSR1* locus is intact, the probes hybridize to the centromeric (*red*) and telomeric (*green*) regions flanking the gene. The spectral overlap of the two signals in juxtaposition produce a yellow signal. Thus in cell lacking rearrangement of this locus, two yellow signals are present, representing the two copies of chromosome 22 lacking rearrangement (*right*); (**B**) When rearrangement occurs, such as the balanced translocation with chromosome 12 depicted here, the centromeric probe (*red*) is retained by the derivative chromosome 22 while the green probe is transferred to the derivative chromosome 12. Thus in the nuclei one yellow signal indicates the intact chromosome 22 while the derivative 12 and 22 chromosomes segregate freely as single green and red signals, respectively (*right*).

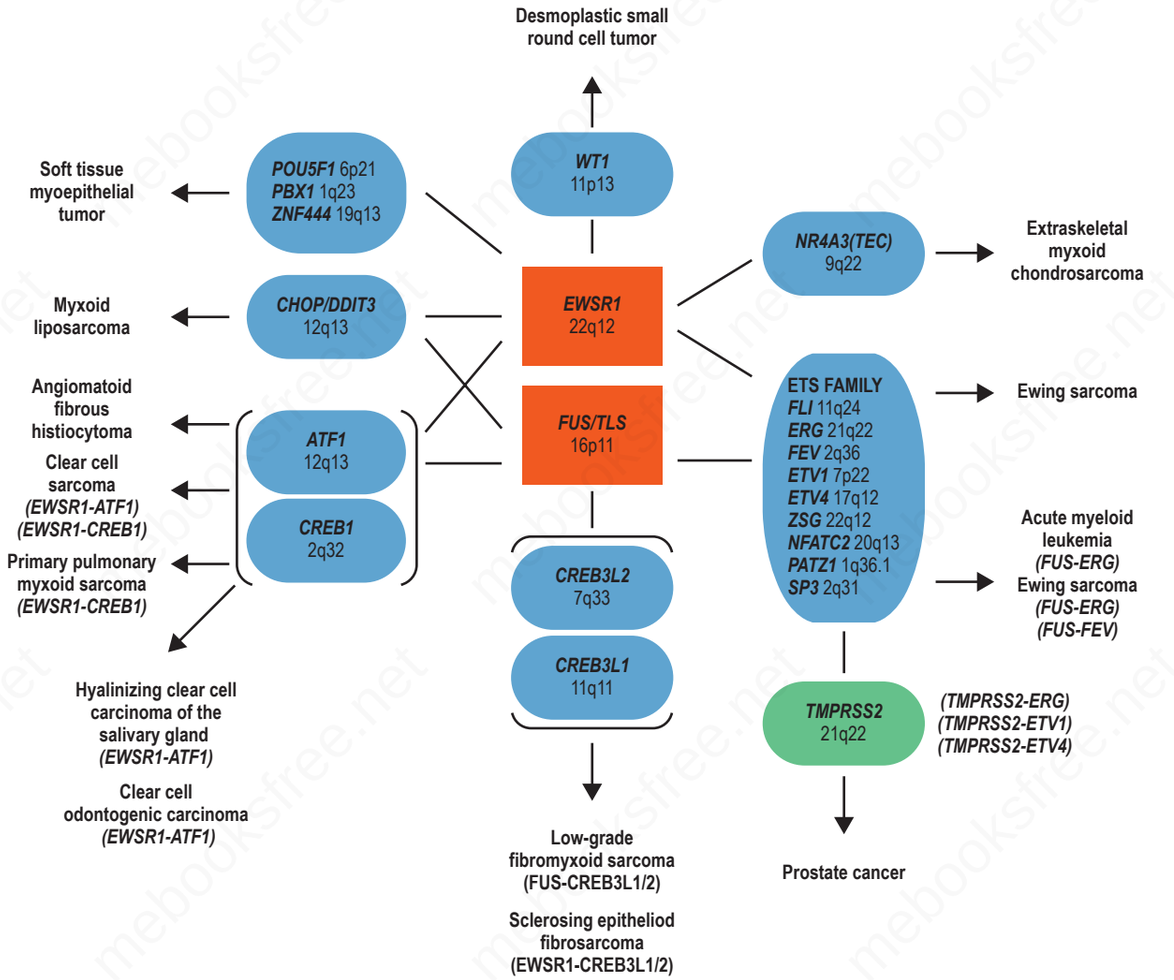

Fig. 2.26
Multiple translocations involve *EWSR1* and the homologous gene, *FUS*: both *EWSR1* and *FUS* can often substitute for one another and both are involved in balanced translocations with multiple genes resulting in a variety of neoplasms. Since FISH only indicates that a single locus, such as *EWSR1*, is rearranged and nothing about the fusion partner, results must be interpreted carefully within the clinical and morphologic context of a tested case. Sometimes techniques such as RT-PCR must be used to verify the fusion partner.

the interpretation of complex karyotypes. Computer-assisted pseudocoloration can also facilitate semi-automated karyotyping.[12]

Comparative genomic hybridization (CGH)

CGH can be used to demonstrate gains and losses of DNA through the entire genome of a tumor sample. While initially a research tool, its application has led to important discoveries that have been translated into focused genetic tests. In other cases, more global information is needed and this test is increasingly applied in the clinical setting, such as distinguishing melanoma from melanocytic mimics.[13]

CGH demonstrates for the entire genome:

- regions of chromosomal loss (often containing tumor suppressor genes),
- regions of chromosomal gains (often containing oncogenes),
- overall patterns of gains and losses (rather than just a few focused regions).

As originally described, CGH detects and maps DNA sequence copy number variation throughout the entire genome onto a cytogenetic map supplied by metaphase chromosomes (*Fig. 2.27*).[14] CGH can be regarded as a variation of FISH in which the entire genome of a sample such as DNA from a skin tumor is used as a hybridization probe. The tumor is freed as much as practically feasible from contaminating normal cells by manual dissection, the DNA extracted, and labeled with a fluorochrome (green, for example). In addition, a reference probe of normal genomic DNA from a healthy donor is labeled with a different fluorochrome (red, for example). Equal amounts of the green- and red-labeled DNA are mixed and hybridized onto a substrate, which represents the entire human genome. Originally, these were metaphase spreads of normal human chromosomes prepared from lymphocytes of a healthy donor that represented a cytogenetic map. More recently, this substrate has been replaced by manufactured microarrays composed of nucleotide probes that are printed at high density on a solid surface.[15] Depending on the number and lengths of these nucleotide probes, the entire genome can be represented on an array. By using smaller probes, higher resolution of genetic gains and losses can be achieved. During the hybridization, the red- and green-labeled DNA populations compete for binding to corresponding regional microarray targets. For each array target (or region of a chromosome in the original protocol) the ratio of red and green fluorescence intensity ratio is determined. A ratio of 1 indicates a balanced situation at this locus, i.e., no gain or loss in the tumor (see *Fig. 2.28*). In the presence of deletions in the tumor genome, less green probe will be available to hybridize to the corresponding targets, which will result in a decreased green to red fluorescence intensity ratio (<1). In the presence of increased copies, the corresponding targets still show a green to red fluorescence intensity ratio greater than 1. The ratio of red and green fluorescence intensity can be used to quantify the copy number change. A ratio of 1 indicates normal copy number, a ratio <1 indicates a loss, and a ratio >1 indicates

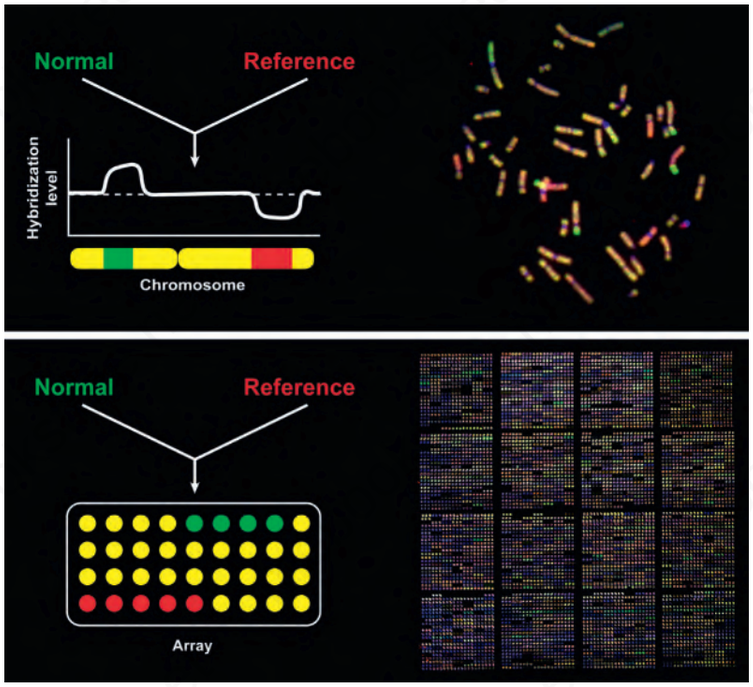

Fig. 2.27
Comparative genomic hybridization (CGH) on a metaphase chromosome spread (*upper panels*) and a microarray (*lower panels*): the regions of the chromosomes (*upper panel*) that appear red are affected by deletions, whereas the regions that appear green are affected by gains or amplifications (*bright green*). Yellow indicates an area with normal DNA complement–no gain or loss. The lower panel on the right shows a DNA microarray with approximately 2500 targets printed as triplicates spots. Triplets that appear green indicate gains whereas those that appear red indicate loss. The array targets are not printed in order of their genomic position which can help control for technical variations. The precise genomic location of the DNA copy number changes detected by the measurement only becomes apparent after plotting the average ratios of red to green fluorescence intensities corresponding to their genomic position as illustrated in *Fig. 2.28*.

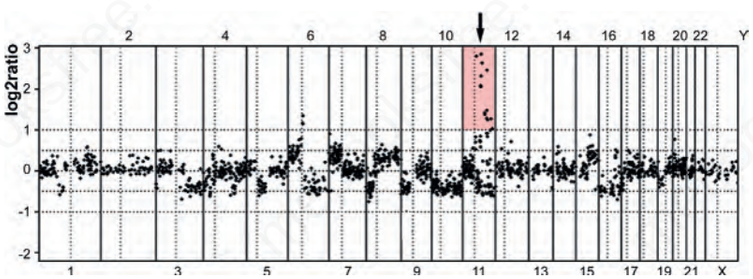

Fig. 2.28
DNA copy number changes as detected by array comparative genomic hybridization of an acral melanoma: the graph shows the $\log_2$ of the ratio of the fluorescence intensity ratios of tumor to reference DNA plotted according to their genomic position on the *x*-axis. The numbers at the top and at the bottom indicate the chromosomes. A $\log_2$ ratio of zero corresponds to normal copy number. As can be seen, multiple contiguous chromosomal regions showed losses and gains. The arrow corresponds to an amplification of chromosome 11q13 interval containing the gene that encodes cyclin D1.

a gain. Gains with a high ratio that only affect portions of a chromosomal arm are termed amplifications. They arise from multiple independent events (chromosomal breakage and fusions) that accumulate under positive selection, typically because the genomic region present in the amplicon contained an oncogene, i.e., a gene that provided a growth advantage to the tumor cells with increased copies of the gene.

The full experimental protocol for CGH is slightly more complex than outlined above. A third, unlabeled DNA population is needed to ascertain that repetitive regions that are scattered throughout the genome do not cross-hybridize and interfere with the measurement. This blocking DNA is highly enriched for repetitive regions and suppresses unwanted cross-hybridization between repetitive regions in the labeled DNA populations and the chromosomes which serve as substrate. CGH has revolutionized the cytogenetic analysis of solid tumors. Compared to conventional cytogenetic analysis, CGH does not require culture of cells for karyotypic analysis, which brings the major advantage that CGH can be performed on archival tissue. It is important to note that the DNA copy number measurement obtained with CGH represents an average of the entire cell population from which the DNA was extracted. For this reason, only the copy number alterations present in a substantial portion of the cells are detected by the method. Depending on the type and amplitude of aberration – amplifications can be detected most easily – the copy number change needs to be present in about 30% to 50% of the cells in order to be identifiable. Alterations affecting only a minority of cells remain undetected. A further limitation is that CGH only detects genomic aberrations that result in DNA copy number changes. Balanced translocations and point mutations are not detected. Copy number neutral rearrangements that arise through chromosomal recombination and LOH (see above) are also not detectable by CGH. More recent implementations that use oligonucleotides to determine single nucleotide polymorphisms (SNPs) allow the genome-wide simultaneous assessment of DNA copy number and LOH in unfixed tumor tissue.[16,17] Due to lack of sensitivity, these methods are not routinely used for clinical diagnosis.

Polymerase chain reaction (PCR)

In the diagnostic setting, PCR is used primarily to acquire sufficient DNA for analysis by sequencing or other methods, primarily to demonstrate a mutation or other genetic change or the presence of a specific gene or messenger RNA.

PCR is an extremely flexible technique and can be adapted to:

- detect mutations (base pair substitutions, insertions and deletions) in genes,
- demonstrate novel fusion transcripts (gene fusions),
- demonstrate clonality,
- demonstrate loss of heterozygosity (loss of one allele),
- detect DNA or RNA associated with infectious organisms,
- detect the levels of expression of messenger RNA.

The ability to specifically amplify and detect any segment of DNA in the human genome has opened many diagnostic doors. In this technique, a pair of short sequences of DNA (called primers) that hybridize to two sequences of genomic DNA (or RNA reverse transcribed to DNA) are designed to amplify a specific region of DNA. Using a DNA polymerase that is stable at high temperatures, a series of annealing, extending, and melting/denaturing cycles amplifies the DNA between the two probes. This technique can be used on nucleic acids extracted from formalin-fixed, paraffin-embedded tissue, although probes must be designed to amplify shorter segments of DNA since the starting material has been cross-linked and fragmented from the formalin treatment. A variety of techniques based on PCR can be used to amplify DNA and then determine its sequence. Direct sequencing of genomic DNA allows detection of point mutations in cancer, such as BRAF or NRAS in melanoma.[18] Generally, one can detect a mutation in 1 in 5 cells with this technique. More sensitive techniques such as pyrosequencing can reduce this to 1 in 10 or 20 cells by analysis for a precise mutation. Allele-specific PCR can be used to detect a known point mutation in as little as 1 in 50 or 100 cells. This technique has applications such as detecting *KIT* D816V mutation in mastocytosis in skin where the neoplastic cells may be sparse relative to the surrounding normal tissue.[19] Digital droplet PCR can also provide high sensitivity and is focused on a single precise nucleotide change.[20] Insertions and deletions in genes can also be detected, usually by Sanger sequencing.[9] Real-time PCR allows indirect visualization of the desired PCR product (amplicon) through the amplification cycles and can provide rapid assessment of a positive or negative result.[21]